Treatment of Blast Furnace Wastewater and Utilization of LD Slag from Steel Industry

Deepti

Treatment of Blast Furnace Wastewater and Utilization of LD Slag from Steel Industry

Thesis submitted in partial fulfillment of the requirements

for the degree of

DOCTOR OF PHILOSOPHY

by

Deepti

Roll No: 166152103

Centre for the Environment

Indian Institute of Technology Guwahati

Guwahati-781039, India

Dedicated to my Parents,

brother and husband for their

faith, love, understanding

and support

Centre for the Environment
Indian Institute of Technology Guwahati
Guwahati 781039, India

CERTIFICATE

It is certified that the work reported in the thesis entitled "**Treatment of Blast Furnace Wastewater and Utilization of LD Slag from Steel Industry**", by **Deepti (Roll No: 166152103)**, has been carried out under our supervision. The work documented in this thesis has not been submitted to any other University or Institute for the award of any degree or diploma.

Dr. Mihir Kumar Purkait
Professor
Department of Chemical Engineering
Indian Institute of Technology Guwahati
Guwahati 781039, India
Date:25/02/2022

Dr. Utpal Bora
Professor
Department of Biosciences & Bioengineering
Indian Institute of Technology Guwahati
Guwahati 781039, India
Date:25/02/2022

Acknowledgements

I owe a debt of gratitude to many people who have helped me in completing this research work directly and indirectly. I would like to acknowledge them all. To begin with, I wish to express my deepest acknowledgement to my supervisor, **Dr. Mihir Kumar Purkait** for providing me inspiring guidance throughout the entire course of this work. I am indebted to him for his useful suggestions and constant encouragement throughout the entire period. I am grateful to him for his great support, encouragement which helped me to finish this work within time. I always admire his advises, energy and hard work for all his students.

I would like to thank **Prof. Utpal Bora,** my co-supervisor for providing me guidance, suggestions and support throughout the course.

I feel very fortunate that I got a chance to work with such experienced and enthusiastic supervisors, whom I will admire throughout my career.

My sincere thanks to all my doctoral committee members, **Prof. Subrata K. Majumder**, **Prof. Animes Kr. Golder** (Department of Chemical Engineering), and **Prof. Pranab Kr. Ghosh** (Department of Civil Engineering) for their valuable suggestions and constructive criticism during the project evolutions, which helped me to make necessary improvements in various stages of my research work. I would specially like to thank **Prof. Subrata K. Majumder,** my doctoral committee for the rigorous and remarkable questions that he raised during the seminar presentations which had helped me a lot in understanding many facts related to my work.

I am also thankful to all the faculty members of Centre for the Environment and Chemical Engineering Department for their encouragement and help at various stages during my stay in both Centre and Department.

I must thank to all the technical and office staffs of my Centre specially, **Dr. Deepmoni Deka**, **Mr. Partha Protim Bakal, Mr. Kaustubh Rakshit**, **Mr. Rajiv Kumar**

Gogoi and Mr. Mridul Das. The experimental works presented in this thesis would never have been possible without the help of these proficient technicians. I am also very thankful to **Mr. Bijoy Kumar Choudhury** (Senior Technician, Department of Mechanical Engineering), who helped me in installing my experimental setup.

I am thankful to the **Central Instrument Facility** of IIT Guwahati for allowing me to utilize their experimental resources.

My seniors like, **Dr. Randeep, Dr. Murchana, Dr. Piyal, Dr. Abhik, Dr. Dibyajyoti, Somnath, JayaKrishnan, Dr. Arnab and Dr. Sushma Chakraborty**. Thanks to all of them for their help and support. I was fortunate enough to get excellent labmates **Ankush, Anweshan, Pranjal, Simons, Niladri, Vikas, Prangan, Rajshekar, Mukesh**. Thanks to all of them for their friendly support, timely assistance and co-operation throughout my research work. I am also thankful to **Bharat, Chetana, Shweta, Debasis and Remya** for their friendly behavior and assistance.

I have no word to thank **GOD** who is my strength and wisdom.

I also wish to extend my loving thanks to my father **Mr. Prabhakaran Nair**, my mother **Mrs. Indira Prabhakaran** and my little brother **Mr. Kiran** for their constant moral support. Their love, affection, blessings and sacrifices made me stronger to overcome my huddles and achieve my goal. I express my humble regards to my **parents-in-law** and acknowledge their love and blessings. A special thanks to **all my school and college teachers** for leading me towards the path of research.

Finally, I express my enormous gratitude and indebtedness to my husband, **Mr. Naveenkumar** for his utmost care, unlimited patience and constant endorsement at all stages of this work during these five years. Thank you for the encouragement and the appreciation for even the littlest things go right.

Deepti

Abstract

Steel industries are one among the major industries which contribute to the world's economic growth. However, waste generation within the industry is enormous due to its high production rates. Large quantity of water is used in the steel industry for different processes like cooling operations, dust scrubbing and descaling. Most of the steel industry releases about 90% of water, which needs to be treated and then reused or discharged into the environment. The wastewater generated from all the processes contain high pH, chlorides, calcium bicarbonate, fluoride, sulphates, cyanide, total suspended solids, volatile suspended solid, TDS, cyanide, thiocyanates, phenol traces, iron and magnesium oxides. Nanofiltration (NF) is been used as a tertiary treatment system for the blast furnace (BF) wastewater in TATA Steel Ltd., India, which is one of the leading steel industries in the world. The volume of the reject stream varies between 20-30 % of feed steam. This membrane reject stream contain the concentrated monovalent and divalent ions (3- 4 times of feed). Available technologies for the treatment of NF reject are not efficient and economically viable due to high energy and space requirement (eg. Solar concentrator). Therefore, there is an urge for a more efficient, economical and facile technique for the treatment of membrane reject stream. Similarly, around 2 – 4 tonnes of waste per tonne of steel are being generated within the industry. Linz Donawitz (LD) slag is one among the wastes in integrated steel industry. Globally, production of LD Slag is around 47 MT per annum. Hence there is a need for use of the LD slag in much persuading way through either conversion of slag into useful material or recycling as process material. Taking all these issues into considerations, the main objectives of this work are divided into two sections. First section deals with the treatment of highly saline wastewater from blast furnace unit of steel industry. And the second section deals with the utilization of LD slag which is a by-product of steel industry.

Abstract

Firstly, the work is focused on the removal of chlorides and sulphates from nanofiltration rejected water which is generated in the blast furnace unit of steel industry by the method of precipitation using miscible organic solvents such as diisopropylamine (DIIPA), isopropylamine (IPA), and ethylamine (EA) in different proportions. Solvent based precipitation showed that miscible organic solvents such as DIPA/IPA/EA is effective in precipitating salts from NF rejected water and thereby reducing the concentrations of chlorides and sulphates. Sulphate and chloride removal efficiency of 99.82 % and 77.50 % respectively, was observed. Effects of solvent to water ratio, pH, temperature and mixing time was thoroughly investigated and optimized using central composite design (CCD). However, due to the recalcitrant nature of brine, treating highly saline wastewater with only one treatment system is insufficient. The drawbacks of a single treatment can be resolved by using combined treatments, resulting in a more effective treatment process and improved outcomes**.** Therefore, the above-mentioned work is extended with a novel concept of integration of closed-circuit reverse osmosis (CCRO) technology and solvent-based precipitation as a means of producing an exceptional quality of water by separating the salts especially chlorides and sulphates from highly saline nanofiltration (NF) rejected stream of the steel industry. The outcome of this work showed that the overall removal efficiency of sulphate and chloride was found to be 99.88 % and 91 %, respectively. Preliminary treatment cost was estimated and found to be around 7.35 $/m^3. The treated water can either be recycled in the system or safely released into the environment.

Further, work is focused on utilizing the solid waste generated from steel industry for the fabrication of porous ceramic membrane from Linz Donawitz (LD) slag. Membranes were fabricated using uniaxial method sintered at three different temperatures like 650 ^oC, 850 ^oC and 950 ^oC. Porosity, pore size distribution, flexural strength, chemical stability was determined and pure water flux experiments were conducted to evaluate the efficiency of the

prepared membranes. Considering the raw materials cost, the cost of the fabricated membranes was estimated in the range of 32.55 - 55.7 USD/m^2. This work gives a potential path to develop microfiltration ceramic membrane with, high porosity and great quality in terms of strength and chemical stability. The fabricated membranes were utilized in a hybrid technique (flocculation followed by microfiltration) for the treatment of cold roll mill (CRM) wastewater generated from steel industry. However, LD slag contain significant amounts of chromium and releasing them into the environment creates some environmental issues. Hence the removal of chromium from Linz Donawitz (LD) slag from the steel industry as a part of environmental quality improvement of the slag material for further use was carried out. Removal of chromium from LD slag is done by the process of roasting and leaching using potassium hydroxide and water respectively. The efficiency of the roasting process for Cr removal was increased by optimizing the mass ratio of potassium hydroxide to the slag, roasting temperature and time. At the optimum condition such as mass ratio = 0.25, temperature = 450 ^oC, roasting time = 3 h and slag particle size = < 25 µm. Approximately 96 % of chromium was removed from LD slag. In this work, the residual slag is used as an adsorbent for the treatment of Congo red polluted wastewater.

Research Publications

1. Patents

- M. K. Purkait, **Deepti**, A Sinha, P. Biswas, S Sarkar, "Separation of ions from the rejected stream of industrial wastewater", Application Number: 201831044754. Date of filing: 27/11/2018. Patent No. 358257, **Granted on 11/02/2021**.
- M. K. Purkait, **Deepti**, "Process for removal of chromium from Linz-Donawitz slag", **Application Number: 202231007598. Date of filing: 13/02/2022**

2. Books

- **Wastewater treatment techniques for steel industry: Case study** authored by, Mihir Kumar Purkait, Piyal Mondal, Pranjal Prathim Das, **Deepti**. Imprint: CRC Press (Taylor & Francis) *(Ongoing)*.

3. Book chapters

- **Deepti**, Piyal Mondal, Mihir Kumar Purkait. Utilization of advanced ceramics towards treatment of wastewater. Volume: Advanced Ceramics. Publisher: Springer.
- **Deepti**, Piyal Mondal, Mihir Kumar Purkait. Emerging technologies and its advancements towards wastewater treatment from various industries. Volume: Emerging technologies in wastewater treatment. Publisher: CRC.
- **Deepti**, Anweshan, Simons, Mihir Kumar Purkait. Membrane and disinfection technologies for industrial wastewater treatment. Publisher: Springer Nature.

4. Journal articles

- **Deepti**, Sinha, A., Biswas, P., Sarkar, S., Bora, U., Purkait, M.K., 2020. Separation of chloride and sulphate ions from nanofiltration rejected wastewater of steel industry. J. Water Process Eng. 33, 101108. https://doi.org/10.1016/j.jwpe.2019.101108.
- **Deepti**, Sinha, A., Biswas, P., Sarkar, S., Bora, U., Purkait, M.K., 2020. Utilization of LD slag from steel industry for the preparation of MF membrane. J. Environ. Manag. 259, 110060. https://doi.org/10.1016/j.jenvman.2019.110060
- **Deepti**, U. Bora, M.K. Purkait, Promising integrated technique for the treatment of highly saline nanofiltration rejected stream of steel industry, J. Environ. Manag. 300 (2021) 113781. https://doi.org/10.1016/j.jenvman.2021.113781.

5. Awards and Achievements

Best Paper presentation Award (2020): Research paper entitled " Studies on separation of chloride and sulphate ions from NF rejected stream of steel industry using precipitation method" at National conference on issues and challenges in water treatment and allied research for sustainable environment (WATER 2020) organized by Centre for the Environment, IITG, Guwahati, India

6. Conferences/ Seminars/ Workshops

- **Deepti**, U. Bora and Mihir Kumar Purkait, " Integrated technique for the treatment of highly saline nanofiltration rejected stream of steel industry " at International Conference on Advances in Chemical, Biological and Environmental Engineering organised by Department of Chemical Engineering Malaviya National Institute of Technology, Jaipur

- **Deepti**, U. Bora and Mihir Kumar Purkait, " Utilization LD slag from steel industry for the fabrication of ceramic membrane" at National Conference on Recent Innovations in Chemical Engineering RICE-2021 organised by Department of Chemical Engineering MANIT, Bhopal
- **Deepti**, U. Bora and Mihir Kumar Purkait, "Separation of chloride and sulphate ions from steel industry using chemical precipitation" at National conference on issues and challenges in water treatment and allied research for sustainable environment (WATER 2020) organized by Centre for the Environment, IITG, Guwahati, India
- National workshop on “Rise of Arsenicosis and Fluorosis like diseases in the North-Eastern states of India – Technologies and techniques for mitigation” Conducted by Centre for Technological Excellence in Water Purification”, IIT Guwahati Sponsored by “Knowledge Incubation for TEQIP Centre for Educational Technology”
- National workshop on “Cleaner Technologies and waste minimization for prevention of industrial pollution and Four R’s – Reduce, Reuse, Recycle and Recover –Case studies” Conducted by IIT Guwahati Sponsored by CPCB.
- Participated in EU-India Water Call: information and networking event, sponsored by Department of Science and Technology and Department of Biotechnology, Govt. of India and Delegation of European Union to India.

CONTENTS

CONTENTS

CONTENTS

LIST OF FIGURES

LIST OF FIGURES

LIST OF TABLES

Nomenclature

Notations

V_R	Volume ratio
C_i	Initial anion concentration
C_f	Final anion concentration
Q	Volume of permeated water
A	Effective membrane area
Δt	Sampling time
F_f	Feed flow
C_f	Concentrate flow
J1	Pure water flux before fouling
J2	Pure water
ds	Average pore diameter
di	Diameter of the i^{th} pore
ni	Number of pores with diameter di
n	Total number of pores
Mw	Mass of the membrane saturated with water
Md	Dry mass of the membrane
Ma	Mass of the membrane at dipping condition
Ce	Liquid phase concentration
Qo, b	Langmuir isotherm constants
Kf	Freundlich constant
n	Deviation from linearnity

Abbreviations

TDS	Total dissolved solids
VSS	Volatile suspended solid
TSS	Total suspended solid
LD	Linz-Donawitz
BF	Blast furnace
EAF	Electric arc furnace
COD	Chemical oxygen demand
CRM	Cold roll mill
UF	Ultra-filtration
NF	Nano filtration
RO	Reverse osmosis
FO	Forward osmosis
MF	Micro filtration
IPA	Isopropylamine
DIIPA	Diisopropylamine
EA	Ethylamine
CCD	Central composite design
CCRO	Closed circuit reverse osmosis
FESEM	Field emission scanning electron microscopy
XRD	X ray diffraction
FTIR	Fourier-transform infrared spectroscopy
EDS	Energy dispersive spectroscopy
FRR	Flux recovery ratio
EPA	Environmental protection agency
CR	Congo red

Chapter 1:

Introduction

Chapter 1
Introduction

This chapter provides a brief overview of the processes involved and the waste generated in the iron and steel industry. It summarises the state-of-the-art in saline wastewater treatment, the use of Linz-Donawitz (LD) slag in various applications, and the background of the problem addressed in this work, namely the treatment of highly concentrated brine generated from blast furnace units, as well as the use of LD slag directly for the preparation of ceramic membranes and the presence of chromium in LD slag. Finally, the objectives of the present work are highlighted.

1.1. Background

Industrialization is not just the key factor of a country's economic development, yet in addition the key factor for the augmentation of strong waste creation. The main solution is to recycle and reuse the waste inside the industry [1]. Steel industries are one among the real ventures which add to the monetary development of the nation [2]. Because of its high production rates, waste generation within the industry is gigantic.

In an integrated steel industry, molten iron which is obtained from blast furnace is sent to the basic oxygen furnace with the presence of oxygen for manufacturing of steel. Steel is also produced alternatively in electric arc furnace from steel scraps along with the fluxes like limestone or dolomite. Scraps and fluxes are heated with the help of electric current, during which the fluxes combine with non-metallic components of scrap and ill-sorted elements of steel to form a liquid slag. The liquid slag is converted into crystalline slag by air cooling process. Before casting, the crude steel is refined by lowering dissolved gases and impurities by adding some alloying agents. Other operational process is taken place in ladles. Steel billets, steel blooms, slabs are produced by continuous casting. Structural sections are made

in the rolling mill from the obtained semi-finished steel [3][4]. **Fig. 1** shows the process of integrated steel industry.

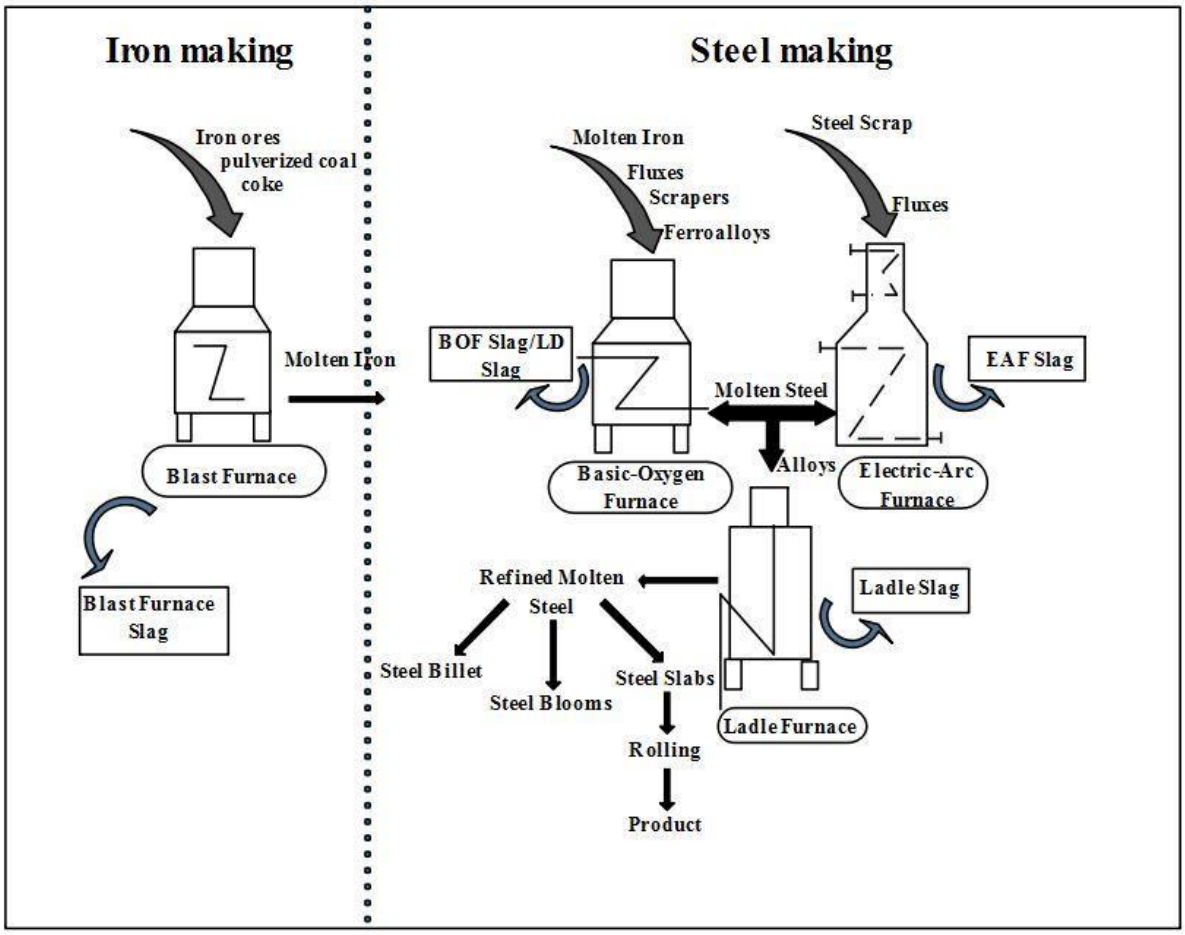

Fig. 1.1. Iron and steel making process in integrated steel industry

1.2. Waste generation: A steel industry perspective

Large quantity of water is used in the steel industry for different processes like cooling operations, dust scrubbing, descaling. Integrated steel plant utilizes water in an average of 28.6 m^3/tonne of steel produced, and water discharge with an average of 25.3 m^3/tonne of steel. Therefore, per tonne of steel produced consumes low water of about 1.6m^3 - 3.3 m^3.Water losses is due to evaporation. Around 90 % of water is discharged or reused [5]. Iron and steel plants generate wastewater from different processes like mining, smelting of pig

iron in blast furnace, LD convertors, rolling mills as shown in the **Fig. 2**. Wastewater resulting from different processes have particular characteristics [6,7].Overall, the wastewater generated from all the processes contain high pH, chlorides, calcium bicarbonate, fluoride, sulphates, cyanide, total suspended solids ,volatile suspended solid, TDS, cyanide thiocyanates, phenol traces, iron, magnesium oxide [2,5,8–12].

Likewise, Per tonne of steel production produce 2-4 tonne of wastes [13]. The solid wastes produced per tonne of steel is around 1.2 tonne in India compared to 0.55 tonne of that in abroad [3].Various solid waste gets generated from different process as depicted in **Fig. 2** includes blast furnace slag, blast furnace flue dust, LD slag ,LD sludge, mill scale, mill sludge, EAF slag, EAF dust [10,13]. Previously, these wastes were either discarded or dumped in the open space. However, due to a lack of space and environmental concerns, many studies are being conducted on the reuse and recycling of these wastes. [14][15].

1.3. Characteristics of various wastewater and slags generated from various units of steel industry

1.3.1. Mining wastewater

The composition of wastewater from the mining sector is diverse. Many of the constituents found in wastewater from the steel industries can also be found in water from the mining industry. Mining water must be drained because otherwise, normal mine operations will be difficult, if not impossible. The amount of drainage water varies throughout the year depending on local hydrogeological conditions. The subterranean water in most mines is only mildly polluted and clear enough to be dumped into rivers or used for a variety of purposes without further treatment. Mine water is frequently neutral or slightly alkaline, although it can also be acidic due to large levels of carbon dioxide or sulphuric acid. The drainage water

in the latter instance will contain significant levels of iron salts. Sulphides may be present in mine water, which must be eliminated through oxidation or aeration [7].

1.3.2. Coke oven wastewater

Coke, a crucial component for creating steel, uses roughly 4000 m3 of freshwater to produce 1000 tonne of coke, which is one of the reasons for the excessive use of water in the iron and steel sector. At the end of the operation, over 1000 m3 of extremely hazardous effluent is produced [16]. Coal carbonization produces gas and other byproducts such as anthracene, toluene, naphthalene, benzene, and coal-tar compounds, Large amounts of organic and inorganic contaminants, such as ammonium, sulphate, cyanide, thiocyanate, and TDS, are found in the effluent produced by the quenching of coke. Treated wastewater discharged from the steel plant cannot meet the required effluent standard due to the difficulty in eliminating organic matter; thus, the released effluent becomes an undesirable matter. The polluted effluent from the coke plants is formed by the washing of the ammonia stills, and it collects in the gas coolers as a result of condensation/sedimentation. Various studies have indicated that biological treatment, such as biodegradation, and pre-treatment studies, such as steam chemical coagulation, sludge concentration, stripping, and aeration, have been used to treat coke oven wastewater to lessen unfavourable environmental conditions. Treatment of wastewater containing various combinations of thiocyanate (SCN), ammonia-nitrogen ($NH4^{+}$–N), cyanide (CN–), and phenol compounds is difficult since the pollutants resist removal. For the treatment of these substances, electrocoagulation, ozonation, and hybrid approaches have been investigated [17,18].

1.3.3. Steel making wastewater

The principal source of wastewater and the primary usage of water in basic oxygen furnace steelmaking are air pollution control systems designed to clean furnace off-gases before they are released into the atmosphere. Excess slag quench water, hood cooling water losses, cooling tower blowdown, and equipment cleaning water are examples of minor wastewater sources that differ by site. Total suspended solids, COD, chlorides, sulphates, organic carbon, and iron are the most common constituents of this effluent. [9].

1.3.4. Cold roll mill wastewater

With numerous sub-processes such as pickling, rolling, annealing, and tempering, the cold rolling mill (CRM) operation imparts hardness, thickness reduction, and desired finishing on steel. During the process, a significant amount of oily wastewater is produced, the most difficult of which is emulsion wastewater from cold-rolling. CRM wastewaters are steel-making process residues with strong carbonation potential due to their very alkaline properties [19]. A typical discharge of CRM effluents contains alkaline, acid, oil and grease, phenol, and iron. Other compounds may also be present such as various salts of chromium, copper, nickel, and zinc in the effluent, depending upon the steel composition. The quality of wastewater should be controlled to their limit before discharging it to the environment. Conventional treatment methods followed are adsorption, biochemical treatment, membrane technology, coagulation -flocculation, electrocoagulation and ozonation [20].

1.3.5. Linz-Donawitz slag

Linz Donawitz (LD) slag is one among the wastes in integrated steel industry. It has been found that the density of LD slag lies between 3.3-3.6g/cm^3. Due to its high Fe content, steel slag looks in appearance a loose collection, and appears hard and wear resistant. The LD slag mainly consists of SiO_2, CaO, Fe_2O_3, FeO, Al_2O_3, MgO, MnO, P_2O_5 Cr_2O_3. The main

mineral phases contained in steel slag are dicalcium silicate (C2S), tricalcium silicate (C3S), RO phase (CaO-FeO-MnO-MgO solid solution), tetra- calcium aluminoferrite (C4AF), olivine, merwinite and free-CaO

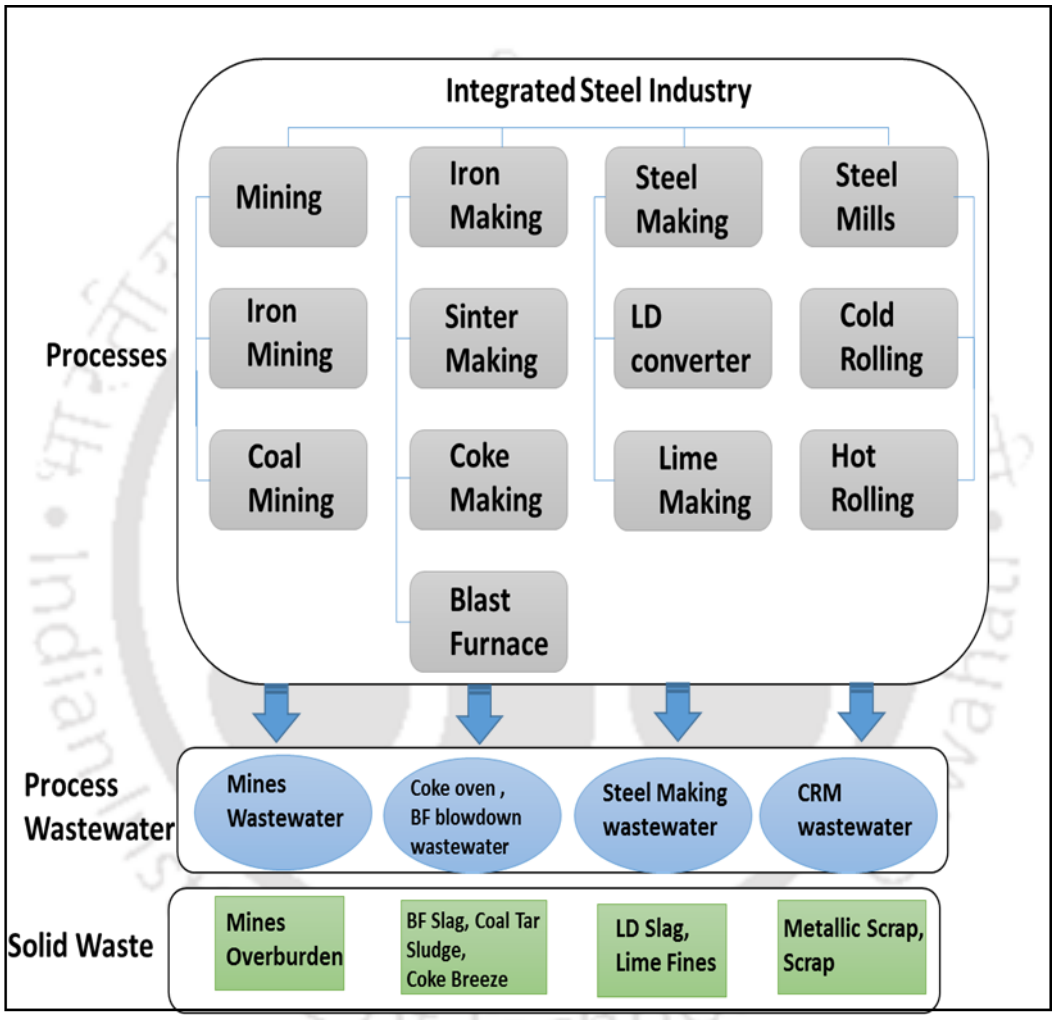

Fig. 1.2. Wastes generated in integrated steel industry

1.4. State of the art

With a brief overview of the contemporary research, this section outlines the research outcome of various literatures so as to identify few promising areas of research that needs to be addressed in this thesis. The state of the art has been presented for treatment of effluents

from blast furnace and cold roll mill units, as well as the utilization of LD slag from the steel industry

1.4.1. Separation of chloride and sulphate ions from nanofiltration rejected wastewater of steel industry

Literature survey

Over the last decade, membrane-based technology (UF, NF and RO) is used globally for the treatment of contaminated drinking water or industrial effluent in the polishing step. Tata Steel Ltd, India, one of the renowned steel industries in the world, has developed a tailor-made ion-selective charged nanofiltration membrane technique for the treatment of chloride and sulphate rich effluent from blast furnace unit of steel industry. However, the rejected stream of this technology contains chloride, sulphate, sodium, and magnesium ions in concentrations greater than 8000 - 10000 mg/L. Highly concentrated NF rejected water without undergoing any treatment can affect equipment within the industry. In particular, chlorides (> 600 mg/L) and sulphates (> 400 mg/L) above their permissible limits can lead to metal corrosion, scaling and blockage in the pipelines [9]. Additionally, if discharged into the environment, it can cause soil and groundwater contamination which in turn makes it unsuitable for human consumption causing diarrheal symptoms, dehydration and hypertension [21]. Managing the concentrate from the NF plant is quite challenging as it can result in an adverse effect if reused or discharged without any treatment. Consequently, there has been consistent investigation to deal with the membrane filtration reject stream. Several methods have been reported to dispose of the rejected stream of membrane filtration such as deep well injection, discharge to sewers, ocean outfall and evaporation ponds, [22]. Furthermore, some treatment techniques are available and have been reported such as thermal evaporation, crystallization [23], ion exchange [24,25], electro- dialysis, RO-NF integrated

system [26–28], solar and geothermal desalination [29], biosorption [30], forward osmosis (FO), ozone oxidation[31] and vacuum membrane distillation (VMD) [32,33]. Because of strict environmental guidelines, discharge standards, size and complexity of the equipment, high energy and low output, equipment with larger physical footprints make it less viable for industrial use. From another point of view, the colossal amount of free energy stored in the brines, which might have been rummaged through proper methods, is squandered in the existing disposal methods [34].

There are reports in the literature which reported the separation of ions from aqueous solutions the important ones include MSH Bader 1998 [35] which reported an experimental database for the precipitation of chloride and sulfate salts associated with six cations (sodium, potassium, magnesium, calcium, barium, and strontium) from aqueous solutions was generated using isopropylamine as the precipitation agent. Another work by Bader reported a process based on the concepts of membrane distillation (MD) and liquid–phase precipitation (LPP) for selective removal of sulfate from seawater is provided. The MD–LPP process uses a small amount of energy and additive, generates minimal waste with suitable disposal paths, extracts economic values from discarded streams or species, and offers a rapid economic deployment. Patents of interest include US Patent no. 9,828,270 which discloses a treatment system is provided and comprises a precipitation unit and a recovery unit. The precipitation unit is configured to treat a solution using one or more miscible organic solvents like diisopropylamine and isopropylamine to produce a mixture of precipitate solids and a liquid.

Another one is US Patent no. 4,548,614 which discloses a process in that low boiling, water soluble organic solvent is added to a saturated brine to thereby reduce the salt solubility of the brine and cause precipitation of the salt. The precipitated salt is filtered out and dried. The remaining brine-solvent mixture is distilled to remove the solvent which is reused. Unsaturated brine that is generally free of solvent is returned for resaturation with salt.

Miscible organic solvents may precipitate salts by its solventing out (reduction in the solubility of the salt) properties [35]. In this work, solvents are selected such that these a) can cause high salt precipitation, b) boiling point close to ambient temperature, c) less expensive and d) less environmental risk. In addition, the solvents used are widely used as herbicide in the agricultural purpose [35]. The quick vaporization of the organic solvents on the use of vacuum is increasingly affordable when contrasted with conventional strategies, for example, distillation to achieve the required heat transfer. In addition, these solvents have additional properties of i) excellent blending among species, ii) better control of its dose and transport, iii) allowing better separation of species and 4) useable at various conditions [36,37].

Possible scope for further research

Although there are several reports for the precipitation and separation of inorganic ions but none of the report discloses a simple and economically viable process for separation of chloride and sulphates ions from rejected stream of industrial wastewater by using the miscible organic solvents.Therefore, this part of the thesis focussed to develop a simple and economically viable process for separation of chloride and sulphates ions from rejected stream of nanofiltration from iron and steel industries by using the miscible organic solvents. Miscible Organic solvents are used as precipitating agent. Though there are many miscible organic solvents available, the opted ones are isopropylamine (IPA), diisopropylamine (DIPA) and ethylamine (EA) those which is effective in precipitating the salt and economical. Four important parameters such as volume of the solvent, pH, temperature and contact time were considered for precipitation and optimized using central composite design (CCD). The method carried out in this part of thesis will be a benefaction to the steel industry in terms of handling nanofiltration rejected water containing high chlorides and sulphate ions. To the best of our knowledge, no work has been reported on use of solvent based technology for the treatment of NF rejected effluent of steel industry.

1.4.2. Integrated technique for the treatment of highly saline nanofiltration rejected stream of steel industry

Literature survey

Treating highly saline wastewater with only one treatment system is insufficient, due to the recalcitrant nature of brine. Usually, a single treatment system is ineffective to produce treated water that meets regulatory standards. The treatment method would incur very high costs to satisfy these conditions. According to [38], water containing complex compounds, such as monovalent and divalent ions, heavy metals, and dyes, should be treated with a combination of treatments since one is insufficient. The drawbacks of a single treatment can be resolved by using combined treatments, resulting in a more effective treatment process and improved outcomes. In a previous study, [39], studied the treatment of brine, by a hybrid process of electrocoagulation and two stage reverse osmosis (RO). Furthermore, [34], investigated the importance of the hybrid system that combines reverse electrodialysis and reverse osmosis for brine management. [40] emphasised the importance of implementing an integrated treatment approach, stating that a single treatment method is no longer feasible in the modern world due to more stringent legislation and that a variety of treatment methods should be used for more technically and economically viable alternatives. A hybrid process, in turn, is cost-effective and time-saving because it combines multiple processes into one [41]. Considering the advantages of combined techniques, the hybridization/integration of two techniques can be investigated for better treatment results for the treatment of concentrated brine. Reverse Osmosis (RO) is a pressure-driven process used to remove salts and pollutants, especially treating wastewater with high conductivity like the iron and steel industry [42]. Another alternative is the semi-batch process, also referred to as closed circuit reverse osmosis (CCRO), which has some of the same characteristics as batch RO. The basic

principle of CCRO is that fresh feed continuously dilutes recycled brine, resulting in minimal energy increase. The use of CCRO to enhance treatments has lately gained a lot of interest. [43,44] and [45] studied the performance of CCRO and they suggest that this technique appears to have the ability to promote high rejection and low fouling propensity. However, this method for a second time generates a very high concentrated rejected stream which has to be treated again with one more process. In the integrated approach, the chemical precipitation process is used as a second system, where organic solvents are used to precipitate the salts from concentrated RO rejected stream using solventing out phenomenon. This process reduces the solubility of salt in water and hence can separate the salt from the water. Organic solvents selected in this study are isopropylamine, diisopropylamine and ethylamine that can meet certain criteria viz., (a) all are miscible in water, (b) having favourable properties such as low boiling point, high volatility and importantly, no azeotrope formation with water and (c) chemically stable and cost-effective [46].

Possible scope for further research

The literature review shows that, given the benefits of combined techniques, the hybridization/integration of two techniques can be examined for improved results in the treatment of concentrated brine.

Available technologies for the treatment of NF reject are not efficient and economically viable due to high energy and space requirement (eg. Solar concentrator). Therefore, there is an urge for a more efficient, economical and facile technique for the treatment of membrane reject stream. Investigation on CCRO with solvent-based precipitation technique might be a novel one for the treatment of highly saline wastewater from the steel industry.

In this part of the thesis, an attempt was made to investigate the integrated technique of closed-circuit reverse osmosis (CCRO) and solvent-based precipitation to treat concentrated nanofiltration reject. The performance of the membrane, factors affecting precipitation and to

scrutinize whether the proposed design benefit in reducing the brine concentration to benefit the steel industry for better management of the rejected stream of NF process is investigated. Moreover, a preliminary economic assessment was carried out for the integrated process. Reverse osmosis system analysis (ROSA 7.0 - FilmTec's) software, was used to estimate the water production cost, common technical assumptions, design parameters and specifications for the RO system. The system used here is an attempt to increase the quality of the NF rejected stream using a hybrid technique while also achieving zero liquid discharge. The system is expected to be a better technology than the previous one as mentioned in the previous section (Section 1.4.1).

1.4.3. Utilization of LD slag from Steel Industry for the Preparation of MF Membrane

Literature survey

Linz Donawitz (LD) slag is one among the wastes in integrated steel industry. LD slag produced per ton of crude steel in India is said to be 150-180 kg/t. Globally, production of LD Slag is around 47 MT per annum [15]. Open dumping and landfill practices are the common techniques adopted for disposal of industrial slag, thus these techniques result in environmental pollution in the form of dust and leachate apart from huge economic accountability [47]. Hence there is much research on utilization of LD Slag for other beneficial uses like road making, construction, agriculture, extraction of valuable products. It has been reported that iron and steel slag have high pozzolanic potential and can be utilized as raw material or blending constituent in cement manufacturing and constructional activities.[5-9]. However, because of its high specific gravity and high volume expansion, it is disadvantageous for road making. Also, as LD slag is exceedingly porous in nature, it demands more water which makes it troublesome in making concrete clinkers. Hence there is

a need for use of the LD slag in much persuading way through either conversion of slag into useful material or recycling as process material.

Ceramic membranes are looking for more consideration over decades because of their high quality, great mechanical and compound soundness, higher life expectancy [50][51,52], and simple cleaning [10-12]. There are many research centred in fabrication of ceramic membranes using diverse raw materials like α-alumina, zirconia, silica.[13-15]. However, the expense of these crude materials stayed high and prompted focus around less expensive crude materials[56–58]. Industrial wastes such as fly ash, charred wastes, coal ash, as well as agricultural wastes like rice husk, sugarcane bagasse, clays have been investigated and studied as economical and convenient raw materials for the fabrication of ceramic membranes [16-18]. M. Changmai et al. [62] have fabricated low cost ceramic membranes using thermal power plant slag with additional precursors. Similarly H. Abdallah et al. [63] utilized rollers kiln waste as the main raw material for the fabrication of ceramic support. The composition of these materials made it possible to fabricate ceramic support which motivates further research towards cost effective membranes of great demand [64].

Steel industry uses cold rolling to harden, reduce thickness and provide special finishing on steel. Acid, alkaline and oily wastewater are discharged during cold steel rolling. It also contribute to zinc, nickel, copper, tin, chromium and iron depending upon the varieties of steel. The quality of wastewater should be controlled to their limit before discharging it to the environment. Conventional treatment methods followed are adsorption, biochemical treatment, membrane separation, and coagulation - flocculation [65]. Coagulation – flocculation is a simple physiochemical technique commonly used for water and wastewater treatment. Inorganic metal salts namely, aluminum (alum) sulfate, ferric chloride, ferrous sulfate, and ferric chloro-sulfate are generally used in coagulation–flocculation [66]. However, polymerized forms of metal coagulants are of great demand in recent years due to

their wider availability, higher removal of organic matters, lower alkalinity intake and reduced cost [24,25]. Xue-Ni Cheng et al. [69] have used coagulation for the treatment of oily wastewater from cold rolling mill. During coagulation, the amorphous precipitate create flocs, which therefore needs further treatment to hold back the water quality parameters in terms of turbidity, conductivity and total dissolved solids. Based on the floc size, microfiltration was considered in the subsequent steps. It was found that particle size of the flocs produced was in the range of 5 to 130 μm [70–72] .

Possible scope for further research

It may be envisaged from the above literature that LD slag has been used in wide range of applications including construction, road making and agriculture. However, considering the growing demand of ceramic membranes (CM), use of LD slag for the fabrication of CM might be addition of current research. In this part of the thesis, an attempt was made to fabricate porous ceramic membranes by LD slag along with other precursors by uniaxial method. Three different sintering temperatures (650 ^{o}C, 850 ^{o}C and 950 ^{o}C) were selected for the study. Modification of the slag was carried out for the improvement of the membrane. Morphological and permeation experiments were conducted to investigate the properties of the membrane. Treatment of cold roll mill (CRM) wastewater from steel industry was carried out using the hybrid process via coagulation- flocculation followed by microfiltration. The flocs generated after coagulation – flocculation process was separated using the prepared LD slag membranes. Use of LD slag for the fabrication of ceramic membrane is not only an appealing option towards the commercialization of membrane, but also great option to reduce the solid waste which is dumped to the environment.

1.4.4. Removal of Chromium from Linz-Donawitz slag

Literature survey

The global average rate of LD slag production is estimated to be around 47 MT per year. In India, it is reported to be between 150 and 180 kg for every tonne of steel produced [20]. Open dumping and landfill operations are the most commonly used methods for disposing of industrial slag, they cause environmental degradation in the form of dust and leachate, in addition to significant economic liability. As a result, extensive research is being performed on the use of LD Slag for a variety of advantageous uses. Because of the composition of slag, it can be used in a variety of applications, which encourages ongoing study towards a more sustainable environment. The composition of these slag varies greatly depending on the source of origin, however, they typically contain some important resources such as CaO, FeO and SiO_2 [73,74].

However, LD slag contain significant amounts of chromium and releasing them into the environment creates some environmental issues. The hazardous chromium is extremely undesirable in terms of pollution [75]. LD slag includes relatively large quantities of chromium (up to 4 wt.%), which is a hazardous substance when in oxidation state +6. Chromium is a redox-active metal that may be found in the environment as Cr (III) or Cr (VI). These two oxidation states have opposing toxicity and mobility properties: trivalent chromium is an important nutrient at low concentrations and a non-toxic element at greater concentrations, and it is generally insoluble in water, but hexavalent chromium is very poisonous and easily transported [76].

Removal of chromium from LD slag might eventually alleviate the environmental challenge by allowing the precious and important metal Cr to be recovered while still being utilised as cement or building material. In reality, the high chromium concentrations in slag have been a

major impediment to slag usage, prompting researchers to investigate chromium removal or recovery.

Only a few research on chromium extraction from steel slag have been reported. The extraction of chromium from chromite in liquid molten sodium salts of NaOH or NaOH-$NaNO_3$ has been reported by several investigators. Some researchers looked at alkali roasting chromite ore with NaOH and Na_2CO_3 to extract chromium from it [77]. Roasting with Na_2CO_3 at 1100 °C is the most common method for recovering Cr from chromite ore. However, because this process takes place at high temperatures, it consumes a lot of energy and is thus inefficient for treating low-grade ore minerals with only a few percentages of Cr. Others have explored Cr leaching from chromite ore using sulfuric acid (60–80 wt%) at elevated temperatures (160–240 °C) with or without $HClO_4$ as an oxidant at elevated temperatures (160–240 °C) [78]. Acid leaching will dissolve the stainless-steel slag matrix materials and result in a large consumption of acid solution since slag materials are typically made of alkaline mineral phases such as CaO, Al_2O_3, and MgO. Although there has been a minimal study on the biological leaching of metals from slag, the bioleaching approach may be a viable option for industrial slags with low metal concentration [79]. According to (*Gomes et al., 2018)* the supernatant of a mixed acidophilic bacteria culture may be utilised to recover aluminium, chromium, and vanadium from Argon oxygen decarburization (AOD) slag. The recovery of metals from the leachate was inadequate since all of the metals were in the third oxidation state (Al_3, Cr_3, and V_3). Alkali pressure leaching was recently reported to recover Cr selectively from SS slag material with a low yield (48%) without dissolving or substantially changing the matrix material [80].

The patents of interest include Indian Patent application publication no. 9004/CHENP/2012 which discloses a system, method for removing chromium from a slug formed by an electric

furnace operation. The system also promotes the desulfurization of chromium-containing hot metal.

Possible scope for further research

Although there are various publications, the patent and non-patent literatures for the recovery of chromium from steel slags, none of them discloses technique for removal of chromium from LD slag of the steel industry by alkaline roasting and leaching. The stated prior art procedures are intricate and have their limitations. All of these factors prompted to investiagte a simple and cost-effective method for the removal of chromium from LD slag of steel industry using a roasting and leaching process. The efficiency of the roasting process for Cr removal was studied with respect to the mass ratio, roasting temperature and time. This method is expected to yield two products: Residual LD slag and chromium-leached liquor. Based on the literature, residual slag has a potential for application in various fields such as agriculture, construction, cement production and wastewater treatment. An attempt was made to investigate the use of residual slag as an adsorbent to treat Congo red polluted wastewater. Also, studies for recovering chromium hydroxide $(CrOH)_3$ precipitates from leached-out liquor containing chromium by adding calcium hydroxide was conducted.

1.5. Objectives of thesis work

Based on the above state of the art, the present PhD thesis incorporates the following objectives

- Separation of Chloride and Sulphate ions from Nanofiltration Rejected Wastewater of Steel Industry
- Integrated technique for the treatment of highly saline nanofiltration rejected stream of steel industry
- Utilization of LD Slag from Steel Industry for the Preparation of MF Membrane
- Removal of Chromium from Linz-Donawitz slag

1.6. Organization of the thesis

Chapter 1 discusses the background of the problem undertaken in this work i.e. the problem associated with the treatment of highly concentrated brine generated from blast furnace units, as well as the use of LD slag directly for the preparation of ceramic membranes and the presence of chromium in LD slag. The objectives of the present work are also highlighted in this chapter. **Chapter 2** describes the use of three different miscible organic solvents such as diisopropylamine (DIIPA), isopropylamine (IPA), and ethylamine (EA) in different proportions for the removal of chlorides and sulphates from nanofiltration rejected stream generated from coke oven unit from steel industry. Four important parameters namely volume of the solvent, pH, temperature and contact time were optimized using central composite design (CCD). **Chapter 3** presents an integrated technique of closed circuit reverse osmosis (CCRO) and solvent-based precipitation to treat concentrated nanofiltration reject. The performance of the membrane, factors affecting precipitation is investigated. A preliminary economic assessment was carried out for the integrated process. **Chapter 4** discusses the fabrication of porous ceramic membranes by LD slag along with other precursors by uniaxial method. Modification of the slag was carried out for the improvement of the membrane. Treatment of cold roll mill (CRM) wastewater from steel industry was carried out using the hybrid process via coagulation- flocculation followed by microfiltration. **Chapter 5** converses the removal of chromium (Cr) from LD slag using roasting and leaching method. The factors affecting roasting was studied in detail. Moreover, the residual slag was utilized as adsorbent for the treatment of Congo red dye polluted wastewater. **Chapter 6** summarized the inferences drawn from the work and provided some suggestions towards future research.

Reference

[1] M. Khunte, Process Waste Generation and Utilization in Steel Industry, 3 (2018) 1–5. https://doi.org/10.11648/j.ijimse.20180301.11.

[2] S.K. Sinha, K. Sinha, S.K. Pandey, A. Tiwari, A Study on the Waste Water Treatment Technology for Steel Industry: Recycle And Reuse, Am. J. Eng. Res. 03 (2014) 309–315. www.ajer.org.

[3] S. Sarkar, D. Mazumder, Solid wastes generation in Steel Industry and their recycling potential, Manag. Util. Wastes from Met. Process. Ind. Therm. Power Station. (2015) 1–14.

[4] J. Waligora, D. Bulteel, P. Degrugilliers, D. Damidot, J.L. Potdevin, M. Measson, Chemical and mineralogical characterizations of LD converter steel slags: A multi-analytical techniques approach, Mater. Charact. 61 (2010) 39–48. https://doi.org/10.1016/j.matchar.2009.10.004.

[5] V. Colla, I. Matino, T.A. Branca, B. Fornai, L. Romaniello, F. Rosito, Efficient use of water resources in the steel industry, Water (Switzerland). 9 (2017) 1–15. https://doi.org/10.3390/w9110874.

[6] V. Colla, T.A. Branca, F. Rosito, C. Lucca, B.P. Vivas, V.M. Delmiro, Sustainable Reverse Osmosis application for wastewater treatment in the steel industry, J. Clean. Prod. 130 (2016) 103–115. https://doi.org/10.1016/j.jclepro.2015.09.025.

[7] S.E. Jorgensen, Waste Water From the Iron and Steel Industry and Mining, Stud. Environ. Sci. 5 (2008) 217–227.

[8] A.. Patwardhan, Industrial wastewater treatment, 2008. https://doi.org/10.1016/0735-1097(93)90602-W.

[9] Usepa, Development document for final effluent limitations guidelines and standards for the iron ans steel manufacturing point source category, Response. (2002) 1062.

[10] R. Mukherjee, M. Mondal, A. Sinha, S. Sarkar, S. De, Application of nanofiltration membrane for treatment of chloride rich steel plant effluent, J. Environ. Chem. Eng. 4 (2016) 1–9. https://doi.org/10.1016/j.jece.2015.10.038.

[11] K. Zhang, S.M. Malone, B. Bras, M. Weissburg, Y. Zhao, H. Cao, Ecologically Inspired Water Network Optimization of Steel Manufacture Using Constructed Wetlands as a Wastewater Treatment Process, Engineering. 4 (2018) 567–573. https://doi.org/10.1016/j.eng.2018.07.007.

[12] W.S. ASSOCIATION, Worl_Steel_Figures_2018, (2018) 1-3O. www.worldsteel.org.

[13] B. Das, S. Prakash, P.S.R. Reddy, V.N. Misra, An overview of utilization of slag and sludge from steel industries, Resour. Conserv. Recycl. 50 (2007) 40–57. https://doi.org/10.1016/j.resconrec.2006.05.008.

[14] D.K. Ambasta, B. Pandey, N. Saha, Utilization of Solid Waste from Steel Melting Shop, Int. Semin. "Start up" "Stand up" India from Mines to Steel, 29-31.1.2016, MECON Community Hall, Shyamali, Ranchi. (2016). http://www.meconlimited.co.in/writereaddata/MIST_2016/sesn/tech_4/3.pdf%5Cnhttp://www.meconlimited.co.in/writereaddata/MIST_2016/session.htm.

[15] M. Shokri, A. Ahsan, H.Y. Liu, N.H. Muslim, An overview of Use of Linz-Donawitz (LD) Steel Slag in Agriculture, Jouranl Adv. Sci. Reseacrh. 5 (2015) 30–41.

[16] L. Mishra, K.K. Paul, S. Jena, Characterization of coke oven wastewater, IOP Conf. Ser. Earth Environ. Sci. 167 (2018). https://doi.org/10.1088/1755-1315/167/1/012011.

[17] R. Kumar, P. Pal, A novel forward osmosis-nano filtration integrated system for coke-oven wastewater reclamation, Chem. Eng. Res. Des. 100 (2015) 542–553. https://doi.org/10.1016/j.cherd.2015.05.012.

[18] A. Kuljian, J. Penny, J. Harrison, Full-scale treatment of a coke oven wastewater using immersed membrane biological reactor technology, AISTech - Iron Steel Technol.

Conf. Proc. 1 (2015) 132–146.

[19] P.P. Das, A. Anweshan, M.K. Purkait, Treatment of cold rolling mill (CRM) effluent of steel industry, Sep. Purif. Technol. 274 (2021) 119083. https://doi.org/10.1016/j.seppur.2021.119083.

[20] Deepti, A. Sinha, P. Biswas, S. Sarkar, U. Bora, M.K. Purkait, Utilization of LD slag from steel industry for the preparation of MF membrane, J. Environ. Manage. 259 (2020) 110060. https://doi.org/10.1016/j.jenvman.2019.110060.

[21] G.U. Semblante, J.Z. Lee, L.Y. Lee, S.L. Ong, H.Y. Ng, Brine pre-treatment technologies for zero liquid discharge systems, Desalination. 441 (2018) 96–111. https://doi.org/10.1016/j.desal.2018.04.006.

[22] A. Subramani, J.G. Jacangelo, Treatment technologies for reverse osmosis concentrate volume minimization: A review, Sep. Purif. Technol. 122 (2014) 472–489. https://doi.org/10.1016/j.seppur.2013.12.004.

[23] D.G. Randall, J. Nathoo, A succinct review of the treatment of Reverse Osmosis brines using Freeze Crystallization, J. Water Process Eng. 8 (2015) 186–194. https://doi.org/10.1016/j.jwpe.2015.10.005.

[24] H. Li, Y. Chen, J. Long, D. Jiang, J. Liu, S. Li, J. Qi, P. Zhang, J. Wang, J. Gong, Q. Wu, D. Chen, Simultaneous removal of thallium and chloride from a highly saline industrial wastewater using modified anion exchange resins, J. Hazard. Mater. 333 (2017) 179–185. https://doi.org/10.1016/j.jhazmat.2017.03.020.

[25] Y. Öztürk, Z. Ekmekçi, Removal of sulfate ions from process water by ion exchange resins, Miner. Eng. 159 (2020) 106613. https://doi.org/10.1016/j.mineng.2020.106613.

[26] S. Chakrabortty, J. Nayak, P. Pal, R. Kumar, P. Chakraborty, Separation of COD, sulphate and chloride from pharmaceutical wastewater using membrane integrated system: Transport modeling towards scale-up, J. Environ. Chem. Eng. 8 (2020)

104275. https://doi.org/10.1016/j.jece.2020.104275.

[27] Z. Yan, L. Zeng, Q. Li, T. Liu, H. Matsuyama, X. Wang, Selective separation of chloride and sulfate by nanofiltration for high saline wastewater recycling, Sep. Purif. Technol. 166 (2016) 135–141. https://doi.org/10.1016/j.seppur.2016.04.009.

[28] T. Foudhaili, O. Lefebvre, L. Coudert, C.M. Neculita, Sulfate removal from mine drainage by electrocoagulation as a stand-alone treatment or polishing step, Miner. Eng. 152 (2020) 106337. https://doi.org/10.1016/j.mineng.2020.106337.

[29] J.A. Sanmartino, M. Khayet, M.C. García-Payo, H. El-Bakouri, A. Riaza, Treatment of reverse osmosis brine by direct contact membrane distillation: Chemical pretreatment approach, Desalination. 420 (2017) 79–90. https://doi.org/10.1016/j.desal.2017.06.030.

[30] E. Iakovleva, E. Mäkilä, J. Salonen, M. Sitarz, M. Sillanpää, Industrial products and wastes as adsorbents for sulphate and chloride removal from synthetic alkaline solution and mine process water, Chem. Eng. J. 259 (2015) 364–371. https://doi.org/10.1016/j.cej.2014.07.091.

[31] W. Liu, R. Zhang, Z. Liu, C. Li, Removal of chloride from simulated zinc sulfate electrolyte by ozone oxidation, Hydrometallurgy. 160 (2016) 147–151. https://doi.org/10.1016/j.hydromet.2015.12.006.

[32] P. Balasubramanian, A brief review on best available technologies for reject water (brine) management in industries, Int. J. Environ. Sci. 3 (2013) 2010–2018. https://doi.org/10.6088/ijes.2013030600020.

[33] A.D. Sontakke, M.K. Purkait, Fabrication of ultrasound-mediated tunable graphene oxide nanoscrolls, Ultrason. Sonochem. 63 (2020) 104976. https://doi.org/10.1016/j.ultsonch.2020.104976.

[34] W. Li, W.B. Krantz, E.R. Cornelissen, J.W. Post, A.R.D. Verliefde, C.Y. Tang, A novel hybrid process of reverse electrodialysis and reverse osmosis for low energy

seawater desalination and brine management, Appl. Energy. 104 (2013) 592–602. https://doi.org/10.1016/j.apenergy.2012.11.064.

[35] M.S.H. Bader, Precipitation and Separation of Chloride and Sulfate Ions from Aqueous Solutions: Basic Experimental Performance and Modelling, Environ. Prog. 17 (1998) 126–135. https://doi.org/10.1002/ep.670170220.

[36] Mansour S. Bader, Precipitation and separation of salts, scale salts, and norm contaminant salts from saline waters and saline solutions, 1995.

[37] M.S.H. Bader, Separation of Salts from Aqueous Saline Solutions: Modeling and Experimental, J. Environ. Sci. Heal. . Part A Environ. Sci. Eng. Toxicol. 29 (1994) 429–465. https://doi.org/10.1080/10934529409376047.

[38] C.X.H. Su, L.W. Low, T.T. Teng, Y.S. Wong, Combination and hybridisation of treatments in dye wastewater treatment: A review, J. Environ. Chem. Eng. 4 (2016) 3618–3631. https://doi.org/10.1016/j.jece.2016.07.026.

[39] S.P. Azerrad, M. Isaacs, C.G. Dosoretz, Integrated treatment of reverse osmosis brines coupling electrocoagulation with advanced oxidation processes, Chem. Eng. J. 356 (2019) 771–780. https://doi.org/10.1016/j.cej.2018.09.068.

[40] F.I. Hai, K. Yamamoto, K. Fukushi, Hybrid treatment systems for dye wastewater, Crit. Rev. Environ. Sci. Technol. 37 (2007) 315–377. https://doi.org/10.1080/10643380601174723.

[41] D. Ghosh, M.K. Sinha, M.K. Purkait, A comparative analysis of low-cost ceramic membrane preparation for effective fluoride removal using hybrid technique, Desalination. 327 (2013) 2–13. https://doi.org/10.1016/j.desal.2013.08.003.

[42] M.A. Al-Obaidi, A.A. Alsarayreh, A.M. Al-Hroub, S. Alsadaie, I.M. Mujtaba, Performance analysis of a medium-sized industrial reverse osmosis brackish water desalination plant, Desalination. 443 (2018) 272–284.

https://doi.org/10.1016/j.desal.2018.06.010.

[43] S.M. Riley, D.C. Ahoor, K. Oetjen, T.Y. Cath, Closed circuit desalination of O&G produced water: An evaluation of NF/RO performance and integrity, Desalination. 442 (2018) 51–61. https://doi.org/10.1016/j.desal.2018.05.004.

[44] N.A. Yaranal, S. Kumari, S. Narayanasamy, S. Subbiah, An analysis of the effects of pressure-assisted osmotic backwashing on the high recovery reverse osmosis system, J. Water Supply Res. Technol. (2019) 1–21. https://doi.org/10.2166/aqua.2019.089.

[45] B. Sutariya, H. Raval, Analytical study of optimum operating conditions in semi-batch closed-circuit reverse osmosis (CCRO), Sep. Purif. Technol. 264 (2021) 118421. https://doi.org/10.1016/j.seppur.2021.118421.

[46] Deepti, A. Sinha, P. Biswas, S. Sarkar, U. Bora, M.K. Purkait, Separation of chloride and sulphate ions from nanofiltration rejected wastewater of steel industry, J. Water Process Eng. 33 (2020) 101108. https://doi.org/10.1016/j.jwpe.2019.101108.

[47] S.K. Nath, Geopolymerization behavior of ferrochrome slag and fly ash blends, Constr. Build. Mater. 181 (2018) 487–494. https://doi.org/10.1016/j.conbuildmat.2018.06.070.

[48] C. Sarkar, J.K. Basu, A.N. Samanta, Removal of Ni2+ ion from waste water by Geopolymeric Adsorbent derived from LD Slag, J. Water Process Eng. 17 (2017) 237–244. https://doi.org/10.1016/j.jwpe.2017.04.012.

[49] N. Ortiz, M.A.F. Pires, J.C. Bressiani, Use of steel converter slag as nickel adsorber to wastewater treatment, Waste Manag. 21 (2001) 631–635. https://doi.org/10.1016/S0956-053X(00)00123-9.

[50] K. Mohanty, M.K. Purkait, Membrane technologies and applications, 2011. https://doi.org/10.1002/0470020393.

[51] M.K. Purkait, P.K. Bhattacharya, S. De, Membrane filtration of leather plant effluent:

Flux decline mechanism, J. Memb. Sci. 258 (2005) 85–96. https://doi.org/10.1016/j.memsci.2005.02.029.

[52] S. Emani, R. Uppaluri, M.K. Purkait, Preparation and characterization of low cost ceramic membranes for mosambi juice clarification, Desalination. 317 (2013) 32–40. https://doi.org/10.1016/j.desal.2013.02.024.

[53] B.K. Nandi, R. Uppaluri, M.K. Purkait, Preparation and characterization of low cost ceramic membranes for micro-filtration applications, Appl. Clay Sci. 42 (2008) 102–110. https://doi.org/10.1016/j.clay.2007.12.001.

[54] L. Zhu, Y. Dong, S. Hampshire, S. Cerneaux, L. Winnubst, Waste-to-resource preparation of a porous ceramic membrane support featuring elongated mullite whiskers with enhanced porosity and permeance, J. Eur. Ceram. Soc. 35 (2015) 711–721. https://doi.org/10.1016/j.jeurceramsoc.2014.09.016.

[55] W. Zhu, Y. Liu, K. Guan, C. Peng, W. Qiu, J. Wu, Integrated preparation of alumina microfiltration membrane with super permeability and high selectivity, J. Eur. Ceram. Soc. 39 (2019) 1316–1323. https://doi.org/10.1016/j.jeurceramsoc.2018.10.022.

[56] M.W.J. Luiten-Olieman, C. Huiskes, M. ten Hove, L. Winnubst, A. Nijmeijer, Hydrothermal stability of silica, hybrid silica and Zr-doped hybrid silica membranes, Sep. Purif. Technol. 189 (2017) 48–53. https://doi.org/10.1016/j.seppur.2017.07.045.

[57] X. Wang, F. Guo, Y. Liu, X. Zhao, P. Xiao, H. Cai, G. Wang, M. Yi, Hydrothermal ageing of tetragonal zirconia porous membranes: Effect of thermal residual stresses on the phase stability, Corros. Sci. 142 (2018) 66–78. https://doi.org/10.1016/j.corsci.2018.06.042.

[58] B.K. Nandi, R. Uppaluri, M.K. Purkait, Effects of dip coating parameters on the morphology and transport properties of cellulose acetate-ceramic composite membranes, J. Memb. Sci. 330 (2009) 246–258.

https://doi.org/10.1016/j.memsci.2008.12.071.

[59] M. Changmai, M.K. Purkait, Detailed study of temperature-responsive composite membranes prepared by dip coating poly (2-ethyl-2-oxazoline) onto a ceramic membrane, Ceram. Int. 44 (2018) 959–968. https://doi.org/10.1016/j.ceramint.2017.10.029.

[60] S. Jana, M.K. Purkait, K. Mohanty, Clay supported polyvinyl acetate coated composite membrane by modified dip coating method: Application for the purification of lysozyme from chicken egg white, J. Memb. Sci. 382 (2011) 243–251. https://doi.org/10.1016/j.memsci.2011.08.011.

[61] B.K. Nandi, B. Das, R. Uppaluri, M.K. Purkait, Microfiltration of mosambi juice using low cost ceramic membrane, J. Food Eng. 95 (2009) 597–605. https://doi.org/10.1016/j.jfoodeng.2009.06.024.

[62] M. Changmai, M. Pasawan, M.K. Purkait, Treatment of oily wastewater from drilling site using electrocoagulation followed by microfiltration, Sep. Purif. Technol. 210 (2019) 463–472. https://doi.org/10.1016/j.seppur.2018.08.007.

[63] H. Abdallah, S.K. Amin, H.H.A. Almaged, M.F. Abadir, Fabrication of ceramic membranes from nano – rosette structure high alumina roller kiln waste powder for desalination application, Ceram. Int. 44 (2018) 8612–8622. https://doi.org/10.1016/j.ceramint.2018.02.077.

[64] V.K. Bulasara, H. Thakuria, R. Uppaluri, M.K. Purkait, Effect of process parameters on electroless plating and nickel-ceramic composite membrane characteristics, Desalination. 268 (2011) 195–203. https://doi.org/10.1016/j.desal.2010.10.025.

[65] Z. Yun-hua, G.A.N. Fu-xing, New Integrated Processes for Treating Cold-Rolling Mill Emulsion Wastewater, 17 (2010) 32–35. https://doi.org/10.1016/S1006-706X(10)60110-0.

[66] S. Ghafari, H. Abdul, M. Hasnain, A. Akbar, Application of response surface methodology (RSM) to optimize coagulation – flocculation treatment of leachate using poly-aluminum chloride (PAC) and alum, 163 (2009) 650–656. https://doi.org/10.1016/j.jhazmat.2008.07.090.

[67] V. Singh, M.K. Purkait, C. Das, Cross-Flow microfiltration of industrial oily wastewater: Experimental and theoretical consideration, Sep. Sci. Technol. (2011). https://doi.org/10.1080/01496395.2011.560917.

[68] S. Ghafari, H. Abdul, M.J.K. Bashir, The use of poly-aluminum chloride and alum for the treatment of partially stabilized leachate : A comparative study, DES. 257 (2010) 110–116. https://doi.org/10.1016/j.desal.2010.02.037.

[69] X. Cheng, Y. Gong, Treatment of oily wastewater from cold-rolling mill through coagulation and integrated membrane processes, (2018).

[70] L.H. Ã, G. Newcombe, Effect of NOM , turbidity and floc size on the PAC adsorption of MIB during alum coagulation, 39 (2005) 3668–3674. https://doi.org/10.1016/j.watres.2005.06.028.

[71] W. He, Z. Xie, W. Lu, M. Huang, J. Ma, Comparative analysis on floc growth behaviors during ballasted flocculation by using aluminum sulphate (AS) and polyaluminum chloride (PACl) as coagulants, Sep. Purif. Technol. 213 (2019) 176–185. https://doi.org/10.1016/j.seppur.2018.12.043.

[72] F. Mohammadi, T. Mohammadi, Optimal conditions of porous ceramic membrane synthesis based on alkali activated blast furnace slag using Taguchi method, Ceram. Int. 43 (2017) 14369–14379. https://doi.org/10.1016/j.ceramint.2017.07.197.

[73] C. Sarkar, J.K. Basu, A.N. Samanta, Microwave Activated LD Slag for Phenolic Wastewater Treatment: Multi-parameter Optimization, Isotherms, Kinetics and Thermodynamics, Chem. Eng. Trans. 57 (2017) 277–282.

https://doi.org/10.3303/CET1757047.

[74] Y.N. Dhoble, S. Ahmed, Treatment of wastewater generated from coke oven by adsorption on steelmaking slag and its effect on cementitious properties, Curr. Sci. 116 (2019) 1346–1355. https://doi.org/10.18520/cs/v116/i8/1346-1355.

[75] I. Netinger Grubeša, I. Barišic, A. Fucic, S.S. Bansode, Characteristics and uses of steel slag in building construction, 2016. https://doi.org/10.1016/c2014-0-03994-9.

[76] P. Chaurand, J. Rose, V. Briois, L. Olivi, J.L. Hazemann, O. Proux, J. Domas, J.Y. Bottero, Environmental impacts of steel slag reused in road construction: A crystallographic and molecular (XANES) approach, J. Hazard. Mater. 139 (2007) 537–542. https://doi.org/10.1016/j.jhazmat.2006.02.060.

[77] Z. Peng, L. Wang, F. Gu, H. Tang, M. Rao, Y. Zhang, G. Li, T. Jiang, Recovery of chromium from ferronickel slag: A comparison of microwave roasting and conventional roasting strategies, Powder Technol. 372 (2020) 578–584. https://doi.org/10.1016/j.powtec.2020.05.103.

[78] E. Kim, J. Spooren, K. Broos, P. Nielsen, L. Horckmans, K.C. Vrancken, M. Quaghebeur, New method for selective Cr recovery from stainless steel slag by NaOCl assisted alkaline leaching and consecutive BaCrO4precipitation, Chem. Eng. J. 295 (2016) 542–551. https://doi.org/10.1016/j.cej.2016.03.073.

[79] H.I. Gomes, V. Funari, W.M. Mayes, M. Rogerson, T.J. Prior, Recovery of Al, Cr and V from steel slag by bioleaching: Batch and column experiments, J. Environ. Manage. 222 (2018) 30–36. https://doi.org/10.1016/j.jenvman.2018.05.056.

[80] E. Kim, J. Spooren, K. Broos, L. Horckmans, M. Quaghebeur, K.C. Vrancken, Selective recovery of Cr from stainless steel slag by alkaline roasting-water leaching, Hydrometallurgy. 158 (2015) 139–148. https://doi.org/10.1016/j.hydromet.2015.10.024.

Chapter 2:

Separation of chloride and sulphate ions from nanofiltration rejected wastewater of steel industry

Chapter 2
Separation of chloride and sulphate ions from nanofiltration rejected wastewater of steel industry

This chapter discusses about the use of three different solvents for the removal of chlorides and sulphates from nanofiltration rejected stream generated from blast furnace unit of steel industry. Miscible organic solvents such as diisopropylamine (DIIPA), isopropylamine (IPA), and ethylamine (EA) was used in different proportions for precipitation. Response surface methodology (RSM) was applied to optimize the parameters for the removal of chloride and sulphate ions. Analysis of variance was used to study the incurred data. Four important parameters namely volume of the solvent, pH, temperature and contact time were optimized using central composite design (CCD). The precipitated salts were characterized by FESEM, XRD and FTIR analysis.

2.1. Experimental

2.1.1. Materials

Seawater used for coke quenching can be identified as an origin for diffusing chloride and sulphate into coke due to its porous structure. These ions diffused coke is used as a raw material for iron making process which increases the chloride and sulphate content of the flue gas discharge from blast furnace. Tata Steel, Jamshedpur (India) uses biochemical oxidation (BO) for the treatment of wastewater coming from coke oven by product. This is very effective for the removal of cyanide and phenol. The treated water after BO process contains

Content of this chapter is published as below:

- **Deepti,** A. Sinha, P. Biswas, S. Sarkar, U. Bora, M.K. Purkait, Separation of chloride and sulphate ions from nanofiltration rejected wastewater of steel industry, J. Water Process Eng. 33 (2020) 101108. https://doi.org/10.1016/j.jwpe.2019.101108.
- M K Purkait, **Deepti,** A Sinha, P. Biswas, S Sarkar, "Separation of ions from the rejected stream of industrial wastewater", Application Number: 201831044754. Date of filing: 27/11/2018. **Patent No. 358257, Granted on 11/02/2021.**

high chlorides, sulphates, fluorides and other ions which make it difficult to discharge to the environment. Hence the polluted water was treated via membrane filtration, with a particular emphasis on removal of ions. The rejected water from this unit was collected for the experiment for the treatment of chloride and sulfate ions.

The collected water was sealed and stored in a dark room at room temperature in order to avoid any compositional change by air oxidation with time. Organic solvents like isopropylamine (IPA), diisopropylamine (DIPA) and ethylamine (EA) with a 99% purity were purchased from Spectrochem Pvt.Ltd, Mumbai, India. Hydrochloric acid, sodium hydroxide, sodium chloride, potassium chloride, calcium chloride, iron chloride, magnesium chloride, manganese chloride are procurred from Merck (India). All chemicals used were utilized without any purification.

2.1.2. Analytical methods

Ion chromatography (Model: Metrohm ion analysis, 792 basic IC , Make: Metrohm Ltd, Herisau, . Column: Metrosep A Supp 5) was used to analyse chloride and sulfate ions. Atomic absorption spectrophotometer (AAS, make: M/s Varian, Netherland, model: Spectra AA 220 FS) was used to analyse iron, magnesium, manganese, sodium, potassium and calcium ions. Vacuum pump (Model VMS; Make: Axiva Sichem Biotech, India) was used for vacuum filtration unit. All the glasswares used in the experiments were supplied by Borosil, India. The pH, conductivity, TDS were measured using microprocessor water/soil analysis kit (Model: VSI-301, Make: VSI Electronics). Identification of functional groups were analysed using Fourier tranform infra-red spectroscopy (Model No.: IRAffinity-1; Make: M/s Shimadzu, Japan). X-Ray diffraction (Model No: D8 Advance, Make: Bruker, Netherlands) was conducted to assess the crystallinity of precipitated salts. The surface and morphological features of the precipitated salt was studied using field emission scanning

electron microscopy (FESEM, make: Zeises, model: Sigma). Energy dispersive X-ray spectroscopy (EDX) was used to determine the elemental information of the precipitated salt.

2.1.3. Experimental method

Nanofiltration (NF) rejected water and organic solvents in various proportion were well mixed in a ceramic vessel using agitator. The solvent to rejected water ratio, (VR) of 0 – 2.66 was considered which is calculated using Eqn. 2.1. For instance, volume of NF rejected water and solvent was considered in the range of 0.9 litres to 1.25 litres. The solution was mixed at 100 RPM for 1h at room temperature (25 ^{o}C). After 30 min, blending was ceased for another 30 min to complete precipitation of salts. The solution was filtered through nylon filter (pore size: 0.2 µm, diameter: 47 mm) using vacuum filtration set up to separate the salts from the solution. A vacuum pump of capacity 50 Hz, and flow rate of 15 L/min was used. The filtrate which was a mixture of organic solvent and water was sent to distillation unit (1 L capacity) to recuperate the solvent. The mixture of water and solvent was heated up to the boilling point of three solvents, separately. The distillate (organic solvent) was collected in a storing chamber for further use. Properties of the organic solvents like Diisopropylamine, Isopropylamine and Ethylamine is shown in **Table 2.1**. A detailed layout of experimental scheme is shown in **Fig. 2.1**. The efficiency of separation of both ions was measured in terms of percentage precipitation factor and calculated using Eqn. 2.2.

$$VR = \frac{\text{Volume of solvent}}{\text{volume of sample}} \qquad (2.1)$$

$$\%P = 1 - (\frac{Cf}{Ci}) \times 100 \qquad (2.2)$$

Where, % P is percentage precipitation factor, Cf is final anion concentration in the filtered sample and Ci is initial anion concentration in the NF rejected water.

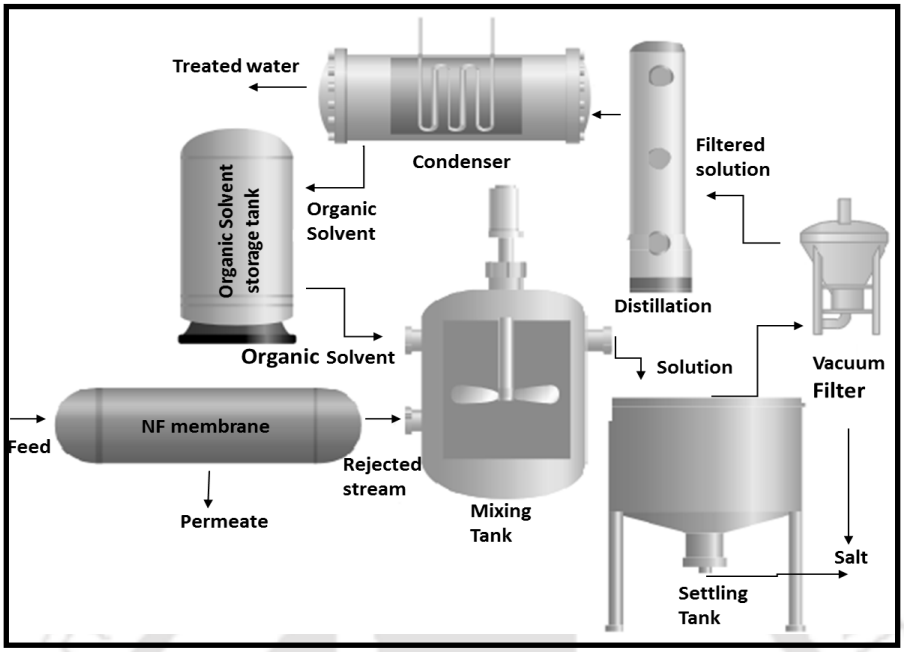

Fig. 2.1. Detailed layout of precipitation process

Table 2.1. Properties of miscible organic solvents [1]

Solvent	Diisopropylamine	Isopropylamine	Ethylamine
Formula	$[(CH_3)CH]_2NH$	$(CH_3)_2CHNH_2$	$C_2H_5NH_2$
Molecular weight (g/mol)	101.19	59.11	45.08
Color	Colourless	Colourless	Colourless
Specific gravity	0.722	0.694	0.689
Melting point (^oC)	-61	-101	-80.6
Boiling point (^oC)	83.5	34	16.6
Water solubility in 100 part	Soluble	Soluble	Soluble

2.1.4. Experimental design

Response surface methodology (RSM) is a collection of statistical and mathematical methods which assess the effect of different factors and their actions on the system response. One of

the main advantages of RSM is to develop and optimize the variables which results in less number of experimental runs. RSM is mainly focused on design of experiments, response surface modelling and optimization [2,3] . Central composite design (CCD) by design expert (version 11.0) was utilized with four different independent factors namely; volume ratio (VR: ratio of volume of solvent to volume of the NF rejected water) [x1], pH [x2], temperature [x3], and contact time [x4] with two dependent responses like percentage precipitation factor (% P) of chloride and sulphate. The volume ratio (VR) ranged from 0.33 to 2.67, pH of the sample varied from 2 to 10, temperature from 10 to 32 ^{o}C and that of contact time ranged from 10 to 30 min. **Table 2.2** shows the parameters and the range dealt by RSM. Eqn. 2.3 was used to show the interaction between the independent variable and dependent responses.

$$\gamma = b_0 + \sum_{i=1}^{k} b_1 X_1 + \sum_{I=1}^{K} b_{ii} X_i^2 + \sum_{i=1}^{k-1} \sum_{J=1}^{K} bi_j XiXj + C \qquad (2.3)$$

Where, b_0 is the value of the intercept, b_i, b_{ii}, b_{ij} are the regression coefficients for linear, second order and interactive effects, respectively. X_i, X_j refers to independent variables and C represents the error of prediction. The analysis of variance gives the information related to lack of fit, p value, F value and R^2 representing the efficiency of the model. “Prob F” less than 0.05 refers that the model terms are significant. Lack of fit more than 0.05 implies the validity of the model. The probability less than 0.05 implies the accuracy of the model.

Table 2.2. Level and ranges of the independent variables in CCD design

Independent variables	**Units**	**- 1 Level**	**+ 1 Level**	**- alpha**	**+ alpha**
V_R	-	0.91	2.08	0.33	2.67
pH	-	4	8	2	10
Temperature	^{o}C	15.5	26.5	10	32
Contact time	min	14.5	25.2	10	30

2.2. Results and discussion

This section is divided into five parts. In the first part, water quality parameters of the NF rejected water of TATA Steel Ltd., India was determined and reported. Variation of precipitation factor (% P) of chlorides and sulphates with VR using three solvents were studied and discussed in second part. The separation of chlorides and sulphates were done in terms of percentage precipitation factor which is calculated using Eqn.1. Third and fourth part deals with the Response surface methodology (RSM) to optimize the parameters for the removal of chloride and sulphate ions. Characterization of the precipitated salt is discussed in fifth part.

2.2.1. Characteristics of NF rejected water

Blast furnace wastewater contains high chlorides and sulfate ions along with other salts. Consequently, reusing without treatment makes the framework pipelines eroded. Along these lines, TATA Steel Ltd., India uses nanofiltration (NF) as tertiary treatment method for the blast furnace wastewater. However, the NF unit contributes to highly concentrated chlorides and sulfates along with different salts much higher than the permissible limit. This makes the rejected water unfit to either reuse or discharge to the streams. The characteristics of obtained NF rejected water was analysed and shown in **Table 2.3**. It is seen from the table that all the water quality parameters are well above the permissible limits especially chlorides and sulphates in the range of 1600 mg/L and 4200 mg/L, respectively. The total dissolved solids have very high value in the range of 8613 mg/L which is highly above the permissible limit (> 2000 mg/L). Similarly, sodium, potassium, calcium and iron are also above the permissible limit. The results after the treatment technique undertaken in this work is also shown in the table and discussed in subsequent sections.

Table 2.3. Characteristics of NF rejected water

Parameters	NF rejected water	After treatment	Permissible limit for surface water [4]
Chloride (mg/L)	1594	358	600
Sulphate (mg/L)	4196	8.4	400
Total dissolved solids (mg/L)	8613	785	2000
pH	8.1	7.25	9.0
Turbidity (NTU)	0.5	0.3	140
Sodium (mg/L)	650	142	200
Potassium (mg/L)	175	4	12
Calcium (mg/L)	183	51	200
Iron (mg/L)	38	4.2	3
Magnesium (mg/L)	198	122	150
Manganese (mg/L)	21	14	2

2.2.2. Precipitation of chlorides and sulphates by organic solvents

Three organic solvents such as diisopropylamine (DIPA), isopropylamine (IPA) and ethylamine (EA) were selected to separate chlorides and sulphates from NF rejected water mentioned in the preceding section. The properties of nanofiltration (NF) rejected water stream is shown in **Table 2.3**. Chloride and sulphate ion concentrations are well above the allowable limit of > 600 mg/l and > 400 mg/l, respectively [4]. Three solvents (IPA, DIPA and EA) were blended independently with NF rejected water. The solvent to rejected water volumetric proportion is named as VR. Experiments were done in room temperature with a blending and settling time of 10 and 30 min, respectively. The variation of precipitation factor with VR is shown in **Figs. 2.2a and 2.2b** for chloride and sulphate respectively, for three solvents considered here. From **Fig. 2.2a** it is seen that chloride precipitation factor increases sharply upto VR value of 1.25 and gradual thereafter. From the figure it may be seen that beyond the VR value of 3 the increase on precipitation factor will be marginal.

Again, precipitation is more for DIIPA that of EA is less for each value of VR. For example chloride precipitation is 80.46 %, 69.54 % and 67.65 % for DIIPA, IPA and EA respectively, for solvent to volume ratio (VR) of 2.67 (**Fig. 2.2a**).

Similar observation is also found for sulphate precipitation shown in **Fig. 2.2b**. However, the sharp increase is observed upto VR of 1.0 instead that of chloride at VR 1.25 and becomes gradual afterward.

From both **Figs. 2.2a and 2.2b**, it is seen that DIIPA shows highest precipitation factor (80% and 100% for chloride and sulphate respectively) followed by IPA and EA. The difference in extent (salt precipitation) capacity was due to the variation of hydrogen bonding capabilities of these three solvents. Soluble salts are salted out (precipitated) when water molecules are easily H-bonded with the amine based solvents and unavailable for salts for solvation. DIIPA has higher H-bonding capacity than that of for IPA and EA thereon. Therefore, extent of chloride and sulphate precipitation is observed in the order of DIIPA>IPA>EA depending on H-bonding capabilities [5]. Considering the operation point of view and boiling point (Table 1) IPA is the best choice [1]. Hence, IPA was chosen for the investigation of various factors influencing the precipitation and discussed in the subsequent sections.

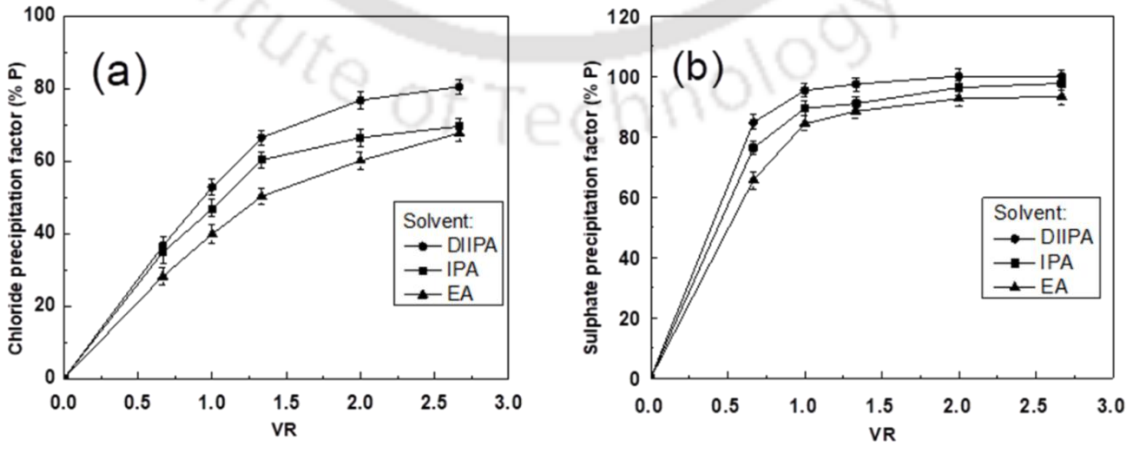

Fig. 2.2. Variation of precipitation factor (%P) with VR. a) For chloride precipitation, and b) for sulphate precipitation. Temperature: 25 ^{o}C and pressure: 1atm

2.2.3. CCD designed model and analysis of variance

Chloride and sulphate precipitation factor model is given by Eqns. 2.4 and 2.5, respectively. The experiments were carried with the volume ratio, VR (A) range from (0.33 – 2.67), pH range (B) from (2 – 10), temperature (C) from (10 – 32) ^{o}C and contact time (D) range from (10 – 30) min. A positive value of coefficient indicates a synergistic effect, and a negative value symbolizes an opposite effect [3].

Chloride precipitation factor (% P) = 76.68-3.04×A-0.91×B-3.82×C-
1.69×D+1.44×A×B+4.48×A×C+0.79×A×D+0.75×B×C-1.86×B×D-4.05 (2.4)
×C×D-2.25× A^2-5.03B^2×C^2-0.050×D^2

Sulphate precipitation factor (% P) = 98.44+0.73×A+0.040×B-0.064× (2.5)
C-0.50×D-0.18×A×B-0.46×A×C+0.65×A×D-0.12×B×C-0.35×B×D+
0.46×C×D+6.32×A^2-0.052×B^2+0.052×C^2+0.17×D^2

Where A, B, C and D are the coded values of variables namely volume ratio (VR), pH, temperature, (^{o}C), and time (min), respectively. Total of 30 experiments with 6 central points have been applied to study the effects of main four independent parameters viz. volume of the solvent, pH, temperature and contact time on chloride and sulphate precipitation. The responses were analysed and the results of ANOVA for precipitation of chlorides and sulphates are shown in **Table 2.4** and **Table 2.5**, respectively. The low probability with F value of 172.8 depicts that the model is accurate. Lack of fit (0.08) more than 0.05 shows that the model is valid. A high R^2 value of 0.99 with adjusted R^2 of 0.98 represents that the model is significant for the chloride precipitation. Similarly, F value about 18 with low probability implies that the model is accurate. Lack of fit (0.82) which is more than 0.05 illustrates that the model is valid. R^2 value of 0.98 represents the sulphate precipitation model is substantial.

Table 2.4. ANOVA result of response surface quadratic model for chloride precipitation

Source	Sum of Squares	df	Mean Square	F value	p-value Prob >F
Model	1661.2	14	118.6	172.8	< 0.0001
A-VR	147.9	1	147.9	215.4	< 0.0001
B-Ph	3.27	1	3.2	4.76	0.0454
C-Temperature	304.8	1	304.8	443.9	< 0.0001
D-Contact time	38.5	1	38.5	56.1	< 0.0001
AB	11.8	1	11.8	17.2	0.0008
AC	224.1	1	224.1	326.5	< 0.0001
AD	3.9	1	3.9	5.7	0.03
BC	4.7	1	4.7	6.8	0.01
BD	17.7	1	17.7	25.8	0.0001
CD	164.3	1	164.3	239.3	< 0.0001
A^2	117.4	1	117.4	171.0	< 0.0001
B^2	0.15	1	0.1	0.2	0.64
C^2	670.6	1	670.6	976.9	< 0.0001
D^2	0.05	1	0.05	0.08	0.77
Residual	10.3	15	0.69	--	--
Lack of Fit	9.0	10	0.91	3.70	0.08
Pure Eror	1.2	5	0.24	--	--
R^2	--	--	--	--	0.99
R^2_{Adj}	--	--	--	--	0.98
R^2_{Pred}	--	--	--	--	0.96
Adequate precision	--	--	--	--	58.6

Table 2.5. ANOVA for Response surface quadratic model for sulphate precipitation

Source	Sum of Squares	df	Mean Square	F value	p-value Prob >F
Model	25.7	14	1.8	18.1	< 0.0001
A-VR	8.4	1	8.4	83.2	< 0.0001
B-Ph	0.006	1	0.006	0.06	0.80
C-Temperature	0.085	1	0.08	0.84	0.37
D-Contact time	3.35	1	3.3	33.1	< 0.0001
AB	0.19	1	0.19	1.84	0.19
AC	2.33	1	2.33	22.9	0.0002

AD	2.67	1	2.67	26.3	0.0001
BC	0.13	1	0.13	1.2	0.27
BD	0.61	1	0.61	6.0	0.02
CD	2.1	1	2.1	20.7	0.0004
A^2	0.001	1	0.001	0.01	0.92
B^2	0.01	1	0.01	0.15	0.70
C^2	0.07	1	0.07	0.7	0.41
D^2	0.62	1	0.62	6.11	0.02
Residual	1.52	15	0.1	--	--
Lack of Fit	0.78	10	0.07	0.52	0.82
Pure Error	0.74	5	0.15	--	--
R^2	--	--	--	--	0.98
R^2_{Adj}	--	--	--	--	0.97
R^2_{Pred}	--	--	--	--	0.96
Adequate precision	--	--	--	--	54.8

2.2.4. Response surface methodology and 3D plotting

Effect of the dependent variables on the percent precipitation factor in 3D graph is shown in **Figs. 2.3 and 2.4** for chloride and sulphate, respectively. The interaction between VR - pH, VR -temperature, VR - contact time, pH - temperature, pH - contact time and temperature - contact time may be seen from these 2 figures. This also depicts the maximum (77.50 % Cl^- and 99.82 % SO_4^{2-}) and minimum (49.48 % Cl^- and 94.21 % SO_4^{2-}) precipitation factor obtained with above mentioned interactions. **Figs. 2.3 and 2.4** represents the higher value points towards the lower value points of the response for chloride and sulphate precipitation factor, respectively. **Fig. 2.3a** shows that the chloride precipitation factor increased with the increase in VR and pH. While from **Fig. 2.3b**, it is seen that the chloride precipitation was maximum (63.05 %) at the middle value of the design space. It can be clearly seen from **Figs.**

2.3c and 2.3e that the contact time does not have much of an impact on chloride precipitation factor with increasing VR and pH. Whereas, the temperature and dosage showed prominent impact on chloride precipitation factor. It may be concluded that 15 minute is the optimum mixing time for precipitating the chloride and sulphate salts in presence of IPA at increasing VR.

Similarly, from **Fig. 2.4a** it is seen that sulphate precipitation factor increases from 97% to 99% with increasing VR . **Fig. 2.4b** shows the effect of temperature and VR on sulphate precipitation factor. This plot shows that sulphate precipitation factor is maximum (98.5 %) at higher VR (2.08) and low temperature (15.50 ^{o}C). From **Fig. 2.4d,** it is seen that there is no much impact on sulphate precipitation factor with increasing temperature and pH. Therefore, the percentage chloride and sulphate precipitation factor is better at the midpoints of the limit as seen in **Figs. 2.3 and 2.4**, respectively.

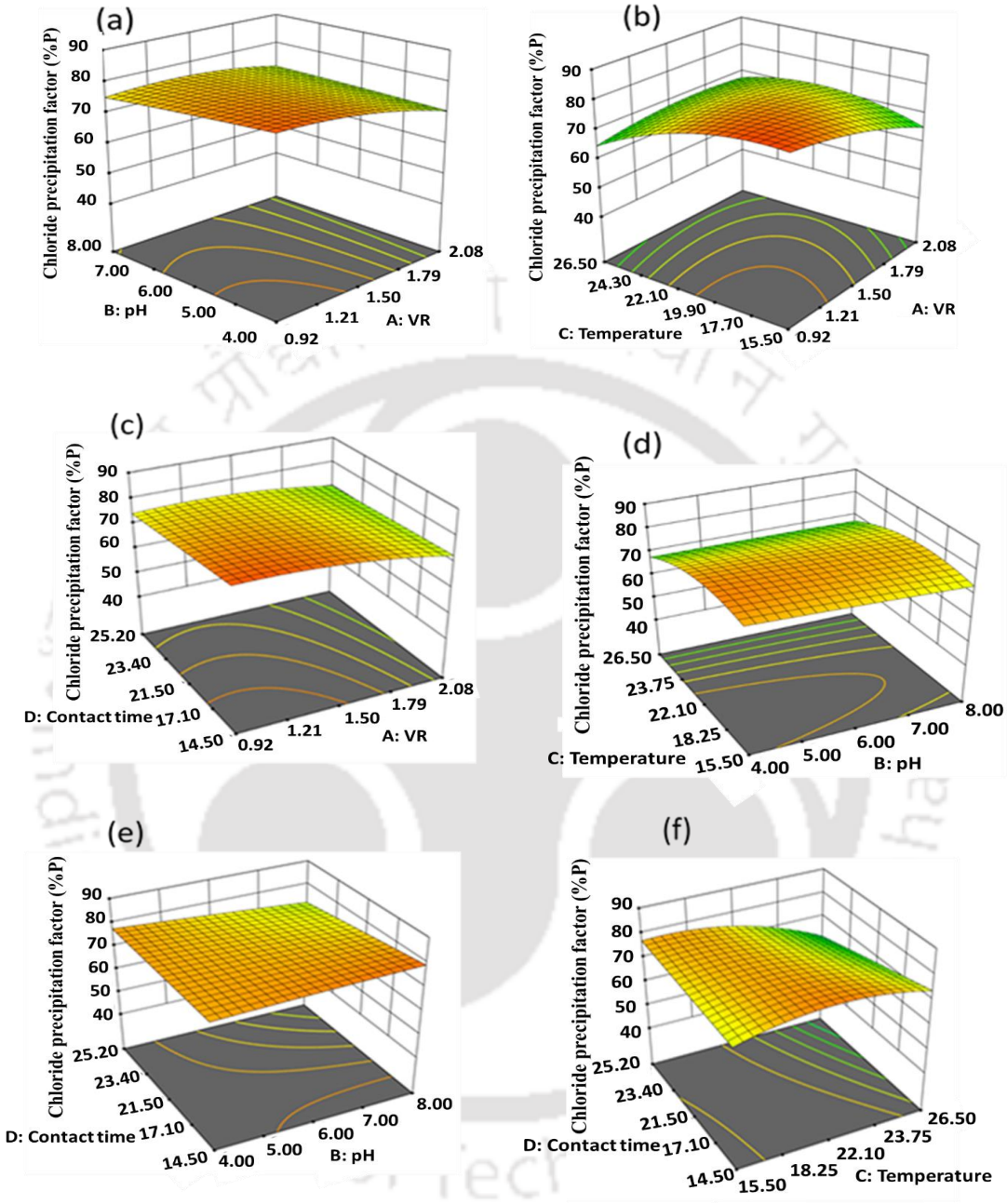

Fig. 2.3. Response surface graphs on chloride precipitation factor showing interactive effect between (a) VR and pH, (b) VR and temperature, (c) VR and contact time, (d) pH and temperature, (e) pH and contact time, and (f) temperature and contact time.

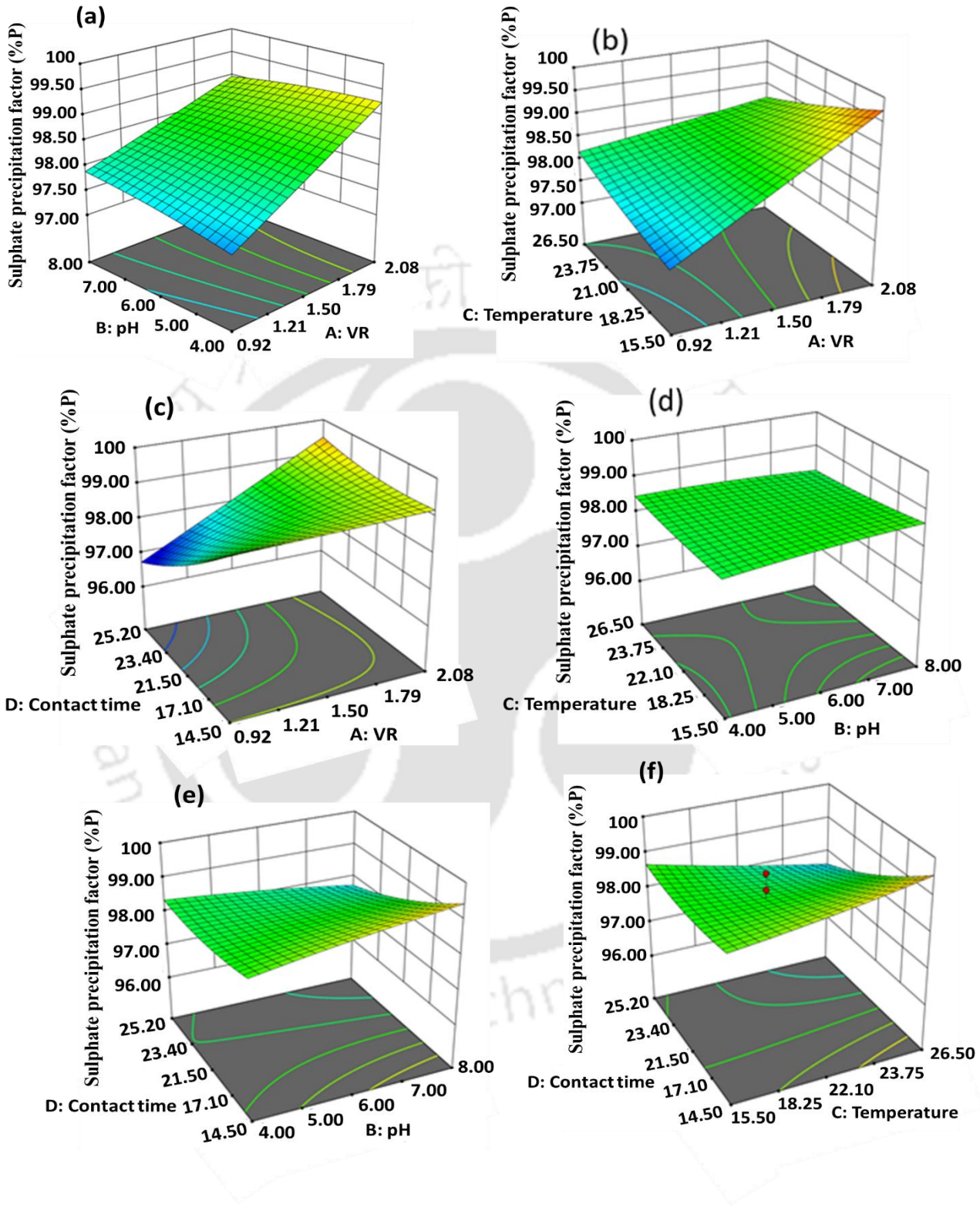

Fig. 2.4. Response surface graphs on sulphate precipitation factor showing interactive effect between (a) VR and pH, (b) VR and temperature, (c) VR and contact time, (d) pH and temperature, (e) pH and contact time, and (f) temperature and contact time.

2.2.5. Interaction studies using factors tool

Interaction study gives a clear picture of changes in precipitation factor with respect to the four parameters considered herein. Interaction study between pH and VR was carried with two pH, 4 and 8 with varying VR and keeping temperature and contact time at 21 ^{o}C and 20 min, respectively. From **Fig. 2.5**, two things can be inferred. Firstly, when the pH of the sample was maintained at 4, the chloride precipitation is higher (80%) at lower VR (0.92). However, as VR was increased, chloride precipitation factor gradually decreased to 72%. On the other hand, at pH 8, chloride precipitation factor was 74.5% and was steady till VR 1.50 and decreased thereafter. Secondly, at pH 4, there is a drastic decrease in chloride precipitation factor but at pH 8 there is no much decrease in precipitation factor with varying VR. This fact would indicate that the chloride ion removal is better when the sample pH is kept in its original (8.1) as shown in **Table 2.3**.

In **Fig. 2.5b,** it is seen that chloride precipitation factor is decreasing gradually from 82.2 % to 65 % at 15 ^{o}C. Whereas at 26.5 ^{o}C, chloride precipitation factor increased from 64 % to 68 % as VR is increased. This fact is advantageous as the temperature is near about room temperature, and precipitation is higher at this temperature, hence there is no need of extra energy which directly favours in terms of cost efficiency. Likewise, in **Fig. 2.5c**, it is seen that chloride precipitation factor shows a decreasing trend with respect to increasing VR when contact time is at 14.5 min and 25.2 min.

In case of interaction study of parameters of sulphate precipitation factor, the trend is exactly opposite to the chloride precipitation factor, which is seen in **Fig. 2.6**. In **Fig. 2.6a**, it is seen that sulphate precipitation factor increases from 97.15 % to 99.25 % and 97.9 % to 98.5 % with increase in VR for both pH 4 and 8, respectively.

In **Fig. 2.6b**, it is seen that at 15 ^{o}C and 26 ^{o}C, sulphate precipitation factor increases sequentially with increasing VR. However, sulphate precipitation factor is highest (99.55 %) when temperature is maintained at 15 ^{o}C. This indicates that sulphate ions are less soluble than chloride at lower temperature.

It may be seen from **Fig. 2.6c** that at 14.5 min of contact time, sulphate precipitation factor remain almost constant at 99.25 % with increase in VR. At 25.2 min, sulphate precipitation factor increases drastically from 97.3 % to 99.7 % as VR is increased from 0.92 to 2.09. Therefore, it may be concluded that, contact time beyond 14.5 min imparts better sulphate precipitation factor.

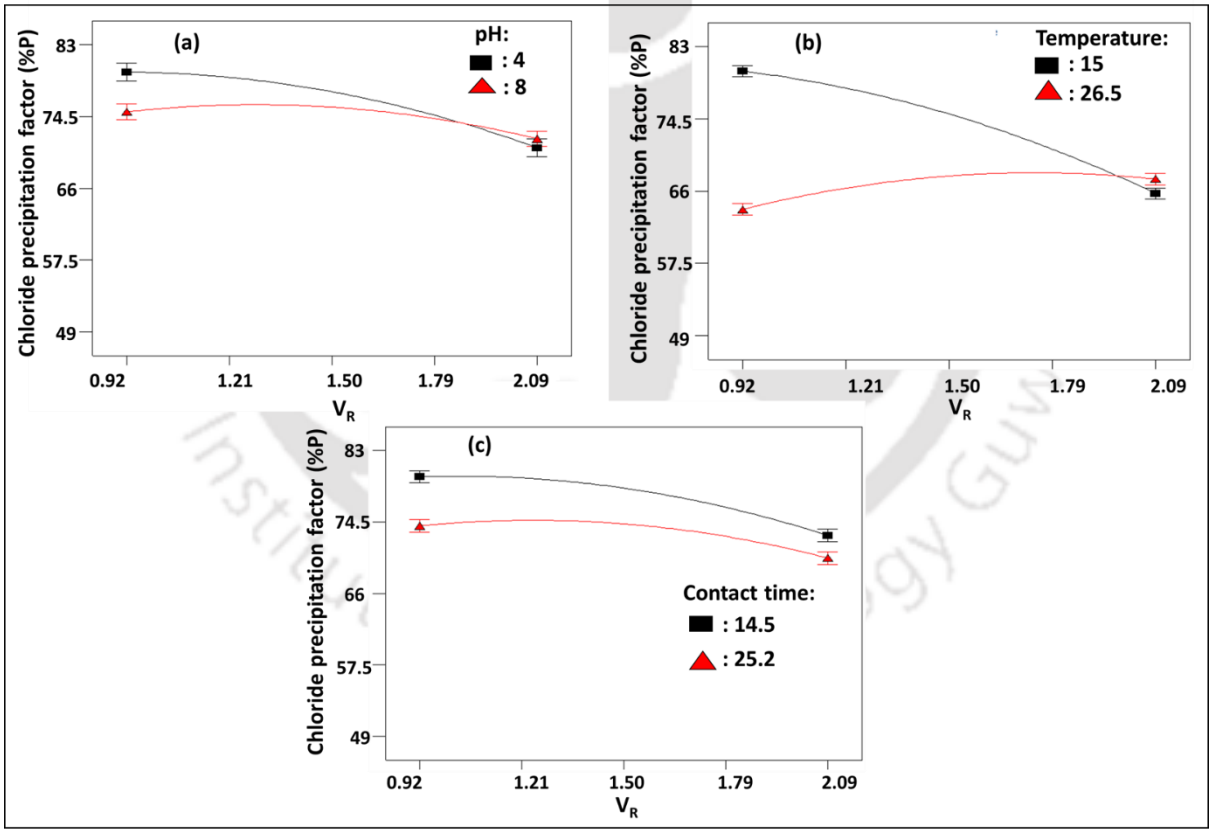

Fig. 2.5. Interactive effect of chloride precipitation factor with. a) pH - VR b) Temperature – VR and c) contact time – VR

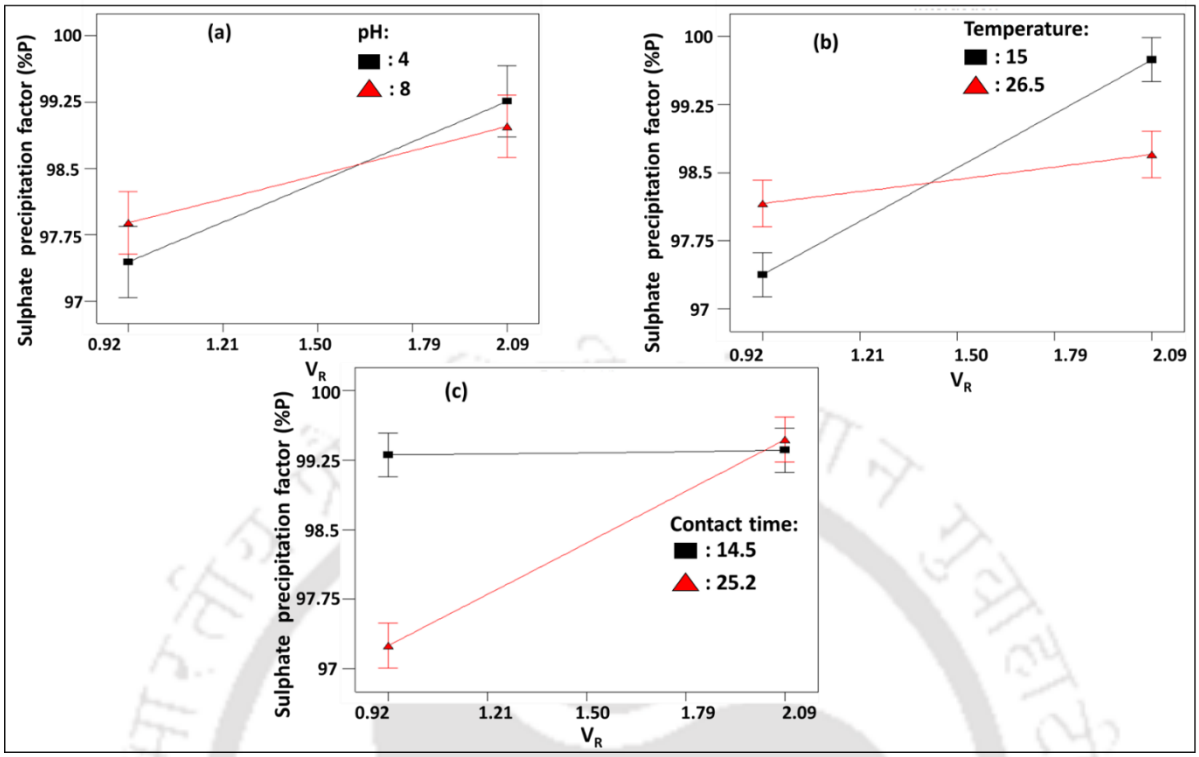

Fig. 2.6. Interactive effect of sulphate precipitation factor with. a) pH - VR b) Temperature – VR and c) contact time – VR

There are limited works focusing on the separation of chloride and sulphate ions from wastewater especially from NF rejected saline water. A comparative study of literatures with the present study is shown in **Table 2.6** [6–10] . From the table, it is envisaged that the use of miscible organic solvents are scant for the separation of chloride and sulphate ions from the industrial effluents. In this context, the present study is advocated to investigate performance of IPA, DIIPA and EA for the separation of chloride and sulphate ions from NF rejected saline water, which highlights the uniqueness of this work.

Table 2.6. Various literatures on separation of chloride and sulphate ions using carious reagents

Method	Reagent	Target	Salt precipitation (%)	References
Precipitation	Barium chloride	Sulphate ion (Pigment industry wastewater)	SO_4^{2-} = 100	[2]
Precipitation	Isopropylamine	chloride and sulphate ions (Synthetic wastewater)	cl^- = 59 SO_4^{2-} = 99	[6]
Precipitation	Dimethylisopropylamine	Sodium chloride (Synthetic wastewater)	-	[7]
Ion exchange	Dowex A-1 and Chelax-100	Chloride, Thallium (Zinc industry wastewater)	cl^- = 60 TI = 97	[8]
Precipitation	Magnesium	Sulphate ion (Synthetic wastewater)	SO_4^{2-} = 99	[9]
Adsorption	Rice straw	Sulphate ion (Synthetic wastewater)	-	[10]
Precipitation	Diisopropylamine Isopropylamine Ethylamine	Chloride and sulphate ions (NF rejected wastewater of steel industry)	cl^- = 81 SO_4^{2-} = 100 cl^- = 70 SO_4^{2-} = 97 cl^- = 68 SO_4^{2-} = 93	**Present work**

2.2.6. Process optimization by desirability function

A desirable value for every input and all the responses were chosen by using numerical optimization. To set an output value for the given conditions, the range of the inputs and target of the responses were considered [11]. The goals for all the inputs were selected "in range" and "maximum" for the responses. The maximum attained percentage chloride and sulphate precipitation factor was obtained at 77.50 % and 99.82 % respectively, at VR of 1.02, pH of 8, temperature at 23.39 ^oC and contact time of 26 min. Validation was confirmed

by carrying out the experiments at the optimized conditions given by the software. The confirmatory experiments depicted percentage chloride and sulphate precipitation factor of 74.50% and 97.6 %, respectively. This suggests that the model is accurate and valid.

2.2.7. Recovery of the solvent

The organic solvents used for the precipitation should have favourable physical properties when recovery is considered. As discussed in table 1, the boiling point of IPA is very low which favours in recovering the solvent from the solution. 96 % - 98 % of isopropylamine (IPA) was recovered using simple distillation. However, 2 – 4 % loss was seen due to evaporation during the operation. This loss may be avoided by state of art distillation facilities. Traces of IPA in the filtered sample was eliminated by simple aeration.

2.3. Characterization of precipitated salt

2.3.1 Field emission scanning electron microscopy

Field emission scanning electron microscopy (FESEM) was performed to analyse the surface morphological features of the obtained precipitated salt as shown in **Figs. 2.7a and 2.7b**. It is seen from **Fig. 2.7b** (higher magnification) that the salts are aggregated by nature. This is due to the presence of mixture of inorganic salts. The quantitative analysis of the salt sample by measuring the elemental composition for every species in the sample was performed using EDX. **Fig. 2.7c** depicts that the precipitated salt contains cations like magnesium, calcium, sodium, iron, potassium which possibly combine with chloride and sulphates to form their respective salts. The presence of chlorine and sulphur makes it evident for the presence of chloride and sulphates.

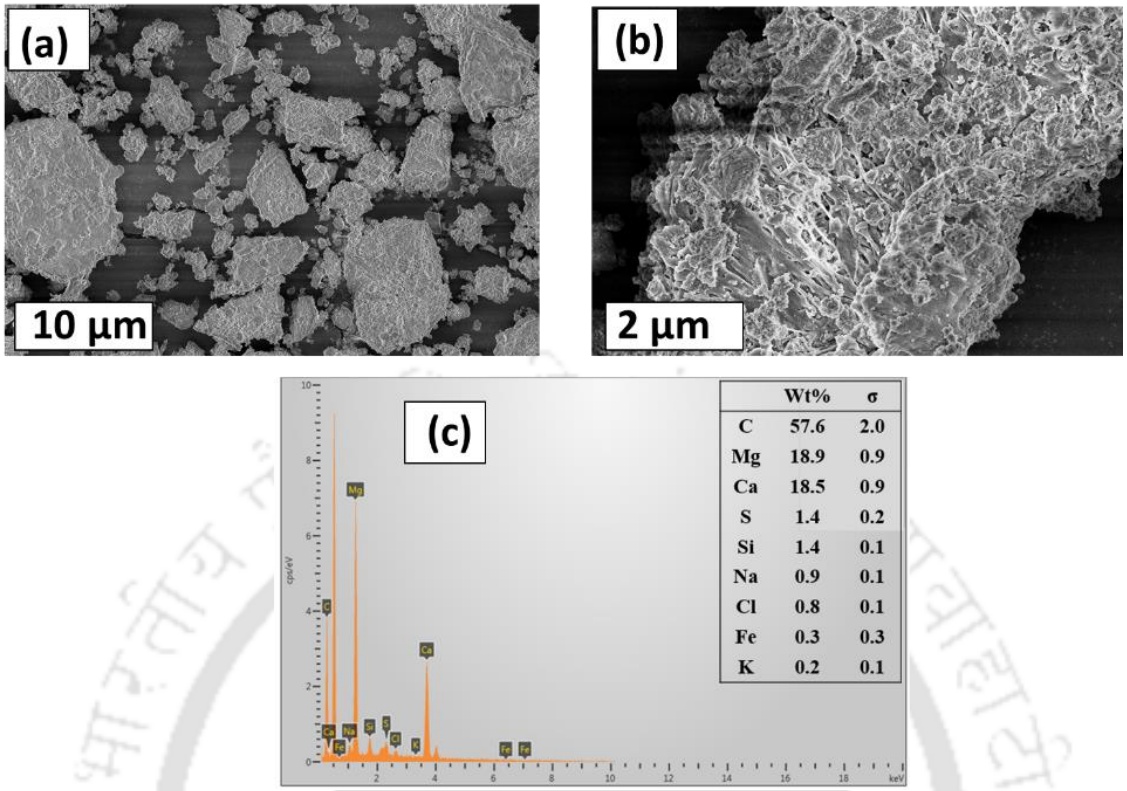

Fig. 2.7. Characterization of precipitated salt. a) and b) FESEM images, c) EDX analysis result

2.3.2. X- Ray diffraction

X- Ray diffraction (XRD) analysis of precipitated salt was performed and is shown in **Fig. 2.8**. The 2θ value at 31° and 45° predominantly show the presence of sodium chloride (NaCl) [12]. Similarly, 30° and 43.4°depicted the presence of magnesium chloride ($MgCl_2$) and calcium sulphate ($CaSO_4$), respectively [13,14]. It is also observed from **Fig. 2.7** that the salts are agglomerated by nature and crystalline in structure. Crystallinity was confirmed by X-ray diffraction (XRD) analysis. This is because of the presence of inorganic salt mixtures, as ensured from the EDS qualitative analysis. Thus the results confirm that the chloride and sulphate is been salted out with the available cations present in the solution.

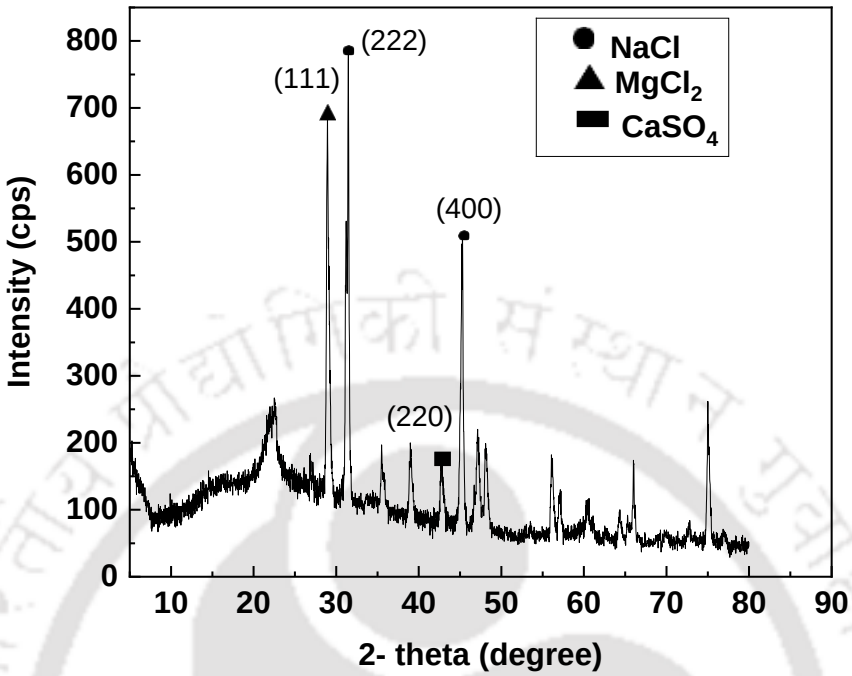

Fig. 2.8. XRD analysis of precipitated salt

2.3.3. Fourier transform infrared spectroscopy

Fourier transform infrared spectroscopy (FTIR) of precipitated salt was carried out between 500 and 4000 cm^{-1}. The spectra obtained is shown in **Fig. 2.9**. Precipitated salt showed inorganic sulphates like calcium sulphate, sodium sulphate and potassium sulphate in the range of 1000 to 1110 cm^{-1}. In addition, peaks around 3694 cm^{-1} and 3377 cm^{-1} showed N-H stretching. This might be due to the presence of trace amount of IPA within the precipitated salt. It is to be noted here that inorganic chlorides will not produce any vibrations as their lattice vibrations are beyond IR range [15].

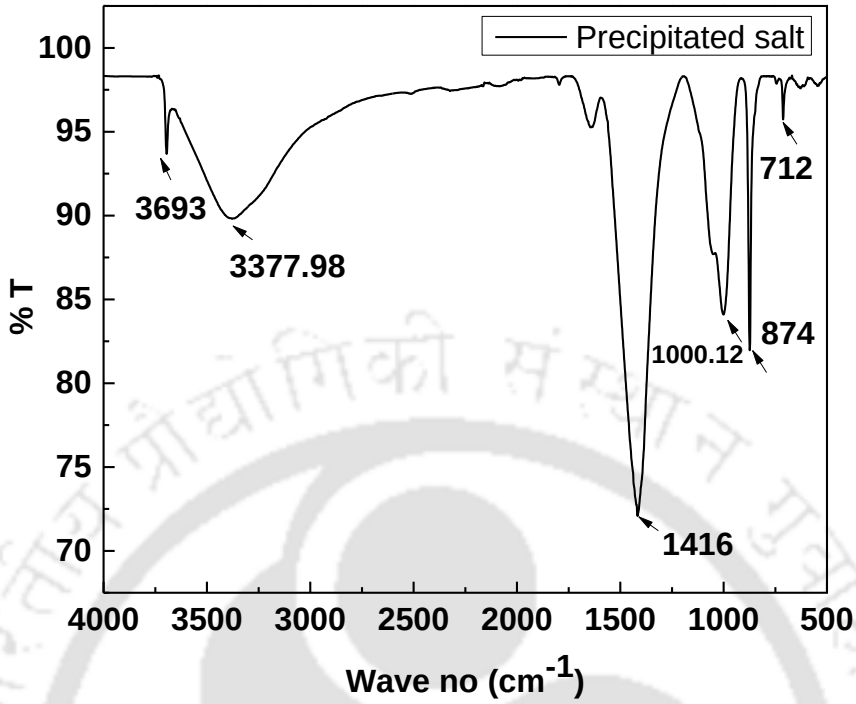

Fig. 2.9. FTIR analysis of precipitated salt.

Summary

The separation of chlorides and sulphates from NF rejected effluent from the steel industry was accomplished using organic solvents such as DIIPA, IPA, and EA. Based on the solventing out phenomena, the chloride and sulphate salts were precipitated in the presence of miscible organic solvents. The degree of chloride and sulphate precipitation is seen in the following order: DIIPA>IPA>EA. The precipitation factor increased as the volume ratio increased (VR). Based on the results of the design experiments, it can be inferred that increasing VR and pH and temperature have little effect on both chloride and sulphate precipitation factor. However, temperature and dose had a significant influence on the chloride precipitation factor.

Reference

[1] D. Perry, R. and Green, Perry's Chemical Engineer's Handbook, 1984. https://doi.org/10.1036/0071511253.

[2] D. Navamani Kartic, B.C.H. Aditya Narayana, M. Arivazhagan, Removal of high concentration of sulfate from pigment industry effluent by chemical precipitation using barium chloride: RSM and ANN modeling approach, J. Environ. Manage. 206 (2018) 69–76. https://doi.org/10.1016/j.jenvman.2017.10.017.

[3] P. Mondal, M.K. Purkait, Green synthesized iron nanoparticles supported on pH responsive polymeric membrane for nitrobenzene reduction and fluoride rejection study: Optimization approach, J. Clean. Prod. 170 (2018) 1111–1123. https://doi.org/10.1016/j.jclepro.2017.09.222.

[4] Usepa, Development document for final effluent limitations guidelines and standards for the iron ans steel manufacturing point source category, Response. (2002) 1062.

[5] I.. Finar, I.L Finar-Vol 1.pdf, (n.d.).

[6] M.S.H. Bader, Precipitation and Separation of Chloride and Sulfate Ions from Aqueous Solutions: Basic Experimental Performance and Modelling, Environ. Prog. 17 (1998) 126–135. https://doi.org/10.1002/ep.670170220.

[7] T.G. Zijlema, H. Oosterhof, G.J. Witkamp, G.M. Van Rosmalen, Crystallization of Sodium Chloride with Amines as Antisolvents, (1997) 230–241.

[8] H. Li, Y. Chen, J. Long, D. Jiang, J. Liu, S. Li, J. Qi, P. Zhang, J. Wang, J. Gong, Q. Wu, D. Chen, Simultaneous removal of thallium and chloride from a highly saline industrial wastewater using modified anion exchange resins, J. Hazard. Mater. 333 (2017) 179–185. https://doi.org/10.1016/j.jhazmat.2017.03.020.

[9] W. Dou, Z. Zhou, L.M. Jiang, A. Jiang, R. Huang, X. Tian, W. Zhang, D. Chen, Sulfate removal from wastewater using ettringite precipitation: Magnesium ion

inhibition and process optimization, J. Environ. Manage. 196 (2017) 518–526. https://doi.org/10.1016/j.jenvman.2017.03.054.

[10] W. Cao, Z. Dang, X.-Q. Zhou, X.-Y. Yi, P.-X. Wu, N.-W. Zhu, G.-N. Lu, Removal of sulphate from aqueous solution using modified rice straw: Preparation, characterization and adsorption performance, Carbohydr. Polym. 85 (2011) 571–577. https://doi.org/10.1016/j.carbpol.2011.03.016.

[11] M. Dastkhoon, M. Ghaedi, A. Asfaram, M.H. Ahmadi Azqhandi, M.K. Purkait, Simultaneous removal of dyes onto nanowires adsorbent use of ultrasound assisted adsorption to clean waste water: Chemometrics for modeling and optimization, multicomponent adsorption and kinetic study, Chem. Eng. Res. Des. 124 (2017) 222–237. https://doi.org/10.1016/j.cherd.2017.06.011.

[12] R. Boopathy, G. Sekaran, Studies on process development for the separation of sodium chloride from residue after evaporation of reverse osmosis reject solution, Sep. Purif. Technol. 183 (2017) 127–135. https://doi.org/10.1016/j.seppur.2017.04.008.

[13] Z. Zhang, X. Lu, F. Pan, Y. Wang, S. Yang, Preparation of anhydrous magnesium chloride from magnesium chloride hexahydrate, Metall. Mater. Trans. B Process Metall. Mater. Process. Sci. 44 (2013) 354–358. https://doi.org/10.1007/s11663-012-9777-5.

[14] E.P. Favvas, K.L. Stefanopoulos, N.C. Vordos, G.I. Drosos, A.C. Mitropoulos, Structural characterization of calcium sulfate bone graft substitute cements, Mater. Res. 19 (2016) 1108–1113. https://doi.org/10.1590/1980-5373-MR-2015-0670.

[15] J.. Derrick, M.R., Stulik, D. and Landry, Scientific tools for conservation: Infrared spectroscopy in conservation science, 1999. https://doi.org/10.1002/9781118162897.ch5.

Chapter 3:

Integrated technique for the treatment of highly saline nanofiltration rejected stream of steel industry

Chapter 3

Integrated technique for the treatment of highly saline nanofiltration rejected stream of steel industry

In this study, an integrated technique of closed circuit reverse osmosis (CCRO) and solvent-based precipitation was used to treat concentrated nanofiltration reject. The performance of the membrane, factors affecting precipitation and to scrutinize whether the proposed design benefit in reducing the brine concentration to benefit the steel industry for better management of the rejected stream of NF process is investigated. The used membranes and precipitated salts were imaged by the FESEM. The corresponding EDS spectra were taken to reveal the morphology of the membrane surfaces and compare them with that of the used membrane. Finally, a preliminary economic assessment was carried out for the integrated process. Reverse osmosis system analysis (ROSA 7.0 - FilmTec's) software, was used to estimate the water production cost, common technical assumptions, design parameters and specifications for the RO system.

3.1. Experimental

3.1.1. Materials

Wastewater from the blast furnace unit steel industry is rich in high dissolved solids, suspended particles and ions. Water is usually treated using nanofiltration (NF) for the removal of ions. The rejected part of this system discharged is highly concentrated brine. For the present study, water from this stage was collected from NF plant of Tata Steel Ltd located in Haldia, West Bengal, India. To avoid any photochemical reactions over time, the water was kept fully airtight and at room temperature in a dark room. Sodium hydroxide, chloride salts of manganese, sodium, potassium, iron and magnesium and hydrochloric acid are

Content of this chapter has been submitted for publication as below:

- Deepti, U. Bora, M.K. Purkait, Promising integrated technique for the treatment of highly saline nanofiltration rejected stream of steel industry, J. Environ. Manage. 300 (2021) 113781. https://doi.org/10.1016/j.jenvman.2021.113781.

purchased from Merck (India). Isopropylamine (IPA), diisopropylamine (DIIPA) and ethylamine (EA) was purchased from Spectrochem Pvt.Ltd, Mumbai, India, with a purity of 99 %. RO membranes (BW60) were supplied by Dow FilmTec, membrane type: Polyamide thin-film composite membrane, maximum operating temperature (45ºC), maximum operating pressure (10 bar), pH range, Continuous operation 2-11. Chemicals used in the experiments were without any further purification.

3.1.2. Analytical methods

Chloride and sulphate ions were analyzed using ion chromatography (Column: Metrosep A Supp 5, Model: Metrohm ion analysis, 792 basic IC, Make: Metrohm Ltd, Herisau,). The concentrations of iron, sodium, magnesium, potassium, manganese and calcium ions were determined using atomic absorption spectrophotometer (AAS, make: M/s Varian, Netherland, model: Spectra AA 220 FS). Water analysis microprocessor kit (Model: VSI-301, Make: VSI Electronics) was used to measure TDS, pH and conductivity of the feed water. A vacuum pump (Model VMS; Make: Axiva Sichem Biotech, India) was used for the vacuum filtration unit.

Gas chromatograph (make: Thermo Electron Corp, Italy, model: Ultra GC T100) equipped with a flame ionization detector (FID) was used for composition analysis of organic solvent in water. Glasswares used in the experiments were supplied by Borosil, India. The surface morphological features of the membranes and precipitated salt was studied using field emission scanning electron microscopy (FESEM, make: Zeises, model: Sigma). Energy-dispersive X-ray spectroscopy (EDS) was used to determine the elemental information of the salt precipitated. Samples were dried in a desiccator and sputtered with gold before EDS analysis.

3.1.3. Experimental procedure

Experiments were conducted on a bench scale integrated reverse osmosis using CCRO cross-flow system and precipitation unit. **Fig. 3.1** shows a schematic diagram of the lab-scale integrated set-up. Commercial RO membranes (Filmtec BW60) were used for this study. Membranes were stored in DI water for a minimum of 24 h before the experiment. Pressure gauge was used to measure the pressure gradient and valves (CV1, CV2 and CV3) were used to control the pressure gradient and flow rate, as shown in **Fig. 3.1**. The booster pump enables acceptable flow rates through RO. Flow-through the membrane cell was at the rate of 42 L/h, and transmembrane pressure was varied up to 7 bars (in the range of low-pressure RO). Conductivity and TDS measurements of feed, permeate and concentrate were carried out using portable pH/TDS/EC meter (make: HANNA instruments, model: HI9810-6) calibrated prior to run. CCRO is a continuous batch process that works by recirculating brine until any coveted recovery level is attained. The initial pressure of each cycle is very low (above the osmotic pressure of the feedwater) and the maximum pressure is above the osmotic pressure of the final brine. Pre-treated water reaches the primary inlet of the RO. The lower salinity feed and the recirculating brine were continually mixed. Fresh feed dilutes the recycled brine over time, resulting in minimum energy consumption. The average osmotic pressure compared to the RO batch increases with this mixing with higher water recoveries. The membranes were initially compacted at high pressure up to 15 bars by DI water until a steady flux was obtained. Samples were collected from permeate and rejected stream at every 5 min of interval for analysis. The performance of the RO system is estimated as permeate flux, salt rejection in terms of total dissolved solids and water recovery which is been calculated using Eqns. 3.1, 3.2 and 3.3, respectively.

$$J = \frac{Q}{A\Delta t} \qquad (3.1)$$

Where, Q is the volume of permeated water (L), A is the effective membrane area (m^2) and Δt is the sampling time (h).

$$\% \text{ Salt rejection} = \frac{\text{Feed}_{\text{Conc}} - \text{Permeate}_{\text{Conc}}}{\text{Feed}_{\text{Conc}}} \times 100 \qquad (3.2)$$

$$\% \text{ water recovery} = \frac{F_f - C_f}{F_f} \times 100 \qquad (3.3)$$

Where, F_f is the feed flow (litres per min) and C_f is the concentrate flow (litres per min).

In addition, the flux recovery ratio (FRR) was determined when the fouled membrane was rinsed and washed with distilled water for 10 min. The flux recovery ratio (FRR) was calculated by Eqn. 4, where J_1 is the pure water flux before fouling and J_2 is the pure water flux after fouling.

$$\text{FRR} = \frac{J_2}{J_1} \times 100 \qquad (3.4)$$

The reject collected after 2 h was sent to the second system, i.e, the precipitation unit. The system adopted here is from an approach described in our previous work [1]. Concentrated brine from RO process was sent to mixing tank, where the brine (from RO process) was blended with the organic solvent (DIIPA, IPA and EA) using an agitator, considering the solvent to rejected water ratio as VR = 0 - 1.4. The volume ratio (VR) for the precipitation process was calculated by Eqn. 2.1.

The solution was mixed at 24 ºC for 10 min at 100 RPM, then stopped mixing and allowed the salts to settle for another 30 min. The solution was filtered by a vacuum filtration system unit (0.2 µm size nylon filter). The filtrate was sent to the distillation and condensation unit wherein the organic solvents were heated up to their boiling points. The distillate was then collected and stored for further use. The efficiency of the precipitation system is measured based on the precipitation factor that is calculated by Eqn. 2.2, where, P is the precipitation factor, Ci and Cf is the initial and final concentration (ppm) of anion in the filtered sample and RO rejected water, respectively.

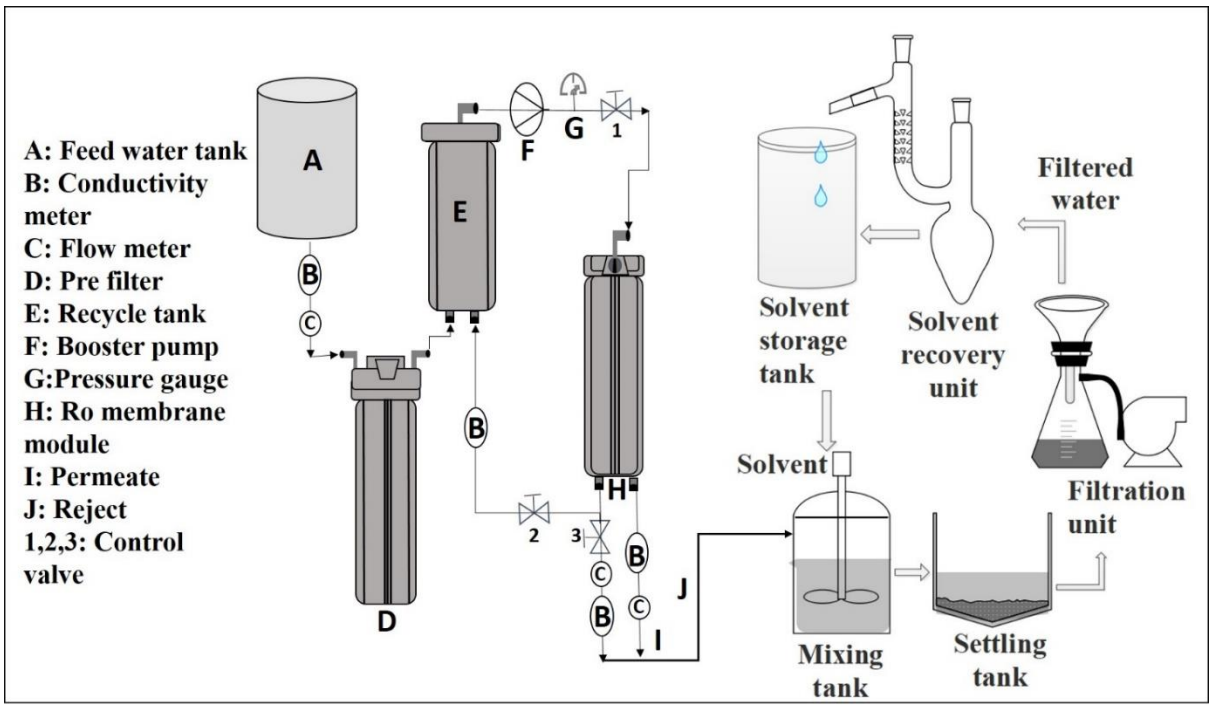

Fig. 3.1. Schematic representation of integrated RO-Precipitation set

3.2. Results and discussion

3.2.1. Quality of feed water

Nanofiltration (NF) is been used as a tertiary treatment system for the blast furnace (BF) wastewater in TATA Steel Ltd., India, which is one of the leading steel industries in the world. NF rejected stream contributes high concentrated salts, particularly chlorides and sulphates much higher than the required desirable limit. Utilization of sea water for coke quenching is identified as the main source for such highly concentrated chloride and sulphate ions. Consequently, the concentrated water cannot be reused or discharged into water bodies. The properties of nanofiltration brine were analysed and shown in **Table 3.1**. All the water quality parameters, such as TDS, chlorides, sulphates, sodium, magnesium, manganese, and other salts, are well above the permissible limit, as shown in the table, which makes them

necessary to treat before reuse or discharge. Results after the integrated methods adopted in this work are also shown in the table and discussed in successive sections.

Table 3.1: Characteristics of feed and treated water

Parameters	NF rejected water	RO Retentate	After precipitation of RO retentate	Permissible limit for surface discharge (EPA)
Chloride (mg/L)	1560	6210	156	600
Sulphate (mg/L)	4212	16800	0.9	400
Total dissolved solids (mg/L)	8100	30305	1316	2000
pH	8.2	7.85	7.5	9.0
Turbidity (NTU)	0.4	0.9	0.2	140
Sodium (mg/L)	418	1600	191	200
Potassium (mg/L)	266	1011	19	12
Calcium (mg/L)	274	1002	206	200
Iron (mg/L)	40	157	2	3
Magnesium (mg/L)	282	1108	132	150
Manganese (mg/L)	28	98	0.9	2

3.2.2. Permeate flux and salt rejection

Vital output parameters of a reverse osmosis (RO) process are permeate flux and salt rejection efficiencies. Flux and rejection are fundamental properties of membrane efficiency under reference conditions like temperature, pressure and feed composition. **Fig. 3.2** represents flux and salt rejection behaviour of RO membrane considered herein with increase in operating time at a feed pressure of 7 bar. After 20 min, the flux decreased sharply from 11 L/m^{2}h to 8 L/m^{2}h and then marginally decreased to 7 L/m^{2}h after 30 min. It is envisaged from the figure that flux decreases sharply in the beginning and gradually thereafter. This may be explained by the phenomenon of concentration polarization (CP). Concentration on the membrane surface keep increasing due to CP. As a result, the effective driving force

decreases due to an increase in osmotic pressure (approximately 3.70 bar) over the membrane surface. Initially, the permeate concentration increases swiftly, thus resulting in a sharp decrease of flux. Permeate flux reduces as feed concentration rises. The gradual decrease in flux was due to the formation of an unaltered polarized boundary layer over the membrane surface. A similar phenomenon is also explained and reported by [2] during the nanofiltration of textile effluent.

The variation of % salt rejection with time is presented in **Fig. 3.2**. At a pressure and temperature of 7 bar and 23 ºC. The time-dependent rejection was decreased sharply from 97 % to 91 % and gradually thereafter. The rapid decrease in rejection of salt with time is because of the formation of a dynamic CP layer on the membrane surface. The gradual decrease in salt rejection was because of the fact that the flux due to backward diffusion from the membrane surface into the bulk solution becomes vying with the convective flux through the membrane as operations are extended. Similar rejection profiles have also been reported by [3], for salt rejections and [4] during NF and RO of leather plant effluent.

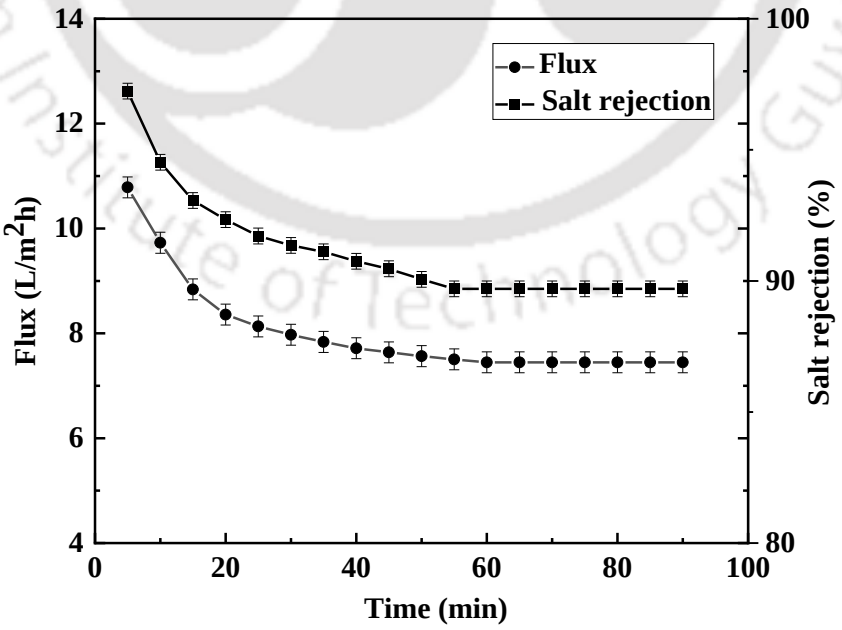

Fig. 3.2. Variation in water flux and salt rejection of RO membrane. Pressure: 7 bar, temperature: 24 ºC and initial TDS: 8100 mg/L

3.2.3. Permeate flux and water recovery

Water flux and water recovery with increasing feed concentration are shown in **Fig. 3.3**. It can be seen from **Fig. 3** that permeate flux is sharply decreasing from 10 L/m^{2}h to 7 L/m^{2}h and gradually thereafter with increasing feed concentration. From **Fig. 3.3 (insert),** the permeate flux is decreasing over time. At constant operating pressure, the permeate flux meets the optimal patterns for different feed concentrations, i.e. flux decreases as feed concentration increases. As feed concentration increases, concentration polarization (CP) increases as well. As a result, the osmotic pressure at the membrane increases. As a result, permeate flux declines sharply with feed concentration. The flux at the end of the process is reduced about 16 % from its initial value with a feed concentration of 8100 mg/L as shown in the figure. At higher feed concentrations, solute formation on the membrane surface is greater, resulting in a steady decrease in permeate flux from 8.1 L/m^{2}h to 7.3 L/m^{2}h.

From **Fig. 3.3,** it was observed that water recovery remained nearly constant around 82 %. Water recovery herein is the ratio of permeate flow to feed flow. The concentration of salt approaches a point where the osmotic pressure of the concentrate equals the applied feed pressure, therefore, the permeate flux reduces and gradually stops. The recovery of water is as high as 82 %. Brine is recirculated until it is released from the system as the system operates at 100 % recovery. Therefore, the recovery rate is an operator-controlled set point. Typically, such desalination plants operate at 75 % product water recovery [5]. The recirculating brine and the lower salinity feed are constantly mixed. In comparison to batch RO, this mixing raises the average osmotic pressure (3.70 bar), resulting in higher recoveries.

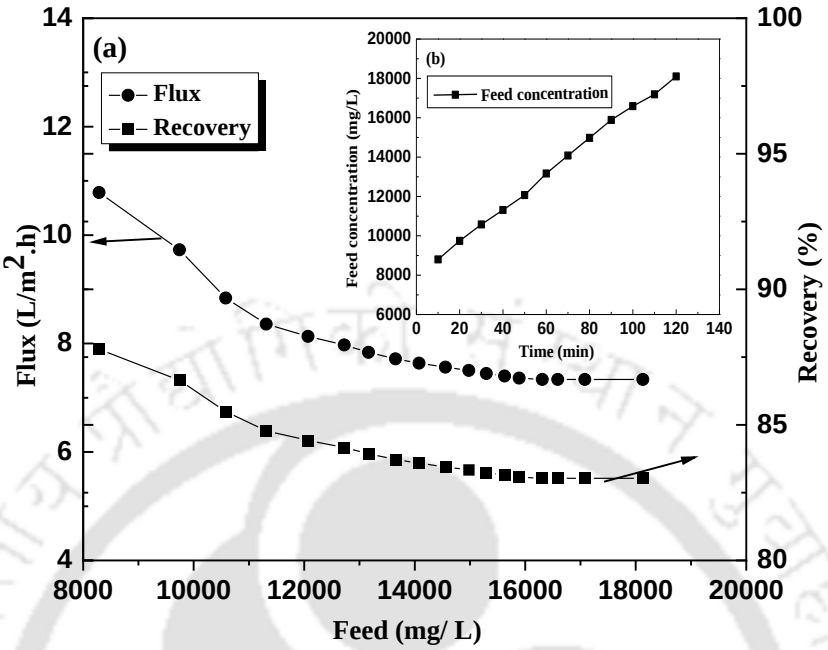

Fig. 3.3. a) Variation of permeate flux and percentage of water recovery with feed concentration. Pressure: 7 bar, temperature: 24 ^{o}C and initial TDS: 8100 mg/L b) Increase in feed concentration with time (insert)

3.2.4. Precipitation of chloride and sulphate ions from RO rejected water

The precipitation fractions for chloride and sulphate ions at various solvent volume ratios (VR) as well as their error analysis is demonstrated in **Fig. 3.4** and **Fig. 3.5,** respectively. Three different organic amines are selected for the experiments, namely diisopropylamine, isopropylamine and ethylamine.

Chloride precipitation factor increases sharply up to 41% at VR value of 0.4 and gradual thereafter and attain a maximum of 91 % at VR = 1.4 (**Fig. 3.4)**. Similarly, from **Fig. 3.5**, it is seen that a sharp increase in sulphate precipitation factor up to VR= 0.4, then increases gradually and becomes constant (99.98 %) at VR = 1. The sharp increase in precipitation is due to the effect of ionic charge on the solubility of the salt in the organic solvent.

Two remarks are implied in the above discussion. First, when the concentrations are far below saturation in aqueous solutions, monovalent chloride or sulphate salts can be co-

precipitated together with other divalent chloride or sulphate salts. Second, it appears that the precipitation factor of chloride and sulphate ions are very much dependent on the solubilities of the salts in the solvent. This is due to the fact that the solubility of chloride salts in organic amines are nearly the same, whereas the solubility of sulphate salts are significantly varied. Furthermore, precipitation increases as solubility decreases. For example, the chloride salts in diisopropylamine have a lower % P (e.g., P = 91 %) than the sulphate salts (e.g., P reaches 99 %), indicating that the chloride salts are more soluble in the solvent than the sulphate salts. Concentration of the salt in the aqueous solution can be the determining factor in initiating precipitation, while the salt solubility in the organic solvent is the governing factor in determining the extent of the precipitation fractions. However, interionic or ion-molecule forces, hydration effect, the polarity of organic solvent, dielectric constants of water and organic solvent, and other variables, as stated by [6], can play a role in determining the effect of the organic solvent in suppressing salt solubility.

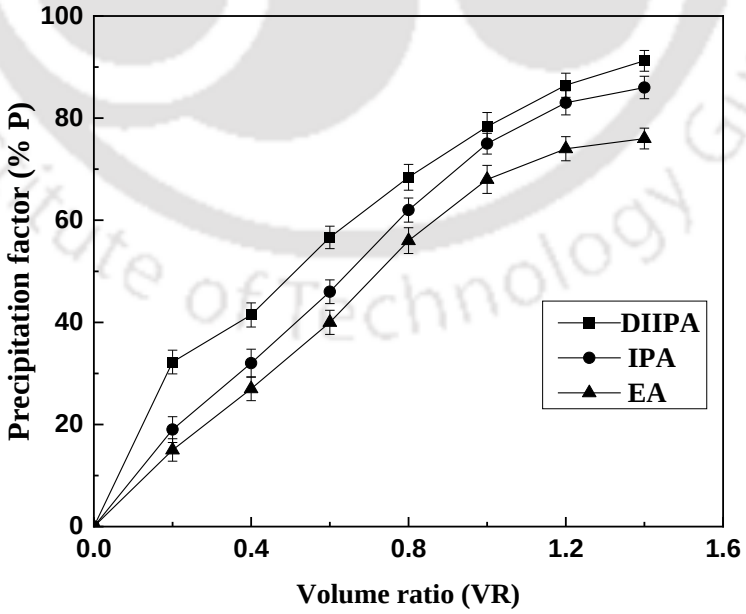

Fig. 3.4. Precipitation of chloride ions from highly concentrated RO brine. pH: 8, temperature: 24 ^{o}C, time: 10 min

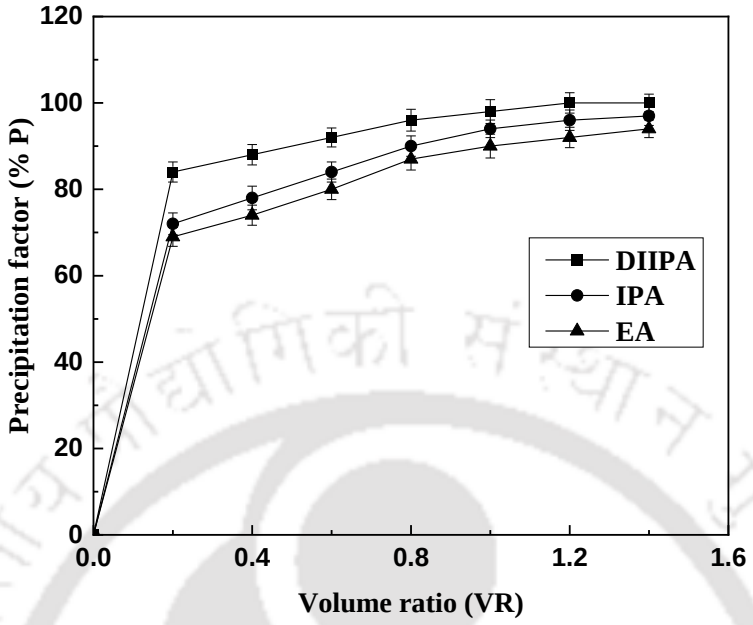

Fig. 3.5. Precipitation of sulphate ions from highly concentrated RO brine. pH: 8, temperature: 24 ^{o}C, time: 10 min

When considering recovery, the organic solvents used for precipitation should have favourable physical properties. IPA has a much lower boiling point (34 ^{o}C) than DIIPA (83.5 ^{o}C), making it ideal for recovering from the solution [1]. Using simple distillation, 96 % to 98 % of isopropylamine (IPA) was recovered. However, during the process, 2 % - 5 % loss was seen due to evaporation which can be eliminated by adjusting distillation facilities. Simple aeration was used to avoid traces of IPA in the filtered sample. **Table 3.1** indicates that integrated CCRO and precipitation techniques proved to reduce the pollutant concentration below the assigned permissible limit. It is seen from the table that results attained after the integrated process showed a significant reduction of all the parameters. Chloride concentration decreased from 1560 mg/L to 156 mg/L, while sulphate decreased from 4212 mg/L to 0.9 mg/L.

3.2.5. Membrane sustainability

The used membranes and precipitated salts were imaged by the FESEM. The corresponding EDS spectra were taken to reveal the morphology of the membrane surfaces and compare them with that of the used membrane. The FESEM images of the pristine membranes showed that the surface had a very smooth morphology. It can be also observed that the membranes are defect-free as shown in **Fig. 3.6a**, compared to a rough surface morphology of used membranes which is shown in **Fig. 3.6b**. From overall system analysis, it was observed that lesser inorganic deposition was taken place for a closed circuit desalination system. From **Fig. 3.6a**, it is clear that very little deposition over the membrane surface has taken place which is a cake or gel formation. This deposition over the membrane can be removed by simply washing with ultrapure water. Fouled RO membranes must be cleaned either chemically or physically regularly, to restore lost permeate flux. Moreover, regular cleaning shortens the life of RO membranes, which has a direct impact on the operational costs of the RO operation. According to [7], replacement costs of membrane vary in the range of 20 % to 30 % of total operating costs; thus, control and prevention of fouling are crucial for increasing membrane operating life, and thereby lowering the cost and overall economics of the desalination process. Therefore, membranes were rinsed with distilled water for about 10 min and pure water flux studies were carried out to know the flux recovery ratio (FRR). FRR value was found to be as high as 90 % even after 6 times of use. Hence, the fouling that occurred here was a reversible one and mitigated with simple washing. Membrane components were cleaned when the average water production rate dropped by 15 % from its initial flow rate. However, long time use will result in irreversible fouling that can be avoided by using chemical agents for cleaning.

It is observed from **Fig. 3.6c** that the salts are agglomerated by nature and crystalline in structure. Crystallinity was confirmed by X-ray diffraction (XRD) analysis. This is because

of the presence of inorganic salt mixtures, as ensured from the EDS qualitative analysis. The precipitated salt was weighed and it was found that about 20 g of salt per litre of feed was recovered. **Fig. 3.6c** indicates that cations such as magnesium, sodium, potassium, iron and calcium which may ally with sulphate and chloride to constitute their respective salts, are present in the precipitated salt.

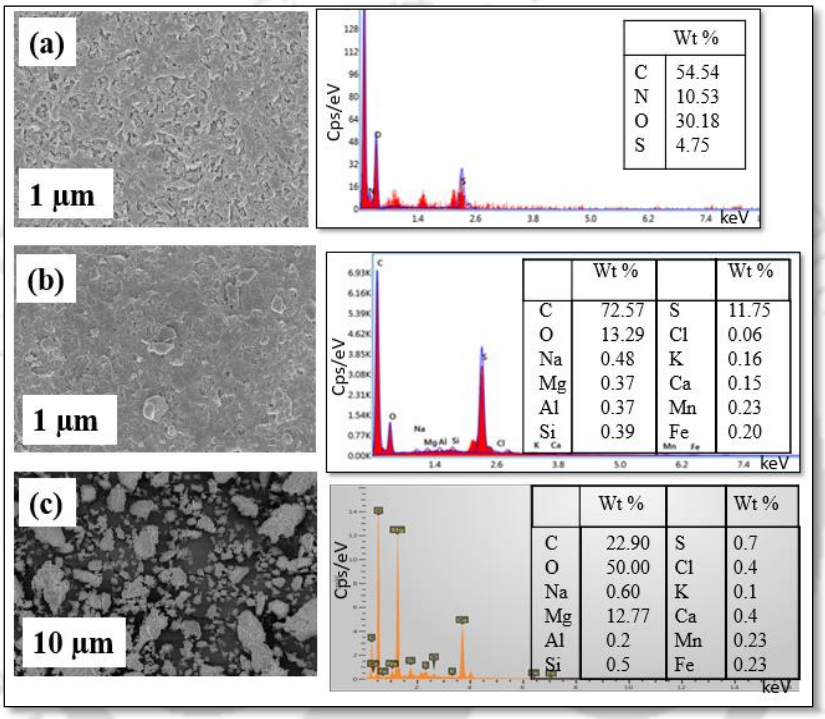

Fig. 3.6. FESEM images and EDX analysis of a) membrane before filtration b) membrane after filtration c) salt precipitated

3.2.6. Cost analysis of the system

Cost is one of the most significant and crucial elements for identifying appropriate technology for the treatment of wastewater. The cost of the water treatment process is calculated by a variety of factors, including economic criteria, plant capital costs and energy costs. The cost of a RO-based desalination system is influenced by the system capacity. The installation, intake, and pre-and post-treatment system costs are all included in the net

expense of such a process. Precipitation system consists of chemical cost, installation cost and operating cost.

Table 3.2. Cost analysis of integrated RO- precipitation system

Parameters	**Integrated RO- precipitation system**
Recovery (%)	82
Operation time (hr/day)	12
Product volume per year (m^3/year), p	150
Membrane life (year)	1
RO plant availability (%), f	90
Capital cost ($)	
RO membrane cost	25
High pressure pump (with 300 GPD)	41
Other accessories	45
Membrane replacement cost,	25
Total cost of membrane system	140
Annual operating cost, A1	33
Unit production cost for RO system, A2 = $\frac{A1}{f \times p}$ ($/m^3. year)	0.25
Unit production cost for precipitation unit	7.1
Annual operating cost include electricity, labour, chemical and cleaning cost. Unit production cost for precipitation unit include accessories, chemicals, operating and maintenance costs. *Annual amortized capital cost is not been included.	

The detailed economic assessment was carried out using reverse osmosis system analysis (ROSA 7.0 - FilmTec's) software for the estimation of water production cost, common technical assumptions, design parameters and specifications for RO system. Water production cost for the RO system estimated as 0.25 $/m^3, which is mainly dependent on water recovery and feed flow rate as mentioned in **Table 3.2**. It was observed that the major share of the cost

was of pump and membrane accessories. Likewise, the water treatment cost of the precipitation unit including all major costs is estimated as 7.1 $/m^3. Therefore, the total cost of integrated treatment is calculated as 7.35 $/m^3. However, the reported value of the process costs is conjectural and can differ considerably based on the time and long-term reliability of the process.

There have been few studies on the separation of ions, especially chlorides and sulphates from different wastewater using various techniques. A summary of the literature with the limitations of the technique used concerning the current study is presented here. The combination of RO with precipitation using miscible organic solvents for the separation of chloride and sulphate ions from industrial effluents is a novel approach, as shown in **Table 3.3**. Apparently, the removal of ions presented in this study is comparably better to that presented in the literature, since this work achieved a higher percentage of removal through integrated techniques. Furthermore, the comparison of targeted parameters and data based on ion removal obtained in this work suggests that the research conducted in this work could serve as benchmark data in the field of treatment of highly concentrated brine from the steel industry. In this context, the current research is recommended to investigate the efficiency of reverse osmosis with a CCRO method, as well as organic solvent precipitation for the separation of chloride and sulphate ions from highly concentrated NF rejected water, illustrating the uniqueness of this work.

Table 3.3. Different literatures on removal of chloride and sulphate ions using various methods with major limitations.

Method	Pollutants	Source	Percentage removal (%)	Limitations
Ion exchange resins [8]	Sulphate ions	Process water	SO_4^{2-} = 60	Regenerant disposal
Nanofiltration [9]	Chloride and sulphate ions	Synthetic saline wastewater	Cl^- = 43 SO_4^{2-} = 98	Highly concentrated reject stream
Electrocoagulation [10]	Sulphate	Mine drainage	SO_4^{2-} = 35	Often replacement of electrodes due to the deposition of film on the electrode surface and high-power consumption
Nanofiltration [11]	Chemical oxygen demand, chloride and sulphate ions	Pharmaceutical wastewater	COD = 98 Cl^- = 98 SO_4^{2-} = 98	Highly concentrated reject stream
Ozone oxidation [12]	Chloride ion	Zinc sulphate electrolyte	Cl^- = 98	Elevated energy cost and hazardous byproducts
Adsorption [13]	Chloride and sulphate ions	Synthetic alkaline solution and mine process water	Cl^- = 74 SO_4^{2-} = 85	Sludge generation
Reverse osmosis – Precipitation **Present work**	Chloride and sulphate ions	NF brine	cl^- = 91 SO_4^{2-} = 99	No sludge and or concentrate problem. However, detailed cost estimation for the cost of recyclable solvent needs to be assessed for the feasibility of this hybrid process.

Summary

Closed circuit reverse osmosis (CCRO) was combined with solvent-based precipitation for the separation of ions especially chlorides and sulphates from highly concentrated brine of nanofiltration reject which is a major concern of blast furnace treatment unit of the steel industry. It has been found that considerable removal of the pollutants such as TDS, chloride, sulphate and other salts was achieved. With increasing feed concentration, the permeate flux decreased. Water recovery was found to be high and relatively constant, equivalent to conventional desalination plant product water recovery. From overall system analysis, it was observed that lesser inorganic deposition was taken place for a closed-circuit desalination system. Also, the precipitation factor increased with increasing volume ratio. The removal of ions presented in this study is comparably better to that presented in the literature, since this work achieved a higher percentage of removal through integrated techniques.

Reference

[1] Deepti, A. Sinha, P. Biswas, S. Sarkar, U. Bora, M.K. Purkait, Separation of chloride and sulphate ions from nanofiltration rejected wastewater of steel industry, J. Water Process Eng. 33 (2020) 101108. https://doi.org/10.1016/j.jwpe.2019.101108.

[2] S. Chakraborty, M.K. Purkait, S. DasGupta, S. De, J.K. Basu, Nanofiltration of textile plant effluent for color removal and reduction in COD, Sep. Purif. Technol. 31 (2003) 141–151. https://doi.org/10.1016/S1383-5866(02)00177-6.

[3] L. Chen, P. Xu, H. Wang, Interplay of the factors affecting water flux and salt rejection in membrane distillation: A state-of-the-art critical review, Water (Switzerland). 12 (2020). https://doi.org/10.3390/w12102841.

[4] M.K. Purkait, V.D. Kumar, D. Maity, Treatment of leather plant effluent using NF followed by RO and permeate flux prediction using artificial neural network, Chem. Eng. J. 151 (2009) 275–285. https://doi.org/10.1016/j.cej.2009.03.023.

[5] R. Singh, Analysis of high recovery brackish water desalination processes using fuel cells, Sep. Sci. Technol. 44 (2009) 585–598. https://doi.org/10.1080/01496390802634414.

[6] Mansour S. Bader, precipitation and separation of salts, scale salts, and norm contaminant salts from saline waters and saline solutions, 1995.

[7] H.Z. Shafi, A. Matin, S. Akhtar, K.K. Gleason, S.M. Zubair, Z. Khan, Organic fouling in surface modified reverse osmosis membranes: Filtration studies and subsequent morphological and compositional characterization, J. Memb. Sci. 527 (2017) 152–163. https://doi.org/10.1016/j.memsci.2017.01.017.

[8] Y. Öztürk, Z. Ekmekçi, Removal of sulfate ions from process water by ion exchange resins, Miner. Eng. 159 (2020) 106613. https://doi.org/10.1016/j.mineng.2020.106613.

[9] Z.Q. Yan, L.M. Zeng, Q. Li, T.Y. Liu, H. Matsuyama, X.L. Wang, Selective separation of chloride and sulfate by nanofiltration for high saline wastewater recycling, Sep. Purif. Technol. 166 (2016) 135–141. https://doi.org/10.1016/j.seppur.2016.04.009.

[10] T. Foudhaili, O. Lefebvre, L. Coudert, C.M. Neculita, Sulfate removal from mine drainage by electrocoagulation as a stand-alone treatment or polishing step, Miner. Eng. 152 (2020) 106337. https://doi.org/10.1016/j.mineng.2020.106337.

[11] S. Chakrabortty, J. Nayak, P. Pal, R. Kumar, P. Chakraborty, Separation of COD, sulphate and chloride from pharmaceutical wastewater using membrane integrated system: Transport modeling towards scale-up, J. Environ. Chem. Eng. 8 (2020) 104275. https://doi.org/10.1016/j.jece.2020.104275.

[12] W. Liu, R. Zhang, Z. Liu, C. Li, Removal of chloride from simulated zinc sulfate electrolyte by ozone oxidation, Hydrometallurgy. 160 (2016) 147–151. https://doi.org/10.1016/j.hydromet.2015.12.006.

[13] E. Iakovleva, E. Mäkilä, J. Salonen, M. Sitarz, M. Sillanpää, Industrial products and wastes as adsorbents for sulphate and chloride removal from synthetic alkaline solution and mine process water, Chem. Eng. J. 259 (2015) 364–371. https://doi.org/10.1016/j.cej.2014.07.091.

Chapter 4:

Utilization of LD Slag from steel industry for the preparation of MF membrane

Chapter 4
Utilization of LD Slag from steel industry for the preparation of MF membrane

This chapter discusses, fabrication of porous ceramic membranes by LD slag along with other precursors by uniaxial method. Three different sintering temperatures (650 ^{o}C, 850 ^{o}C and 950 ^{o}C) were selected for the study. Modification of the slag was carried out for the improvement of the membrane. Morphological and permeation experiments were conducted to investigate the properties of the membrane. Treatment of cold roll mill (CRM) wastewater from steel industry was carried out using the hybrid process via coagulation- flocculation followed by microfiltration. The flocs generated after coagulation – flocculation process was separated using the prepared LD slag membranes. Use of LD slag for the fabrication of ceramic membrane is not only an appealing option towards the commercialization of membrane, but also great option to reduce the solid waste which is dumped to the environment.

4.1. Experimental

4.1.1. Materials

The Materials along with their role which is utilized for fabrication of ceramic membrane is presented in **Table 4.1**. Linz – Donawitz (LD) slag and cold roll mill (CRM) wastewater was obtained from TATA steel Limited, Jamshedpur, India. Sodium metasilicate, boric acid, sodium carbonate, alumina, quartz and poly aluminium chloride (PAC) were obtained from Merck India. Acetic acid (99%) and kaolin was supplied by Loba Chemie, Mumbai, India. All the chemicals were used without any further purification.

Content of this chapter is published as below:

- Deepti, A. Sinha, P. Biswas, S. Sarkar, U. Bora, M.K. Purkait, Utilization of LD slag from steel industry for the preparation of MF membrane, J. Environ. Manage. 259 (2020) 110060. https://doi.org/10.1016/j.jenvman.2019.110060.

Table 4.1: Precursors and scheme used to fabricate 3 different ceramic membranes

Material	M0 (Wt.%)	M1 (Wt.%)	M2 (Wt.%)	Functions
LD slag	55	-	-	-
Modified LD Slag	-	55	60	-
Sodium metasilicate	15	15	15	Binder
Boric acid	5	5	10	Mechanical strength
Sodium carbonate	15	15	0	Pore former
Alumina	10	10	0	Plasticity
Quartz	-	-	15	Mechanical and thermal stability

Scheme of membrane fabrication

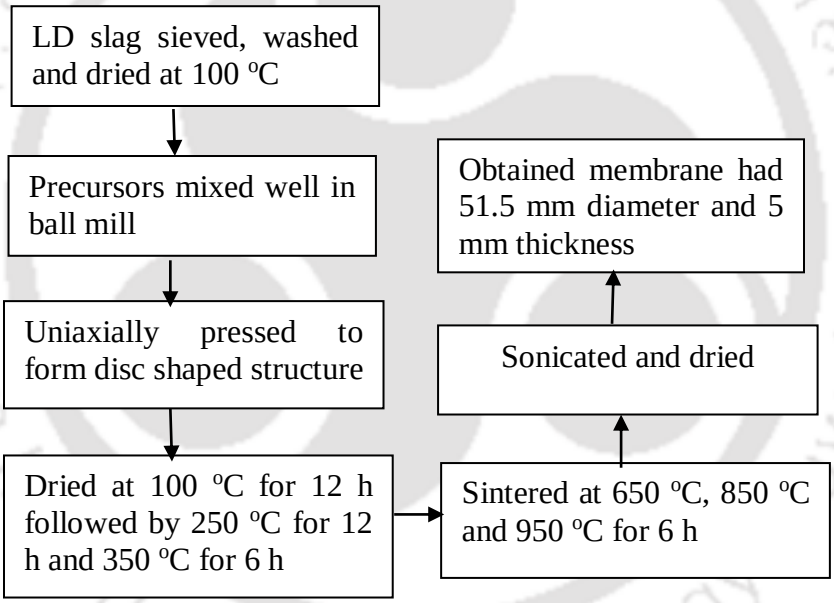

4.1.2. Membrane preparation

The scheme for membrane fabrication is given in **Table 4.1**. LD slag was sieved by 45µm size standard mesh screen. The sieved slag was washed with water and dried at 100 ºC for 12 h. The washed slag (for M0), modified slag (for M1, M2) along with other raw materials as mentioned in **Table 4.1** was mixed well with the help of ball mill maintaining a speed of 60 rpm for an hour. The mixture was uniaxially pressed at a pressure of 100 kg/cm^2 for 2 min using stainless steel mould to obtain a disc shaped structure. The resulted structure was then

dried at 100 ^{o}C for 12 h and at 250 ^{o}C for another 12 h. Before sintering at three different temperatures at 650 ^{o}C, 850 ^{o}C and 950 ^{o}C for 6 h, an intermediate temperature of 350 ^{o}C at 6 h was introduced. Sintering was carried at the heating rate of 2 ^{o}C/min. The obtained membranes were polished using silicon carbide abrasive (C-220) followed by cleaning of the membrane with millipore water in an ultra-sonication bath (make: Elma, model: T460) for 2 h and then dried for 3 h. The obtained membrane had a diameter of 51.5 mm and thickness of 5 mm which was characterized for their morphological properties and for permeability tests.

4.1.3. Modification of LD slag

Composition of LD slag consists of CaO: 53.5 %, MnO: 0.62 %, P_2O_5: 2.41 %, MgO: 10.1%, FeO: 15.2 %, SiO_2: 12.8 %, Al_2O_3: 1% and others: 5.1 %. It is seen from the composition that almost 50 % of LD slag comprises CaO. It is reported that the high free CaO leads to hydration and causes cracking in structures [1]. Moreover, there is a possibility of leaching of CaO to the permeate after filtration as CaO reacts with water in the form of f-CaO. In this view, modification step was included to overcome the above mentioned issues. Modification of LD slag was carried as shown in **Fig. 4.1a**. The experimental set up composed of a double mouth glass reactor in which 350 g of washed slag was treated with 6 M of acetic acid. The reactor was kept in a water bath to maintain an uniform temperature of 40 ^{o}C with a stirring speed of 500 rpm. Simultaneously CO_2 was purged (2 L/min) as shown in the **Fig. 4.1a**. The whole reaction was kept for 2 h. Then the sample was filtered and the residue was dried for 12 h at 100 ^{o}C. Further the dried modified slag was utilized to fabricate membrane (M1, M2). **Fig. 4.1b** shows the scheme of reaction in modification. When calcium hydroxide reacts with acetic acid, it forms calcium acetate by neutralization reaction. Calcium acetate when reacted with carbon dioxide gives calcium carbonate and acetic acid. With this modification step, most of the CaO is converted to $CaCO_3$, which is said to be a very good precursor for the membrane and thereby reducing the adverse effects of CaO.

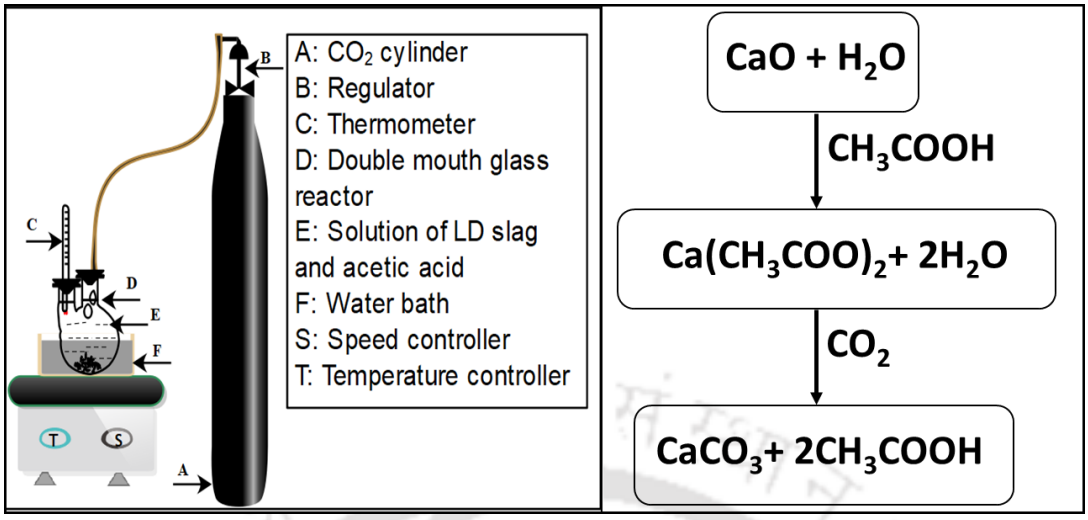

Fig. 4.1. Modification of LD slag. a) Experimental setup, and b) Scheme of modification

4.1.4. Characterization techniques

Characterization of the raw materials and prepared membranes were performed in detail. The composition of LD slag was analysed using X-ray fluorescence (XRF, make: PANalytical; model: Axios). Size distribution of all the raw materials and the membrane mixture was analysed using particle size analyser (Model No.: Delsa Nano C; Make: M/s Beckman Coulter, Swtizerland). Weight transformations of slag and membrane mixture were conducted using Thermogravimetric analysis from 30 ^{o}C – 1000 ^{o}C (TGA, Make: M/s Netzsch, Germany; model: TG 209 F1 Libra). Field emission scanning electron microscopy (FESEM, make: Zeiss; model: Sigma 300) was used to analyse the pore size and any defects present in the membrane. Sputter coating of gold was applied onto the sample before analysis, to avoid any charging of the specimen. Image J software was used to estimate the average pore size of the membranes from FESEM micrographs [2]. Permeation experiment was conducted to evaluate the performance of the membranes in separation application.

Bulk porosity of the prepared membranes were determined by Archimedes method considering water as wetting liquid [3].

Chemical stability of the prepared ceramic membranes was determined by submerging these

in strong base (pH 12) and in strong acid (pH 4) for 24 h. Concentrated HCl and NaOH solutions were used to maintain the pH of the medium. Wet membranes were weighed subsequently dried at 110 ^{o}C for 3 h. Weight losses of the membranes sintered at various temperatures were evaluated.

A permeation set up of 300 ml capacity was used to carry out liquid permeation experiment. The setup consists of a membrane housing with a tubular cell and flat plate base. Membrane was placed in a casing which was sealed using epoxy resin and placed in a membrane housing. Deionised water was filled in the tubular cell. Compressed air was used to pressurize the cell. All the experiments were conducted in a room temperature. Permeate flux of the membranes were determined using following Eqn. 3.1, Where Q is volume of water permeated (m^3), A is effective membrane area (m^2) and Δt is sampling time (h) [4].

4.1.5. Treatment of cold roll mill (CRM) wastewater

CRM wastewater was treated using a hybrid process which include coagulation – flocculation followed by microfiltration. In this study poly aluminium sulphate (PAC) was used as a coagulant. Coagulation – flocculation experiments were carried out using jar – test apparatus (make: Phipps & Bird, Richmond, Virginia) equipped with 6 numbers of 1 L jar with rectangular blades. The experiment was done in two batches. The dosage of the coagulant varied from 30 mg/L to 500 mg/L. The operating parameters were set as follows: (Rapid mixing speed: 120 rpm for 1 min; slow mixing speed: 40 rpm for 20 min; settling time: 30 min). The parameters were set using an automatic controller. Tests were conducted thrice and the mean value is reported. The coagulated water was then filtered using the prepared LD slag membrane.

4.2. Results and discussion

4.2.1. Membranes prepared with raw LD slag

Membranes were fabricated by using raw slag along with different precursors as discussed in **Section 4.1.2**. The fabricated membranes ought to have great quality and characteristics. However, as LD slag comprises of high calcium oxide, leaching of calcium oxide to the permeate was seen as CaO reacts with water in the form of free CaO present in LD slag. Moreover, it was additionally noticed that the permeate had an exceptionally high pH of 14. Thus a modification step was required to resolve these issues. Here, LD Slag was altered utilizing acidic acid (as discussed in section 2.3) by which calcium oxide was converted to calcium carbonate which is one of the imperative precursors for the membrane. **Figs. 4.2a and 4.2b** shows the membranes fabricated before modification using raw LD slag (M0) and modified LD slag (M1, M2), respectively. From **Fig. 4.2a** it is seen that excess calcium oxide has unevenly distributed over the surface which decreases the quality of the membrane. Whereas, from the **Fig. 4.2b**, it is seen that membrane is in good quality and do not have any cracks over it.

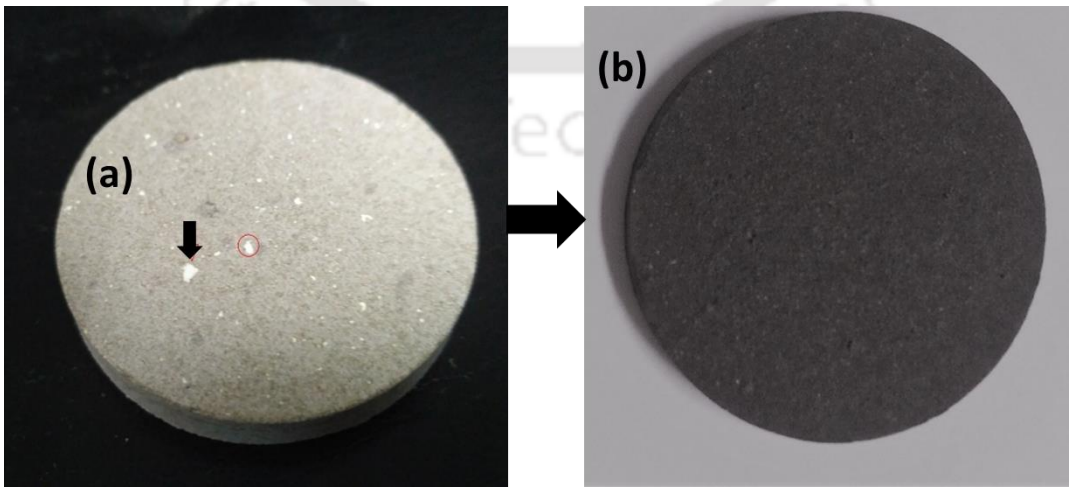

Fig. 4.2. Fabricated LD slag membrane. a) Before modification, b) After modification

4.2.2. Structural characterization

4.2.2.1. Particle size distribution

Particle size distribution analysis was carried out for the raw materials before sintering and shown in **Fig. 4.3**. The figure demonstrates a wide range of particle size distribution of raw materials used for the fabrication of ceramic membranes. These particles support the membrane to get a compacted structure with a homogenous porosity subsequent to sintering by topping off the void spaces by smaller particles between the larger particles. It is seen from the figure that modified slag had the smallest size of 1.6 µm, while quartz had the highest size of 5.6 µm. Different materials like alumina, sodium carbonate, boric acid, sodium metasilicate had sizes of 3.5 µm, 2.3 µm, 3.8 µm and 2.1 µm, respectively. At the point when all these raw materials granulated and blended well before fabrication, the average particle size of M1 mixture is 3.5 µm, D50 is 3.4 µm and mean diameter is 3.3 µm and average particle size that of for M2 is 2 µm , D50 is 1.4 µm mean diameter is 2 µm.

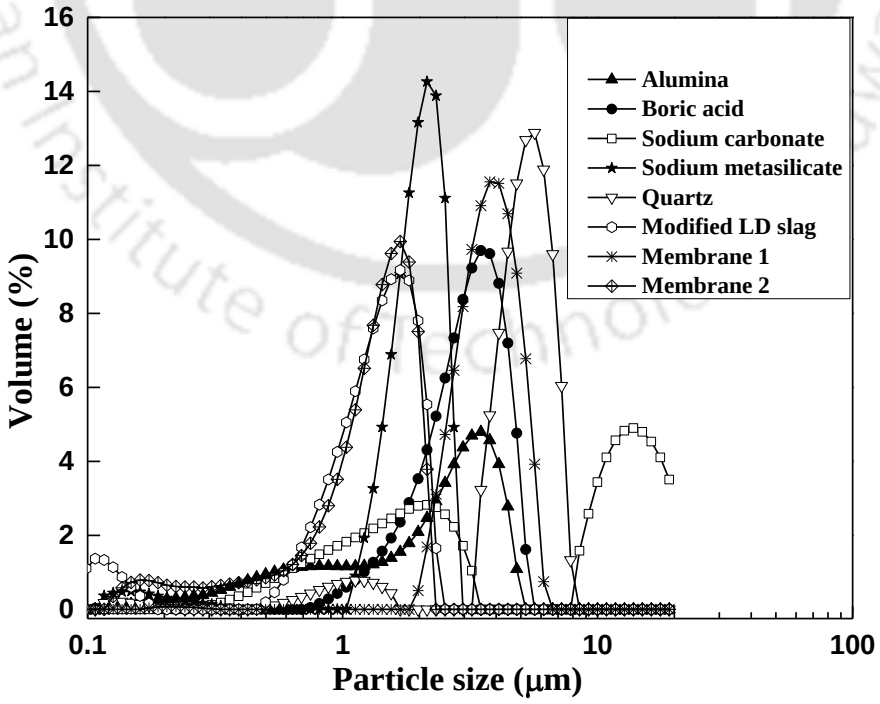

Fig. 4.3. Particle size distribution of raw materials and membrane mixtures

4.2.2.2. Thermogravimetric analysis

Thermogravimetric analysis (TGA) is an important analysis done to investigate the temperature behaviour of the raw slag, modified slag and membrane composition (**Fig. 4.4**). From the figure, it is seen that membrane mixture showed a weight loss at two locations basically one for water loss and the other one for decomposition of calcium carbonate. It was also observed that there was no change in weight loss above 820 ^{o}C. From this it can be inferred that the minimum sintering temperature for the fabrication of the membrane has to be above 820 ^{o}C. It is also seen that an endothermic peak at 420 ^{o}C corresponds to the dehydration of magnesium and iron hydroxides. The weight loss after 600 ^{o}C is caused either by dehydroxylation of calcium hydroxide to calcium oxide or partial degradation of silicates or decomposition of carbonates with the release of CO_2 [5].

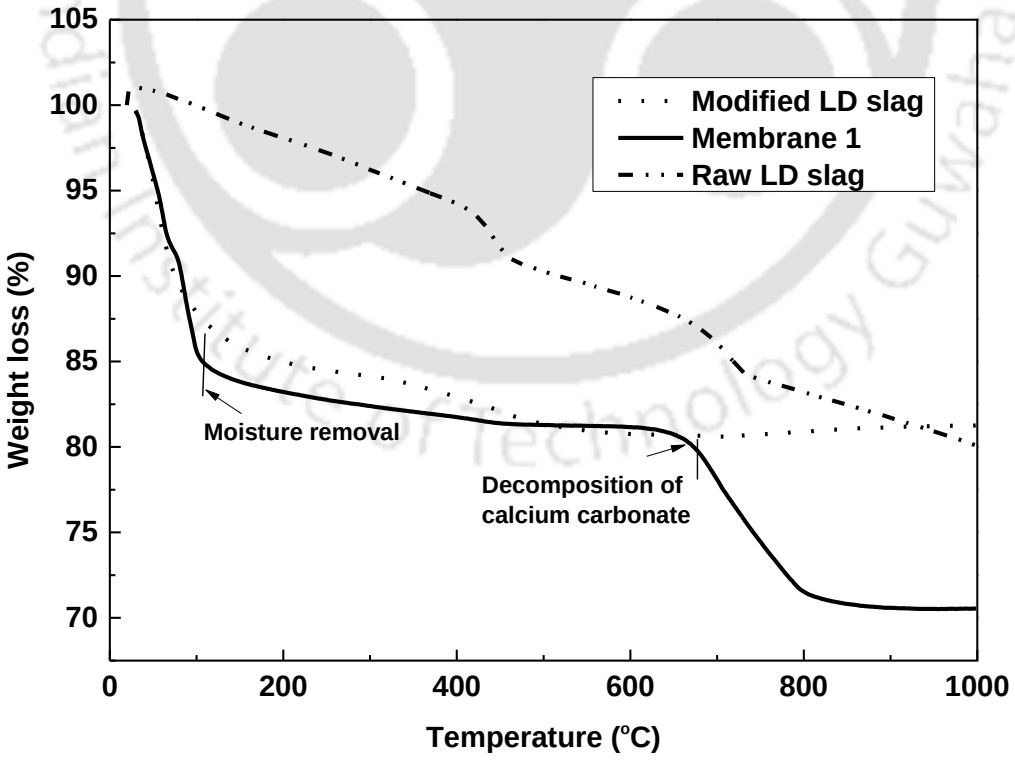

Fig. 4.4. TGA analysis of raw LD slag, modified LD slag and membrane mixture

4.2.2.3. Surface morphology

The surface morphology like pore distribution, shape and size was investigated using field emission scanning electron microscopy (FESEM). The FESEM images of the prepared membranes M1 and M2 are shown in **Figs. 4.5a and 4.5b** at sintering temperatures of 650 ºC, 850 ºC and 950 ºC. The surface of all the membranes are considerably compacted within the sintering temperatures. Moreover, it is seen from the figure that pore size and pore diameter increase with increasing sintering temperature. The membranes at 650 ºC had very less pores compared to the other membranes. While the membranes sintered at 850 ºC and 950 ºC show highly porous structure due to the fact that the sintering temperatures over 650 ºC enhances the grain growth that leads to the large pores. Futhermore, M1 shows highly porous than that of M2. Coroborating with the TGA results, it is confirmed from FESEM images that sintering temperature should be higher than 650 ºC for a porous structured membrane. It can be also observed that the fabricated membranes are defect free and the average pore size lies within 10 µm which reveals that the membranes are suitable for microfiltration applications [6].

4.2.2.4. Pore size distribution

Pore size distribution of all the membranes were carried out using a software called ImageJ with the help of FESEM images [7]. Four FESEM images of every membrane were taken for sampling and evaluated using the said software. **Figs. 4.6a and 4.6b (insert)** represents the pore size distribution of M1 and M2 membranes respectively, with three different sintering temperatures. The porous texture can be seen from these figures. The average pore diameter from FESEM analysis of the membrane is determined using Eqn 4.1, considering that the pores were cylindrical in nature [4].

$$d_s = \left[\frac{\sum_{i=1}^{n} n_i d_i^2}{\sum_{i=1}^{n} n_i} \right]^{0.5} \qquad (4.1)$$

Where ds is area average pore diameter, d_i is the diameter of the ith pore, ni is the number of pores with diameter d_i and n is the total number of pores calculated from FESEM images. The average pore diameters of M1 are 5.3 µm, 6.8 µm and 8.5 µm and that of for M2 are 3.6 µm, 7.5 µm and 8.3 µm for 650 ºC, 850 ºC, and 950 ºC, respectively. It can be observed that the prepared membrane has a wide pore size distribution although lies within microfiltration range. It can also be observed that the pore size distribution is broadened with increase in temperature by forming large pores and apparently eliminating smaller pores. [8].

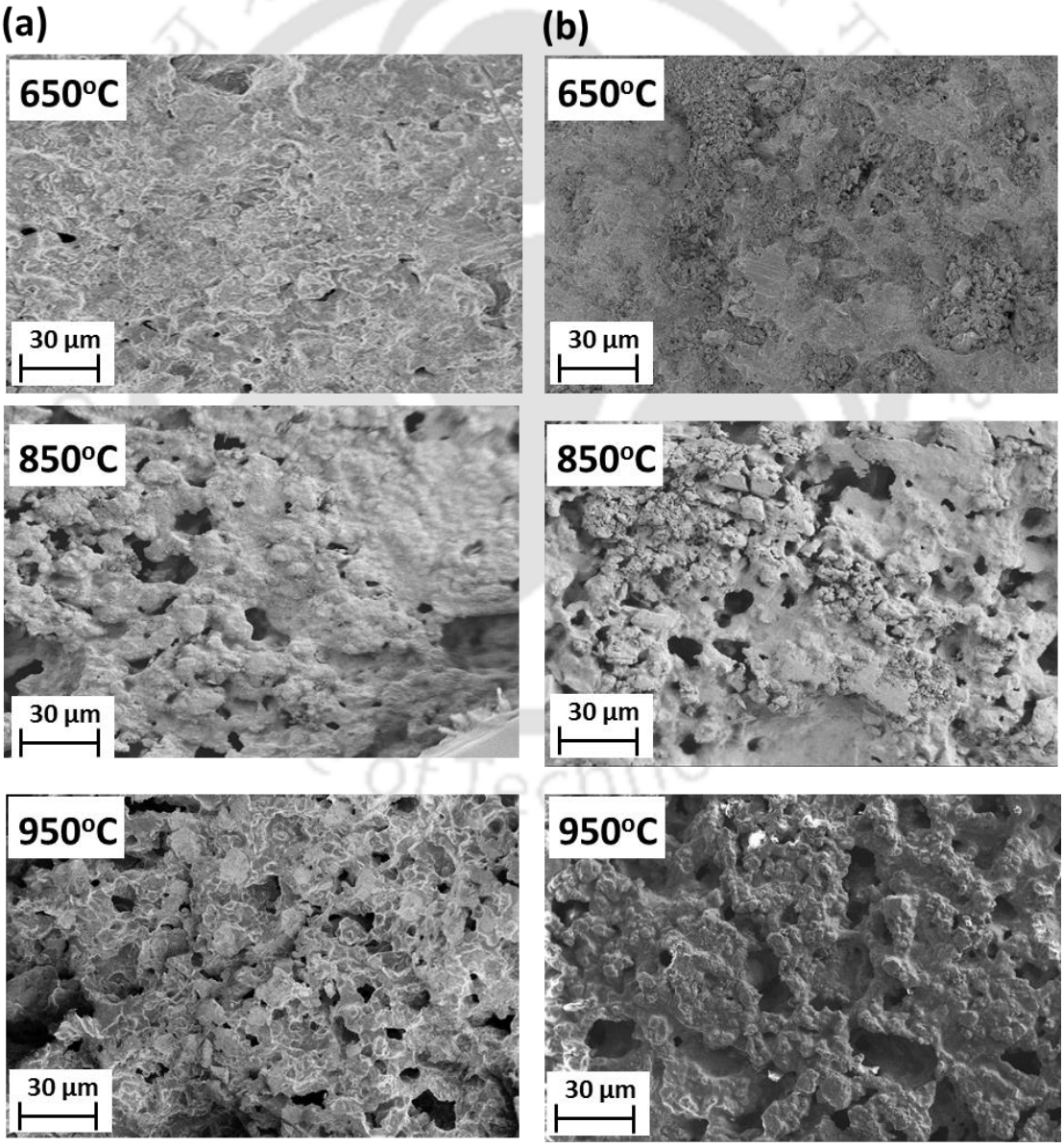

Fig. 4.5. FESEM images of ceramic membranes at different temperatures. a) M1 and b) M2

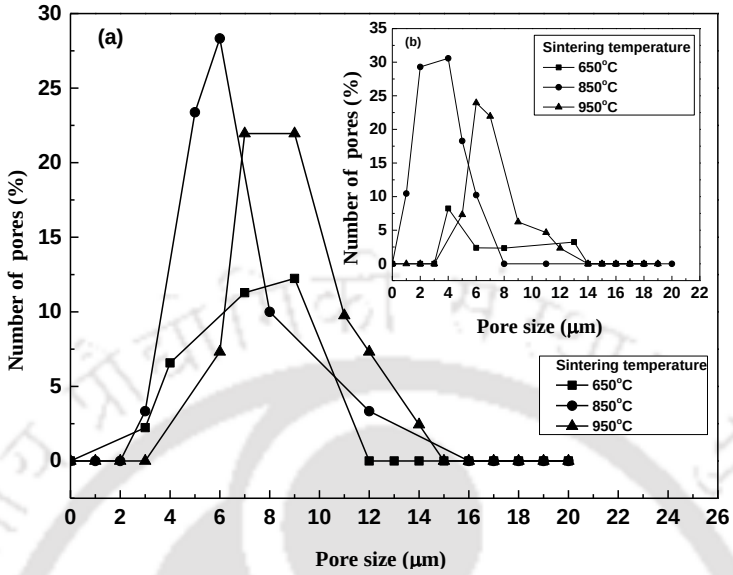

Fig. 4.6: Pore size distribution of the prepared ceramic membranes sintered at various temperatures. a) M1 and b) M2 (insert)

4.2.3. Permeation experiments

4.2.3.1 Water permeation experiment

The fabricated membranes M1 and M2 sintered at 650 ºC, 800 ºC and 950 ºC were subjected to water permeation test to determine the water flux of the membrane in batch mode operation using deionised water. Transmembrane pressure of 101 kPa was maintained throughout the experiment. Each membrane was pressurized at 294.2 kPa to unblock all the pores before carrying out the flux studies. From **Fig. 4.7,** it is seen that the flux was very high initially then gradually decreased and attained steady state within 26 min of operation. Also, it is observed that both M1 and M2 follows increasing trend of flux with increase in sintering temperature. This is due to the increase in porosity with increase in temperature. From **Fig. 4.7**, it may also be seen that at the beginning flux was, 431 L/(m^2.h) , 704 L/(m^2.h) and 818.18 L/(m^2.h) and reached steady state value of 160 L/(m^2.h), 250 L/(m^2.h) and 341

L/(m^2.h) for M1 sintered at 650 ^{o}C, 850 ^{o}C and 950 ^{o}C, respectively.

The similar flux trend was also seen for M2 membrane (**Fig. 4.7)**. The initial flux was 409 L/(m^2.h), 636 L/(m^2.h) and 704 L/(m^2.h) and reached steady state value of 136 L/(m^2.h), 205 L/(m^2.h) and 319 L/(m^2.h) for membranes sintered at 650 ^{o}C, 850 ^{o}C and 950 ^{o}C, respectively at the end of 25 minutes of operation. It is observed that both M1 and M2 showed almost similar flux values. This variation in flux values was due to the change in porosity as discussed in preceding section.

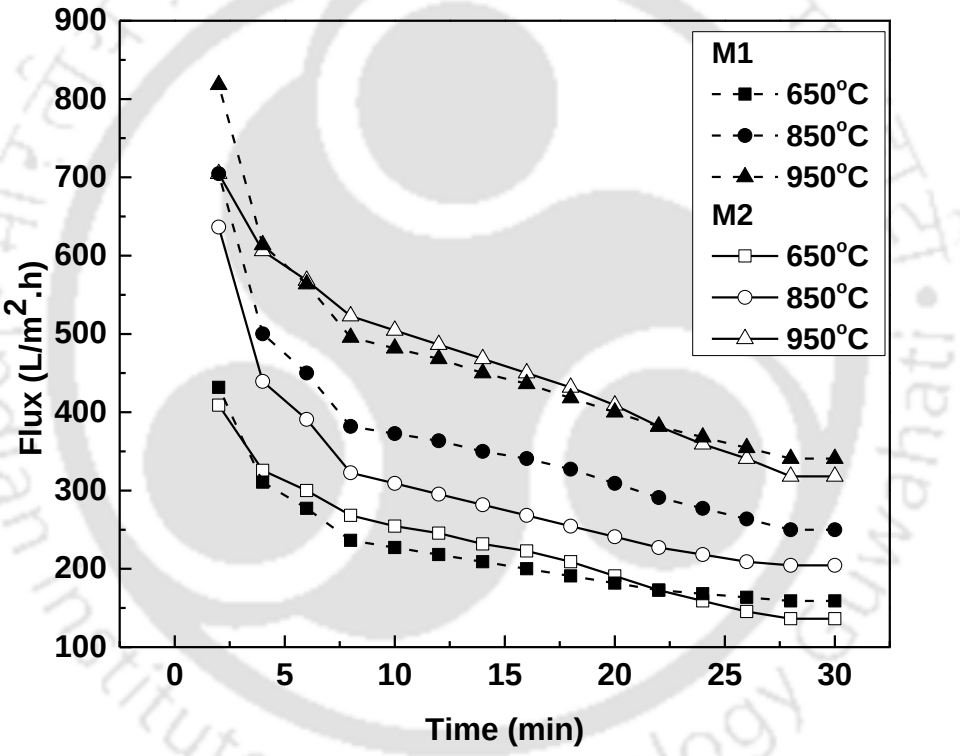

Fig. 4.7: Pure water flux of the microfiltration membranes sintered at various temperatures.

4.2.3.2. Bulk porosity

Bulk porosity of the membranes were determined using Archimedes' principle by following equation [3].

$$p = \frac{(M_W - M_d)}{(M_w - M_a)} \times 100 \qquad (3)$$

Where M_w is the mass of the membrane saturated with water, M_d is the dry mass of the

membrane, M_a is the mass of the membrane taken at its dipping condition in water. **Fig. 4.8a** demonstrates the bulk porosity of membranes M1 and M2 at various sintering temperatures. It tends to be seen from the **Fig. 4.8a** that the porosity has increased from 46% to 63% as sintering temperature was increased from 650 ^oC to 950 ^oC for M1 membrane. Similarly, for M2 membrane the increase in porosity was from 53% to 71% with the same range of temperature change. The increase in porosity was due to the fact that, the volatile materials leave the surface making it porous during sintering. Opening up of pores was initiated with the increase in temperature [9].

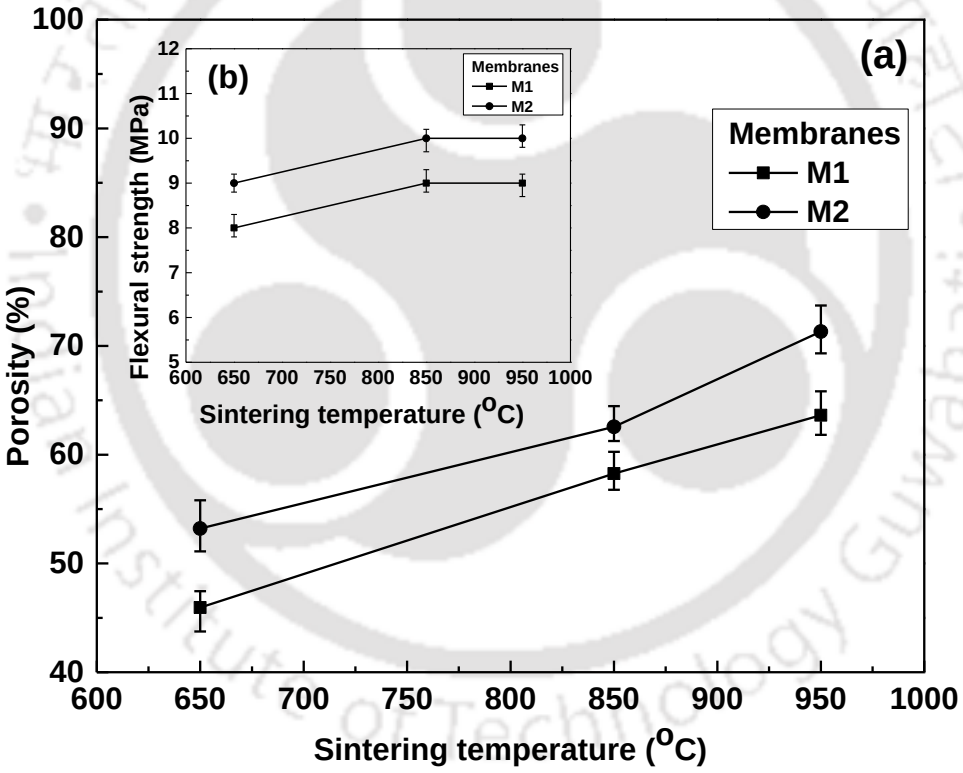

Fig. 4.8: a) Porosity and b) Flexural strength (insert) of the ceramic membranes sintered at various temperatures.

4.2.4. Physical characterization

4.2.4.1. Flexural strength

Three-point bending strength method was adopted to find the mechanical strength of the fabricated microfiltration membranes. The flexural strength of the ceramic membranes

sintered at different temperatures is shown in **Fig. 4.8b (insert)**. As depicted in the figure, M1 shows a flexural strength of 8 MPa at 650 ^{o}C and increases to 9 MPa at 850 ^{o}C and remains almost constant at 950 ^{o}C. Similar trend was observed in case of M2. Flexural strength was 9 MPa at 650 ^{o}C and increases upto 10 MPa for both 850 ^{o}C and 950 ^{o}C. M2 shows higher mechanical strength when compared to M1. The increase in mechanical strength with increase in sintering temperature is due to the grain growth within the membrane which ultimately results in densification [6].

4.2.4.2. Chemical stability

The weight loss of the ceramic membrane in acidic and basic medium sintered at different temperatures is shown in **Fig. 4.9**. From the figure, it is seen that as sintering temperature was increased, the percentage weight loss was decreased for both the membranes. It was observed that weight loss percentage was high during acid treatment than that of base treatment for both the membranes. M1 shows more weight loss both in acid and basic medium compared to M2. It can be detailed that after the acid treatment, the percentage weight loss was found to be from 14 % to 8 % for M1 and 3 % to 0.5 % for M2 at sintering temperatures of 650 ^{o}C and 950 ^{o}C. Similarly, a weight loss from 13 % to 8 % and 0.5 % to 0.08 % for M1 and M2 respectively, at 650 ^{o}C and 950 ^{o}C were found after base treatment of the ceramic membranes. At higher temperatures, ceramic materials are said to be tough to strong acidic and basic medium. Hence this supports that the prepared membrane has attained the ceramic properties. The percentage weight reduction in acidic medium is higher because of the fact that the oxidation of the material such as Fe^{2+} would occur which is available in the modified LD slag and also effervescence occurs when any carbonates react with acid [10]. As M1 composition has sodium carbonate, weight loss is higher in M1 compared to that of M2. Hence higher weight loss in M1 is justified as there is sodium carbonate in its composition.

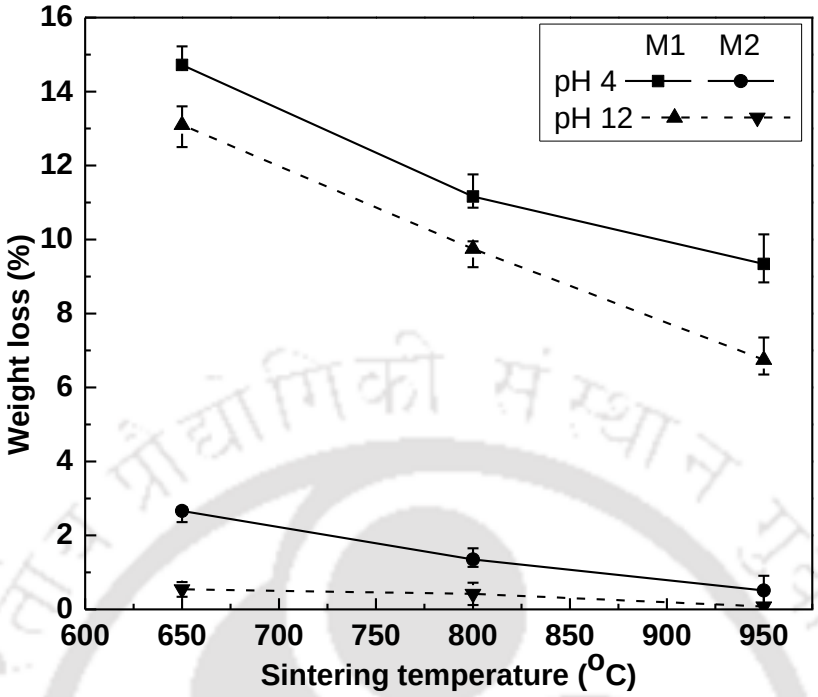

Fig. 4.9: Chemical stability of the microfiltration membranes in strong acidic and basic medium

4.2.4.3. Leaching experiments

The fundamental issue of M0 membrane is leaching of calcium oxide to the filtrate thus making it very basic in nature. Experiments were carried for 5 weeks to study the pH variation and to guarantee that no leaching is seen after the modification. Water was filtered through the membrane for permeation experiments as mentioned in section 3.3. Filtration was carried out for 30 min every day which continued till 5 weeks. pH was measured and noted. The permeate from M0 indicated high pH (14) in day 1. However, it decreased to 13 on 35th day. In case of M1 and M2, the pH was 9.5 in day 1 and gradually decreased to 8.5 and 8.4, respectively, at the end of 28th day and remained consistent till 35th day as shown in **Fig. 4.10**. Therefore, the membrane fabricated with modified LD slag demonstrated to be proficient as far as its basic properties are concerned.

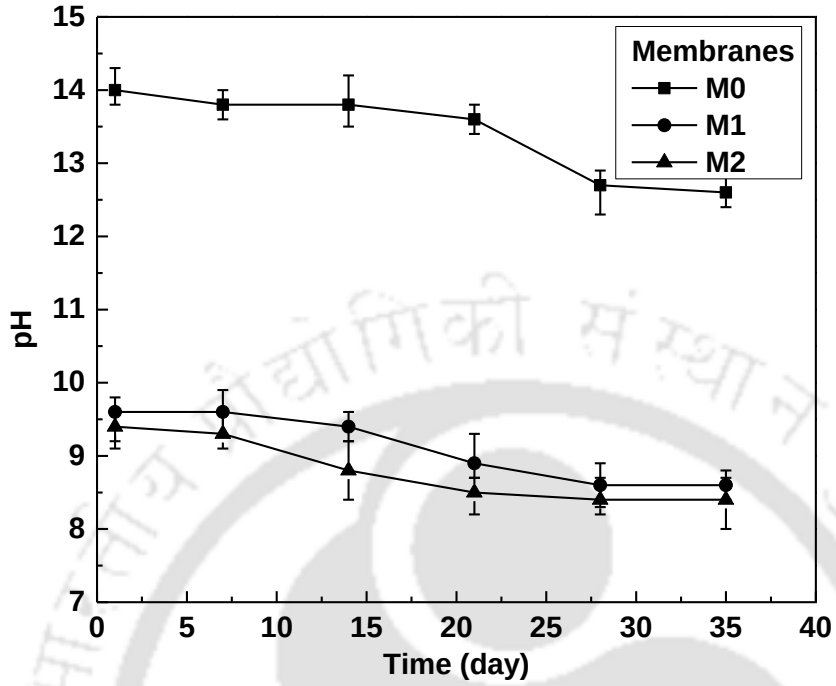

Fig. 4.10: Variation of pH of filtrate. M0: Membrane fabricated before modification of slag, M1, M2: Membranes fabricated after modification of slag

4.2.5. Performance of hybrid process

The performance of coagulation- flocculation and microfiltration was separately analysed in terms of maintaining water quality parameters mainly for chemical oxygen demand (COD), chromium (VI), total dissolved solids (TDS) and iron (III) in the treated water. A preliminary investigation was experimented to determine an approximate range of coagulant dosage. Therefore, wide ranges of concentrations of PAC (30 mg/L – 500 mg/L) were considered to get the optimized dosage of coagulant (PAC) required for treating CRM wastewater as shown in **Table 4.2**. It was observed from the table that at minimum dosage of 30 mg/L, there was no major changes occurred. However, at 50 mg/L, slight change was noticed. As the dosage reached 150 mg/L, formation of flocs started and at the end of 350 mg/L, a complete formation and settling of flocs was seen. Hence, the results revealed that optimum dosage of

PAC for the treatment of CRM wastewater was 350 mg/L. Further experiments were carried with the same dosage.

Table 4.2. Optimization of Poly aluminium chloride (PAC) dose for flocculation of CRM water

PAC dose (mg/L)	Coagulation - Flocculation after 30 min	
0	No change	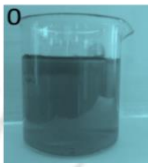
30	Not formed	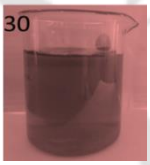
50	Slightly formed	
100	Slightly formed	
150	Flocs formed but not sediment	
200	Flocs formed but not sediment	
250	Flocs formed, slightly sediment	

300	Flocs formed, slightly sediment	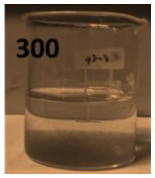
350	Flocs sediment	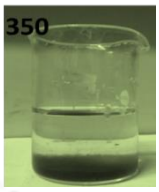
400	Flocs sediment	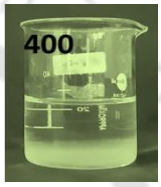
450	Sedimentation completed	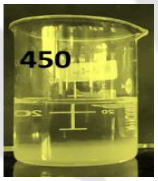
500	Sedimentation completed	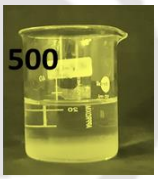

The flocs obtained after coagulation – flocculation was analysed for particle size distribution using particle size analyser. From **Fig. 4.10a**, it is seen that most of the particles were in the range of 10 µm. Comparing the pore size distribution of the membrane (Fig. 6) with the particle size distribution of the flocs generated after coagulation – flocculation (Fig. 10a), it is concluded that prepared LD slag based MF membrane (especially M2) would be better suited for the separation of flocs from coagulated water.

The coagulated water was then filtered through M2 membrane. The permeation experiments were carried as mentioned in section 3.3.2. It is seen from **Fig. 4.10b (insert)** that the steady

flux after 20 min of run was 230 L/(m^2.h) and that of pure water flux was 319 L/(m^2.h) after 20 min of run. The decrease in flux was due to the deposition of flocs on the surface of the membrane thereby blocking the active pores, which is available for microfiltration. However, flux can be recovered > 98% by washing the membrane.

The quality of raw CRM wastewater and treated water, which is compared with the Environmental protection agency (EPA) permissible limit of surface water, is shown in **Table 4.3**. It is seen from the table that results obtained after hybrid process via coagulation – flocculation followed by microfiltration showed considerable reduction of all the parameters. Chromium concentration decreased from 2.26 mg/L to 0.035 mg/L and that of iron decreased from 5.7 mg/L to 0.51 mg/L. Turbidity increased from 12.30 NTU to 16.40 NTU due to the floc formation, however decreased after microfiltration to 0.9 NTU. It is also seen that all the water quality lies within the permissible limits of surface water [11].

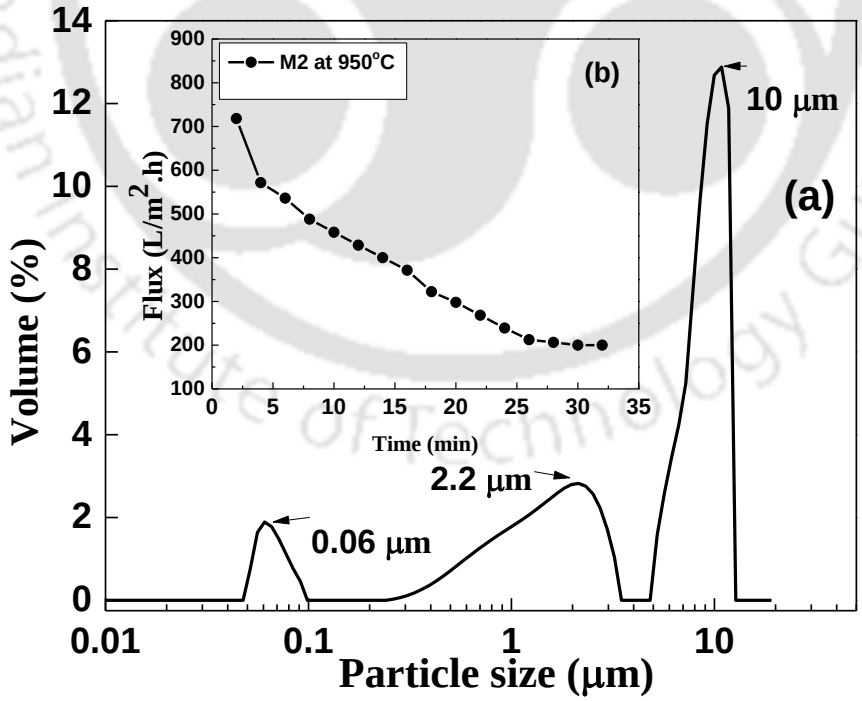

Fig. 4.11: a) Particle size distribution of floc before microfiltration and b) Flux declination pattern during microfiltration of coagulated water (insert). PAC dose: 350 mg/L

Table 4.3. Water quality parameters of cold rolling mill wastewater before and after treatment

Water quality parameters	Feed water	Water after PAC treatment	Water after membrane treatment	Limit for surface water (EPA)
pH	8.32	8.1	7.9	6 - 9
Total dissolved solids (mg/L)	712	324	112	1000
Conductivity	1.28	1.89	0.6	1
Turbidity (NTU)	12.30	16.40	0.9	< 29
Dissolved oxygen (mg/L)	5.43	3.20	1.25	< 3
Chemical oxygen demand (mg/L)	800	230	60	250
Iron (mg/L)	5.7	0.65	0.51	1
Chromium (mg/L)	2.26	0.309	0.05	0.05

4.3. Membrane cost

Cost analysis of a membrane is an important parameter to validate the feasibility of the membrane process. Polymeric membrane which is used for industrial purpose costs around 50 - 200 USD/m^2 [4]. Whereas, inorganic membranes are said to be expensive than that of polymeric membranes which costs around 500 – 1000 USD/m^2 [8]. The raw material cost for the fabrication of the present membrane is evaluated to be 32.55 USD/m^2 and 55.7 USD/m^2 for M1 and M2 membranes, respectively as shown in **Table 4.4**. The total cost including raw materials cost, and manufacturing including electrical cost was estimated be around 100 USD/m^2 and 125 USD/m^2 for M1 and M2 membranes, respectively. Therefore, it can be seen that the cost of the LD slag based membrane is very much similar to that of polymeric membrane, which confirmed the utilization of such solid waste generated in steel industry in an economic way.

Table 4.4. Cost analysis of fabricated membrane

Raw materials	**Unit price ($ kg^{-1})**	**M1 (kg) × 10^{-3}**	**M2 (kg) × 10^{-3}**
Modified LD Slag	-	11	12
Sodium metasilicate	6.6	3	3
Boric acid	8.3	1	2
Sodium carbonate	6.6	3	0
Alumina	8.6	2	0
Quartz	25	0	3
	Total	20	20
Raw material cost of present membrane		32.55 $ m^{-2}	55.7 $ m^{-2}
0.02 kg was needed for one-disc shaped membrane. (51.5 mm diameter and 5 mm thickness) for both M1 and M2			

Summary

Microfiltration ceramic membranes were fabricated using Linz-Donawitz (LD) slag which is a solid waste produced by basic oxygen furnace unit in a steel industry**.** Limitation of using direct LD slag for the fabrication was overcome by modifying the slag. M2 membranes sintered at 950 ^{o}C showed good flexural strength, pure water flux and chemical stability than M0 and M1 membranes sintered at 650 ^{o}C and 850 ^{o}C. A hybrid technique via coagulation – flocculation followed by micro- filtration was chosen for the treatment of CRM wastewater from steel industry. The fabricated LD slag membrane was found suitable for the separation of flocs from coagulated water. Results obtained after hybrid process via coagulation – flocculation followed by microfiltration showed considerable reduction of all the parameters. Cost of the LD slag-based membrane was fairly close to that of a polymeric membrane, indicating that such solid waste generated in the steel industry can be utilised economically.

Reference

[1] M. Shokri, A. Ahsan, H.Y. Liu, N.H. Muslim, An overview of Use of Linz-Donawitz (LD) Steel Slag in Agriculture, Jouranl Adv. Sci. Reseacrh. 5 (2015) 30–41.

[2] M. Changmai, M.K. Purkait, Detailed study of temperature-responsive composite membranes prepared by dip coating poly (2-ethyl-2-oxazoline) onto a ceramic membrane, Ceram. Int. 44 (2018) 959–968. https://doi.org/10.1016/j.ceramint.2017.10.029.

[3] M. Changmai, M. Pasawan, M.K. Purkait, Treatment of oily wastewater from drilling site using electrocoagulation followed by microfiltration, Sep. Purif. Technol. 210 (2019) 463–472. https://doi.org/10.1016/j.seppur.2018.08.007.

[4] D. Ghosh, M.K. Sinha, M.K. Purkait, A comparative analysis of low-cost ceramic membrane preparation for effective fluoride removal using hybrid technique, Desalination. 327 (2013) 2–13. https://doi.org/10.1016/j.desal.2013.08.003.

[5] C. Navarro, M. Díaz, M.A. Villa-García, Physico-chemical characterization of steel slag. study of its behavior under simulated environmental conditions, Environ. Sci. Technol. 44 (2010) 5383–5388. https://doi.org/10.1021/es100690b.

[6] M.K. Purkait, R. Singh, Membrane Technology in Separation Science, 2018. https://doi.org/10.1201/9781315229263.

[7] R. Singh, V.S.K. Yadav, M.K. Purkait, Cu 2 O photocatalyst modi fi ed antifouling polysulfone mixed matrix membrane for ultra fi ltration of protein and visible light driven photocatalytic pharmaceutical removal, Sep. Purif. Technol. 212 (2019) 191–204. https://doi.org/10.1016/j.seppur.2018.11.029.

[8] B.K. Nandi, R. Uppaluri, M.K. Purkait, Preparation and characterization of low cost ceramic membranes for micro-filtration applications, Appl. Clay Sci. 42 (2008) 102–110. https://doi.org/10.1016/j.clay.2007.12.001.

[9] M.K. Purkait, M.K. Sinha, P. Mondal, R. Singh, Stimuli Responsive Polymeric Membranes, 2018.

[10] H. Elomari, B. Achiou, M. Ouammou, A. Albizane, J. Bennazha, S. Alami Younssi, I. Elamrani, Elaboration and characterization of flat membrane supports from Moroccan clays. Application for the treatment of wastewater, Desalin. Water Treat. 57 (2016) 20298–20306. https://doi.org/10.1080/19443994.2015.1110722.

[11] U.S. Epa, Water Quality Standards Handbook Chapter 3 : Water Quality Criteria, (2017).

Chapter 5:

Removal of Chromium from Linz-Donawitz slag

Chapter 5
Removal of Chromium from Linz-Donawitz slag

In this chapter chromium (Cr) is selectively removed from Linz Donawitz (LD) slag, a solid waste produced by a basic oxygen furnace unit in the steel industry. Removal of chromium from LD slag is done by the process of roasting and leaching using potassium hydroxide and water respectively. The variation of percentage of Cr removal was studied by optimizing the mass ratio of potassium hydroxide to the slag, roasting temperature, time and slag particle size. The method adopted for this study yields two products: chromium-leached liquor and residual slag. Residual slag is used as the adsorbent for the treatment of Congo red dye wastewater. Also, an attempt was made to recover chromium from chromium leached liquor in the form of chromium hydroxide by precipitation.

5.1. Experimental

5.1.1. Materials and characterization techniques

Linz – Donawitz (LD) slag was obtained from TATA steel Limited, Jamshedpur, India. Potassium hydroxide, calcium hydroxide, hydrochloric acid, sodium hydroxide and Congo red (CR) of analytical purity was purchased was obtained from Merck (India). CR was dissolved in high purity water to a required concentration in the aqueous solution. All the chemicals were used without any further purification. All the glassware used in the experiments were made by Borosil, India. The composition of LD slag was analysed using X-ray fluorescence (XRF, make: PANalytical; model: Axios). Field emission scanning electron microscopy (FESEM, make: Zeiss; model: Sigma 300) was used to analyse the morphology of slag and distribution of chromium in LD slag, residual chromium-free slag and the precipitated chromium. The concentration of chromium in the raw and the residual slag was analysed using method 3060A [1] and analysed using photometer (Hach; Model DR-900).

The surface area of the residual slag was studied using Brunauer-Emmett-Teller (BET) analyser (Model: AUTOSORB-1; Make: Quantachrome instruments, USA).

5.1.2. Experimental procedure

Composition of raw LD slag consists of CaO: 53.47 %, MnO: 0.62 %, P_2O_5: 2.41 %, MgO: 8.10 %, FeO: 21.6 %, SiO_2: 9.2 %, Al_2O_3: 1 %, Cr_2O_3: 2.3 % and others: 1.3 %. Three mesh screens were used to sift the LD slag: 25 µm, 25 – 45 µm, and 45 – 150 µm. The sieved slag was washed with water and dried for 6 h at 100 ^oC. The dry slag is now combined with a defined amount of KOH and roasted at a predetermined temperature and time in a muffle furnace. The roasted material was then pulverised into very fine powder. After that, the pulverized particles were mixed with water for the leaching process. The roasted pulverised material is stirred with water at 80 rpm for 40 min during the leaching process. After 40 min, the solution is filtered with a vacuum filer (nylon filter with 0.2 µm pore size). This method yields two products: residual slag, which is used as an adsorbent, and chromium-leached liquor. Calcium hydroxide is added to the leached-out liquor containing chromium to form chromium hydroxide $(CrOH)_3$ precipitates. A detailed scheme of the process is given below in **Figure 5.1**. Percentage chromium removal is calculated by Eqn 5.1.

$$\%\ Chromium\ removal = \frac{Cr_{(raw\ slag)} - Cr_{(residual\ slag)}}{Cr_{(raw\ slag)}} \times 100 \qquad (5.1)$$

5.1.3. Utilization of residual slag as adsorbent

After removing the chromium from the LD slag, the remaining slag i.e, residual slag is employed as an adsorbent in the treatment of Congo red dye contaminated water. Residual slag comprises a high concentration of iron, calcium, silica, and other components, making it suitable for use as an adsorbent. A batch system of CR synthetic solution samples was used for all adsorption experiments. Adsorption of CR on residual slag as an adsorbent was measured for different initial concentrations (30-100 mg/L). The pH of the solution was

maintained around 7 by using 0.1M HCl and 0.1M NaOH solution. The concentration of remaining solutions was measured by using UV Vis Spectrophotometer (Model No.: UV-2600, Make: Shimadzu, Singapore) at a wavelength of 496 nm.

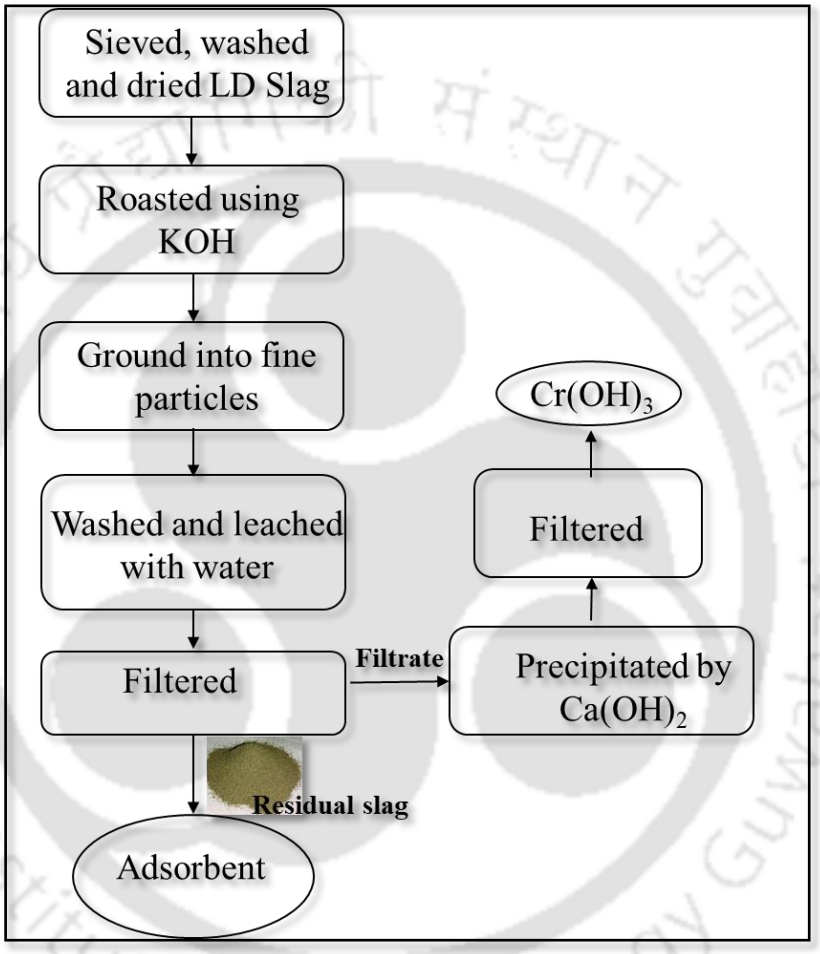

Fig. 5.1. Scheme of removal of chromium from LD Slag

5.2. Results and discussion

This section is divided into main five parts. In the first part, effect of roasting temperature, time and mass ratio of KOH to LD slag on chromium removal is reported. Variation of chromium removal with leaching temperature and time were studied and discussed in second part. Third- and fourth-part deals with the recovery of chromium from leached out liquor in

the form of chromium hydroxide and utilization of residual slag for the adsorption of Congo red dye respectively. Characterization of the raw and residual slag is discussed in fifth part.

5.2.1. Effect of roasting temperature on chromium removal

The influence of roasting temperature on chromium removal is shown in **Fig.5.2**. The temperature range of 300 – 600 °C was chosen for the study with the goal of keeping the temperature as low as possible to optimize the economics of the process. This method enabled the determination of the minimal temperature at which KOH is adequately dissolved. It can be observed from **Fig.5.2**, that the Cr leaching increased abruptly from 57 to 88 % when the temperature was raised from 300 to 400 °C, then increased gradually and eventually stabilized at the temperature range of 450–600 °C for the samples. This is due to the fact that at these temperatures, the interior pores of the slag particles seal, preventing the passage of external O_2 into the particles. The oxidation of Cr_2O_3 inside the particles to soluble potassium chromate become difficult in the absence of diffused O_2. It was observed that the Cr removal was greater in the roasted slag with a darker green color. This was due to the fact that as more Cr^{+3} from the slag was oxidised, the green colour on the surface of the roasted slag got darker. Similar observation was noticed by *Y. ji et al* in his work [2].

5.2.2. Effect of roasting time on chromium removal

The effect of roasting time on removal of chromium is shown in **Fig.5.2**. It is seen that chromium removal increased sharply from 72 % to 94 % at 3 h, then stayed constant from 3 h to 6 h, demonstrating that roasting duration did not effect on longer roasting time. Roasting time less than 1 h were not explored because salt melting and oxygen diffusion require longer time scales. When it reached 3 h, the removal achieved the maximum values of 96 %. There were no obvious changes when the roasting time was more than 3 h. According to the foregoing findings, optimum roasting time for Cr removal is 3 h at 450 °C.

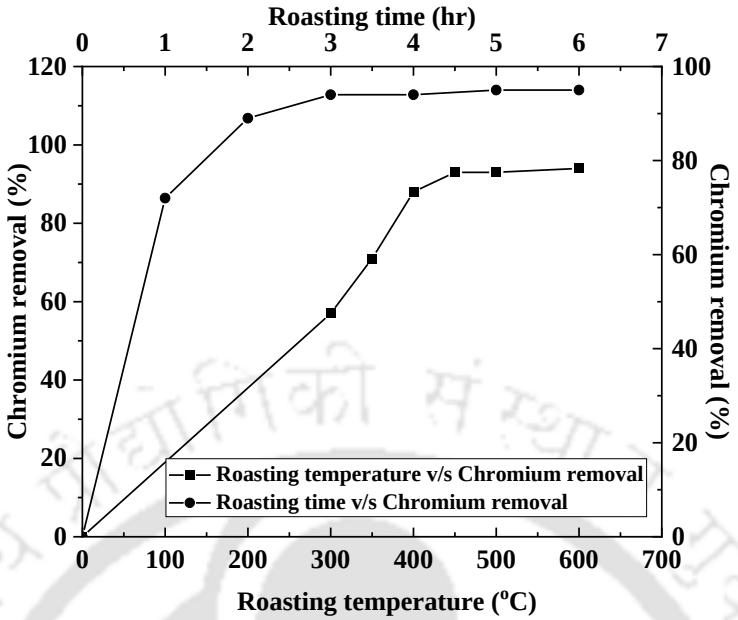

Fig. 5.2. Variation of chromium removal with roasting temperature and time

5.2.3. Effect of mass ratio of KOH on chromium removal

The effect of mass ratio on chromium removal is shown in **Fig.5.3**. The Cr leaching after roasting at 450 °C for 3 h was studied as a function of KOH addition to LD slag before roasting. The Cr leaching sharply increased from 15 % to 69 % with an increasing mass ratio from 0.041 to 0.083. Upon a higher mass ratio, chromium removal is increased up to 96 % till 0.25 and removal did not further increase. Therefore, the optimum mass ratio of KOH to LD slag was determined to be 0.25.

Intuitively, the particle size has an important influence on the leachability of chromium from LD slag. The effect of the particle size of LD slag on Cr leaching for the at 450 °C was investigated. Three particle size ranges of the LD slag were tested, namely, 45–150 µm, 25–45 µm, and < 25 µm. The Cr leaching increases from 85 % to 92 % for the 45–150 µm and 25–45 µm samples, respectively, and reaches a maximum leachability of 96 % Cr for the size fraction < 25 µm. The increased Cr leachability can be attributed to the increase of specific surface area of the slag, as well as a higher reactivity which is induced by grinding which is

also explained by E. Kim [3]. The Cr removal was increased with decreasing particle size. The optimal particle size fraction was found to be < 25 µm.

5.2.4. Variation of chromium removal with leaching temperature and time

The effects of various leaching time (0–60 minutes) on chromium leaching were thoroughly investigated. The leaching was carried out under the following conditions: the liquid-to-solid ratio was 10:1 mL/g, the sample size: 25 µm, the roasting temperature: 450 ^{o}C, and the roasting time: 3 h. At a leaching duration of 10 minutes, the chromium leaching rate quickly reached 84 %, as shown in **Fig. 5.4**. When the leaching time approached 40 min, the rates were practically at their peak (96 %). When the duration was prolonged to 60 min, the leaching rates essentially remained constant. As a result, with a leaching duration of 40 minutes, the leaching of the roasted samples was excellent.

Similarly, the effects of different leaching temperatures (30–80 °C) on chromium leaching were investigated thoroughly. The leaching was done with a leaching time of 40 min and under the same conditions as the leaching time experiments. The leaching was almost constant (95 %) when the temperature varied from 30 °C to 80 °C, as shown in **Fig. 5.4**. This was due to the fact that potassium chromate in roasted samples had a high water solubility (65.2 g/L) and could be rapidly dissolved in water at room temperature [4]. It suggested that the water leaching process could be carried out at room temperature. The leaching temperature was adjusted at 50 °C considering the industrial environmental conditions.

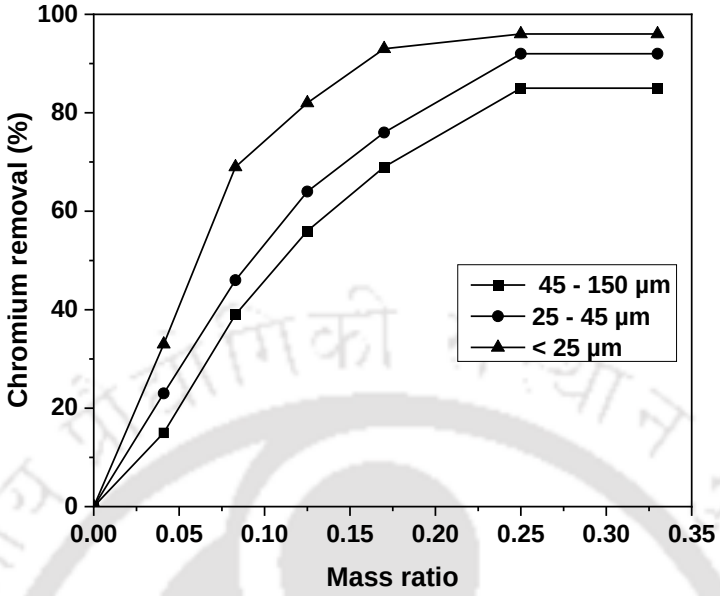

Fig. 5.3. Effect of mass ratio of KOH to LD slag with different particle sizes on percentage chromium removal. Roasting temperature: 450 °C, roasting time: 3 h

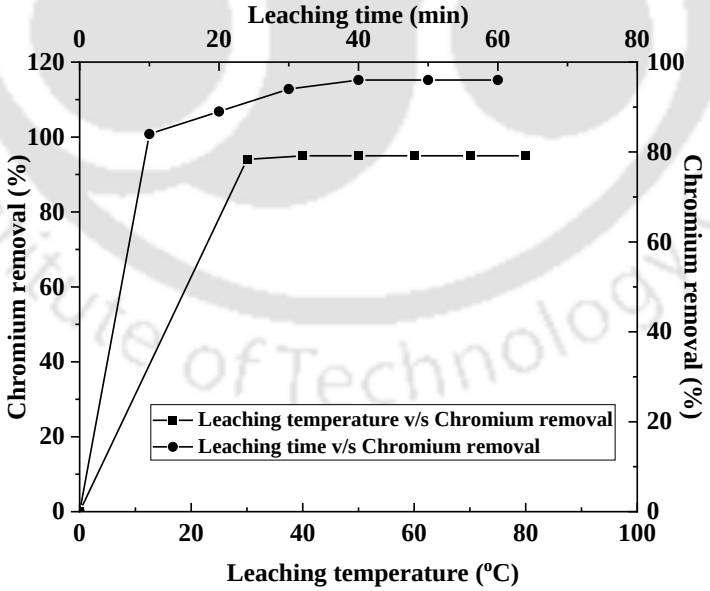

Fig. 5.4. Variation of chromium removal with leaching temperature and time. Roasting temperature: 450 °C, time: 3 h dose: 0.25

5.2.5. Utilization of residual slag as adsorbent

The residual slag obtained after removal of chromium from LD slag is used as adsorbent for the treatment of Congo red dye polluted water. Residual slag contains good amount of iron, calcium, silica and other elements. The surface area of the residual slag was found as 44.16 m^2/g. Congo red (CR) dye, which is an anionic dye, was used as adsorbate for this study. A synthetic wastewater solution of CR was made for the study by dissolving the calculated amount of CR in deionized water. All reagents and solutions were prepared by using deionized water. The effect of residual slag concentration (varying from 1.0 g/L to 5.0 g/L) on the percentage removal of the dyes at different initial dye concentrations (30-100 mg/L) was studied. It was found that dye removal increased with increasing residual slag content. An adsorbent content of 1 g/L was enough for more than 85 % dye removal for 90 mg/L crystal violet solutions. Adsorption efficiency increased to 95 % for congo red dye at 5 g/L residual slag.

5.2.5.1. Adsorption kinetic studies

The kinetic model can be used to estimate the adsorption efficiency and derive an appropriate rate expression for the possible reaction mechanism. According to the time gradient, the adsorption kinetics data for residual slag across 180 min as shown in **Fig. 5.5** were analysed by two typical kinetic models, including pseudo-first-order kinetics model (Eqn 5.2), and the pseudo-second-order kinetics model (Eqn 5.3) [5]. The pseudo-first-order kinetics model, based on the amount of solid adsorption, was applied to the liquid phase adsorption, and the pseudo-second-order kinetic model was based on the assumption that the adsorption rate was controlled by the chemical adsorption mechanism. The equations of the two kinetic models were as follows:

$$\log(q_e - q_t) = \log q_e - \frac{k_1}{2.303} \times t \quad (5.2)$$

$$\frac{t}{q_t} = \frac{1}{k_2 q_e^2} + \frac{1}{q_e} \times t \quad (5.3)$$

where qe (mg/g) is the equilibrium adsorption capacity, qt is the adsorption capacity at time t, and K1 (h^{-1}) and K2 ($g \cdot mg^{-1} \cdot h^{-1}$) are the rate constant of the pseudo-first-order and pseudo-second-order, respectively.

To obtain the rate parameters, fit graphs of the log (qe − qt) vs. t and t/qt vs. t were applied to pseudo-first-order and pseudo-second-order kinetics models respectively. Calculated values of *k*1 and $q_{e,cal}$ are summarized in **Table 5.1**. From **Fig. 5.5a**, it may be observed that the experimental data point does not fit a straight line. From **Fig 5.5a** and **Table 5.1**, it may be concluded that the kinetics of congo red adsorption on residual slag is not probably following the pseudo first order kinetic model and hence not a diffusion-controlled phenomenon.

Fig. 5.5b shows that the plot of *t*/*qt* versus *t* is a straight line with slope of 1/*q*e and intercept 1/*k*2*q*e. Using the value of *q*e calculated from the slope, the value of *k*2 is determined from the intercept. The calculated value of *k*2, *q*e and their corresponding regression coefficient (*R*2) values are presented in **Table 5.1**. The value of regression coefficient is nearly unity (0.99), which confirms that, the sorption kinetics of congo red dye follows a pseudo-second-order process. Thus, it may be concluded that the adsorption of congo red dye on residual slag can be better explained by pseudo-second-order kinetic model than that of first-order kinetic model and the process is chemisorption controlled.

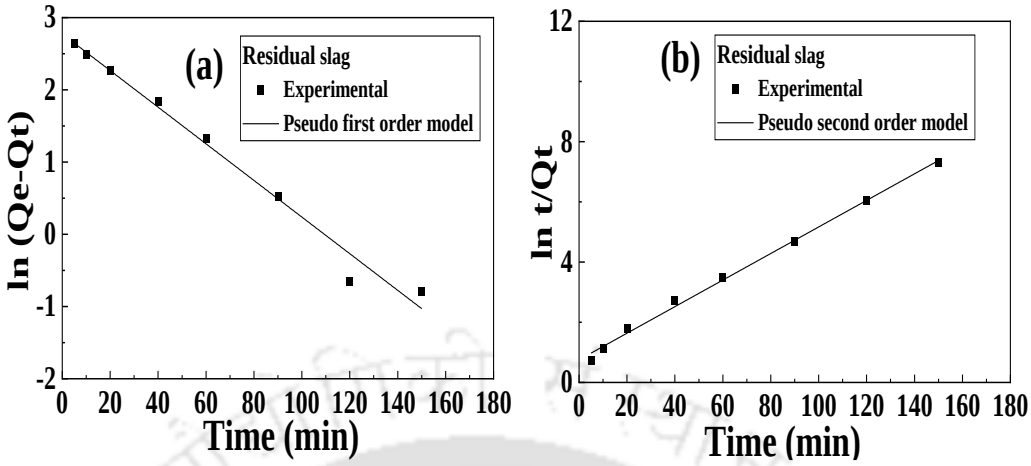

Fig. 5.5. (a)Pseudo-first-order and (b) pseudo-second-order kinetic model, of congo red dye on residual slag

Table 5.1. Parameters of kinetic models for congo red dye adsorption

Adsorbent	**Pseudo first-order model**			**Pseudo-second-order model**		
	$Q_{e,cal}$ (mg/g)	K_1 (min^{-1})	R^2	$Q_{e,cal}$ (mg/g)	$K_2 \times 10^{-3}$ (g/mg.min)	R^2
Residual slag	16.07	0.0253	0.98	22.89	0.0025	0.99

5.2.5.2. Adsorption isotherm studies

Adsorption characteristics and equilibrium parameters, often known as adsorption isotherms, describe how adsorbates interact with adsorbents and provide a thorough knowledge of the nature of the interaction. Isotherms aid in providing information on the best way to employ adsorbents. So, in order to optimise the design of an adsorption system to remove dye from solutions, the most acceptable correlation for the equilibrium curve must be determined. For assessing experimental sorption equilibrium parameters, numerous isotherm equations are available. The Langmuir and Freundlich models, however, are the most prevalent forms of isotherms. The Langmuir isotherm is based on the premise that there are a finite number of binding sites spread uniformly over the adsorbent surface. There is no interaction between

adsorbed molecules since these binding sites have the same affinity for adsorption of a single molecular layer. The Freundlich isotherm model is an exponential equation that applies to adsorption on heterogeneous surfaces with intermolecular interaction and is not limited to the creation of a monolayer. This model implies that as adsorbate concentration increases, so does adsorbate concentration on the adsorbent surface, and that sorption energy reduces exponentially upon completion of sorption centres of the adsorbent [6]. The well-known expressions for the Langmuir and Freundlich models are given as [7]

$$q_e = \frac{Q_o b C_e}{1+bC_e^n} \qquad (5.4)$$

where *C*e (mg/L) and *q*e (mg/g) are the liquid phase concentration and solid phase concentration of adsorbate at equilibrium, respectively, and Q_0 (mg/g) and *b* (L/mg) are the Langmuir isotherm constants.

$$q_e = K_f C_e^n \qquad (5.5)$$

where *K*f is the Freundlich constant [mg/g(L/g)$^{1/n}$] related to the bonding energy, and *n* is the heterogeneity factor. *n* is a measure of the deviation from linearity of the adsorption. It indicates the degree of non-linearity between solution concentration and adsorption.

Since the adsorption is supposed to be the chemisorption in nature, it may be proposed that monolayer coverage of dye molecule is taking place over the residual slag surface. Therefore, adsorption process should be better represented physically by Langmuir isotherm model than Freundlich isotherm model. Both the isotherms for dye—residual slag system is shown in **Fig. 5.6**. This figure provides information on the amount of residual slag required to adsorb a particular mass of congo red under the specified system conditions. Correlation coefficients for Langmuir and Freundlich adsorption isotherm are calculated by fitting the experimental adsorption equilibrium data and are shown in **Table 5.2**. It is also found from the correlation

coefficients (*R*2) that adsorption isotherm for the present system is explained better by Langmuir isotherm model.

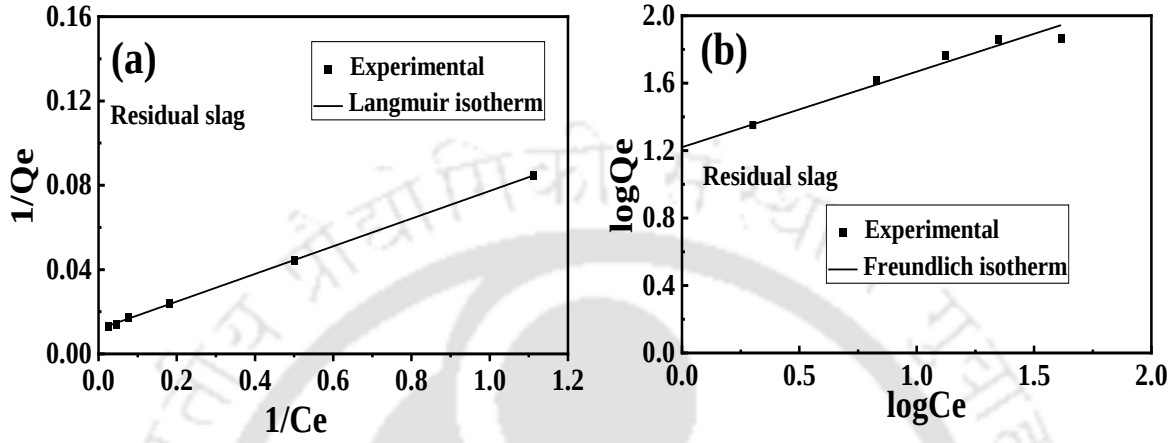

Fig. 5.6. (a) Langmuir and (b) Freundlich adsorption isotherms of congo red dye on residual slag

Table 5.2. Various parameters of Langmuir and Freundlich adsorption isotherm models

Adsorbent	Langmuir isotherm			Freundlich isotherm		
	Q_0 (mg/g)	K_L (L/mg)	R^2	K_F (mg/g) $(L/mg)^{1/n}$	n	R^2
Residual slag	85.40	0.178	0.99	16.60	2.2	0.97

There have been few studies on the adsorption of congo red dye, from different wastewater. A summary of the literature concerning the current study is presented here. The use of residual slag for the adsorption of congo red dye is a novel approach, as shown in **Table 5.3**. Apparently, the removal of dye presented in this study is comparably better to that presented in the literature, since this work achieved a higher percentage of removal through adsorption. Furthermore, the comparison of targeted parameters and data based on dye removal obtained in this work suggests that the research conducted in this work could serve as benchmark data

in the field of treatment of congo red polluted wastewater. In this context, the current research is recommended to investigate the efficiency of residual LD slag, as well as adsorption method for the removal of congo red dye from wastewater, illustrating the uniqueness of this work.

Table 5.3: Different literatures on adsorption of congo red dye using various adsorbents

Method	Pollutant	Adsorbent	Percentage removal (%)
Adsorption [8]	Congo Red dye	Tunics of the corm of the saffron	68
Adsorption [9]	Congo Red dye	Bombax Buonopozense bark Activated-carbon	86.12
Adsorption [10]	Congo Red dye	FexCo3-xO4 nanoparticles	86.12
Adsorption [11]	Congo Red dye	Cabbage waste powder	91
Adsorption [12]	Congo Red dye	Pine cone biochar	94.62
Adsorption [13]	Congo Red dye	Kenaf-based activated carbon	95
Present work	Congo Red dye	Residual LD slag	95

5.2.6. Recovery of chromium hydroxide

Recovery of chromium was carried out using precipitation process. Precipitation experiments were carried out using jar – test apparatus (make: Phipps & Bird, Richmond, Virginia) equipped with 6 numbers of 1 L jar with rectangular blades. The experiment was done in two batches. The dosage of the precipitating agent varied from 100 mg/L to 1200 mg/L. The operating parameters were set as follows: (Rapid mixing speed: 100 rpm for 1 min; slow mixing speed: 30 rpm in the range 10-40 min; settling time: 30 min). The parameters were set

using an automatic controller. The mixture was then filtered using nylon filter paper (0.2 μm). Calcium hydroxide was used as precipitating agent. A preliminary investigation was experimented to determine an approximate range of precipitating agent dosage. Therefore, wide ranges of concentrations of calcium hydroxide (100 mg/L – 1200 mg/L) were considered to get the optimized dosage of precipitating agent ($Ca(OH)_2$) required for recovering chromium as shown in **Table 5.4**. It was observed from the table that at minimum dosage of 900 mg/L, there was major changes occurred with time. However, as the dosage reached 600 mg/L, formation of precipitate started and at the end of 900 mg/L, almost complete formation and settling of precipitate was seen. Hence, the results revealed that optimum dosage of calcium hydroxide and time for the recovery of chromium in the form of chromium hydroxide was 900 mg/L and 30 min respectively.

Table 5.4. Precipitation of chromium from filtrate at various conditions

Time (min)	**10**	**20**	**30**	**40**
Dosage of $Ca(OH)_2$ (mg/L)	Chromium hydroxide precipitation (%)			
100	24	25	28	31
300	32	38	46	47
600	49	58	67	69
900	71	87	91	92
1200	86	90	95	97

5.2.7. Characterizations

5.2.7.1. X-Ray Diffraction

The XRD pattern of the raw LD slag and residual slag is depicted in **Fig. 5.6**. It indicates that the raw LD slag samples were very complex, with several overlapping peaks resulting from the many minerals present in the samples. Major mineralogical phases of the slag were $Ca_3Mg(SiO_4)_2$, akermanite, $Ca_2Mg(Si_2O_7)$, srebrodolskite ($Ca_2Fe_2O_5$), wustite (FeO), Portlandite ($Ca(OH)_2$), Brownmillerite ($Ca_2(Al,Fe)_2O_5$) and Larnite (Ca_2SiO_4) crystalline phases observed and chromium is present in a spinel structure ($(Mn,Ca)x(Fe0_6,Cr0_4)yO_z \cdot nSiO_2$). The crystalline phases, such as bredigite, Ca14Mg2(SiO4)8, merwinite, Ca3Mg(SiO4)2, and monticelite, CaMgSiO4, remained in the residual slag. No chromium was detected, signifying that there were only very small quantities of chromium in the residue. Therefore, this roasting leaching process proven an efficient and feasible technique. Moreover, the residual slag was rich in Si, Fe and Ca. This is an important resource that can be used as adsorbent.

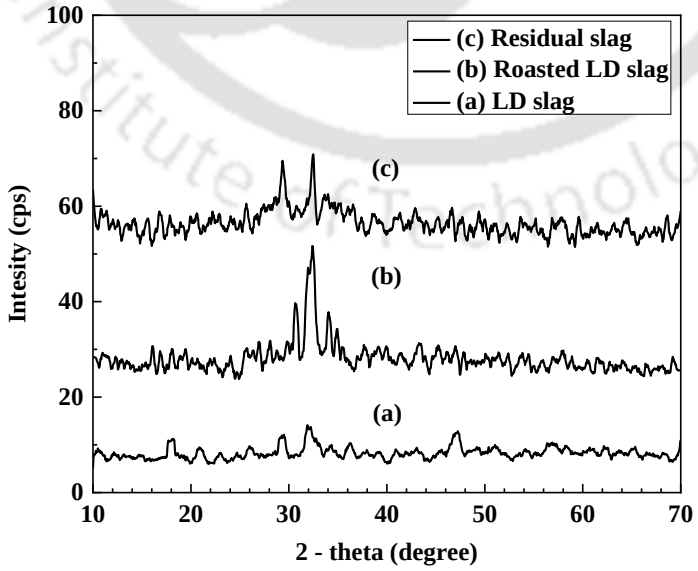

Fig. 5.7. XRD pattern of LD slag and Residual slag

5.2.7.2. Field emission scanning electron microscopy

FESEM-EDS images of the Raw LD slag, roasted slag and residual slag are shown in **Fig. 5.7a, b** and **c** respectively. These indicate that Cr is present in both spinel (Cr oxide) and metal phases. The roasted slag containing spinel structures show that Cr coexists with various metals such as Mg, Al, Mn, Fe and as well as in alloy form. The residual slag becomes rough and porous because of thermal heating of LD slag and chromium leaching by water. it can be seen that the main elements in the residue are Fe, Si and Ca, indicating that most of the Cr was extracted. Moreover, no Cr was detected in the residual slag, signifying that there were only very small quantities of Cr in the residue.

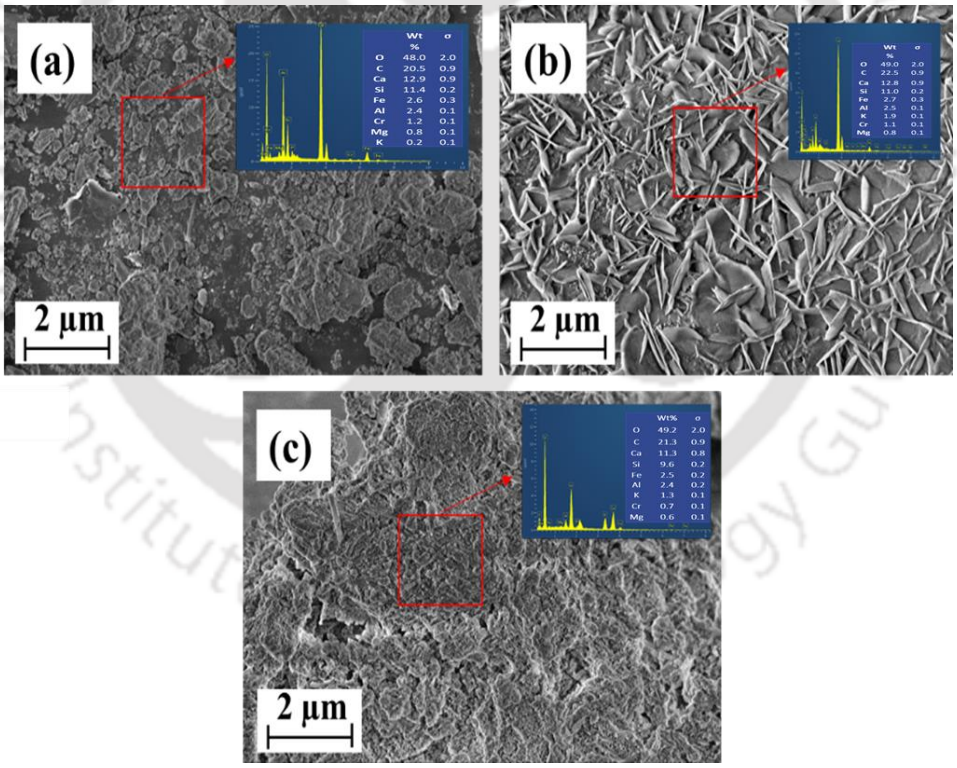

Fig. 5.8. FESEM images of (a)LD slag (b) roasted LD slag and (c) residual slag

Summary

A viable procedure for removing chromium from LD slag produced in the basic oxygen furnace unit of steel industry was successfully explored. Roasting and leaching were used to remove chromium selectively. Based on the experimental findings, the optimum mass ratio of KOH to LD slag, roasting temperature and roasting time was determined. The residual slag was rich in Si, Ca, Fe, and Mg. This matrix was effectively employed as an adsorbent to treat Congo red polluted water. Chromium was recovered from chromium leached liquid using a precipitation procedure with calcium hydroxide as a precipitating agent. The increase in removal percentage of Cr, results into the increase in slag quantity. The Cr concentration in residual slag is reduced to the levels permissible in industrial discharge. Overall, the roasting-leaching method found to be appropriate for removing chromium from LD slag, and the residual slag found to be an excellent adsorbent. Besides adsorbent, the residual slag may be utilized for other applications such as road construction, pavement, and building bricks which gives monetary benefit to the industry.

.

Reference

[1] W.. Mills, C.T., Bern, C.R., Wolf, R.E., Foster, A.L., Morrison, J.M., and Benzel, Laboratory data from testing parameters of EPA Method 3060A on Soils Contaminated with Chromium Ore Processing Residue, U.S. Geol. Surv. Data Release. (2017). https://doi.org/doi.org/10.5066/F7PG1PXD.

[2] Y. Ji, S. Shen, J. Liu, S. Yan, Z. Zhang, Y. Xue, Extracting Chromium from Stainless Steel Slags by NaOH-Added Pellet Roasting Followed by Water Leaching, Steel Res. Int. 88 (2017) 1–8. https://doi.org/10.1002/srin.201600460.

[3] E. Kim, J. Spooren, K. Broos, P. Nielsen, L. Horckmans, K.C. Vrancken, M. Quaghebeur, New method for selective Cr recovery from stainless steel slag by NaOCl assisted alkaline leaching and consecutive BaCrO4precipitation, Chem. Eng. J. 295 (2016) 542–551. https://doi.org/10.1016/j.cej.2016.03.073.

[4] B.E. Poling, G.H. Thomson, D.G. Friend, R.L. Rowley, W.V. Wilding, Section 2: Physical and Chemical Data, 2007. https://doi.org/10.1036/0071511253.

[5] C. Sarkar, J.K. Basu, A.N. Samanta, Synthesis of mesoporous geopolymeric powder from LD slag as superior adsorbent for Zinc (II) removal, Adv. Powder Technol. 29 (2018) 1142–1152. https://doi.org/10.1016/j.apt.2018.02.005.

[6] B.K. Nandi, A. Goswami, M.K. Purkait, Adsorption characteristics of brilliant green dye on kaolin, J. Hazard. Mater. 161 (2009) 387–395. https://doi.org/10.1016/j.jhazmat.2008.03.110.

[7] C. Sarkar, J.K. Basu, A.N. Samanta, Adsorption of Direct Red 23 By Microwave Activated Ld Slag, Chem. Eng. An Int. J. 1 (2017) 1–11.

[8] A. Dbik, S. Bentahar, M. El Khomri, N. El Messaoudi, A. Lacherai, Adsorption of Congo red dye from aqueous solutions using tunics of the corm of the saffron, Mater. Today Proc. 22 (2020) 134–139. https://doi.org/10.1016/j.matpr.2019.08.148.

[9] Y. Achour, L. Bahsis, E.H. Ablouh, H. Yazid, M.R. Laamari, M. El Haddad, Insight into adsorption mechanism of Congo red dye onto Bombax Buonopozense bark Activated-carbon using Central composite design and DFT studies, Surfaces and Interfaces. 23 (2021) 100977. https://doi.org/10.1016/j.surfin.2021.100977.

[10] J. Liu, N. Wang, H. Zhang, J. Baeyens, Adsorption of Congo red dye on Fe x Co 3-x O 4 nanoparticles, J. Environ. Manage. 238 (2019) 473–483. https://doi.org/10.1016/j.jenvman.2019.03.009.

[11] J.N. Wekoye, W.C. Wanyonyi, P.T. Wangila, M.K. Tonui, Kinetic and equilibrium studies of Congo red dye adsorption on cabbage waste powder, Environ. Chem. Ecotoxicol. 2 (2020) 24–31. https://doi.org/10.1016/j.enceco.2020.01.004.

[12] N. Kaya, Z. Yıldız Uzun, C. Altuncan, H. Uzun, Adsorption of Congo red from aqueous solution onto KOH-activated biochar produced via pyrolysis of pine cone and modeling of the process using artificial neural network, Biomass Convers. Biorefinery. (2021). https://doi.org/10.1007/s13399-021-01856-5.

[13] S. Mandal, J. Calderon, S.B. Marpu, M.A. Omary, S.Q. Shi, Mesoporous activated carbon as a green adsorbent for the removal of heavy metals and Congo red: Characterization, adsorption kinetics, and isotherm studies, J. Contam. Hydrol. 243 (2021) 103869. https://doi.org/10.1016/j.jconhyd.2021.103869.

Chapter 6:

Conclusions and scope of future work

Chapter 6
Conclusion, summary and scope of future work

This chapter comprises two section. First part is the conclusions, which include the results drawn from several works presented in this thesis. Second and last section discusses the ideas for the future work.

6.1. Conclusions

The thesis focuses on the treatment of effluents from coke oven and cold roll mill units, as well as the utilization of LD slag from the steel industry. Chapters 2 and 3 discusses on the treatment of concentrated nanofiltration reject generated from the coke oven unit of steel industry, by a solvent-based precipitation approach using organic solvents namely DIIPA, IPA and EA and an integrated technology of closed-circuit reverse osmosis (CCRO) and solvent-based precipitation respectively. Chapters 4 and 5 of the thesis discusses the use of LD slag in the fabrication of a microfiltration ceramic membrane for the treatment of cold roll mill effluent and extraction of chromium from LD slag respectively. The major conclusions from the different studies are presented below.

Separation of chloride and sulphate ions from nanofiltration rejected wastewater of steel industry (Refer Chapter 2):

Separation of chlorides and sulphates from NF rejected wastewater of steel industry was successfully achieved by using organic solvents namely DIIPA, IPA and EA and observations may be summarized as follows:

- Water quality parameters like TDS was reduced from 8613 mg/L to 785 mg/L and that of chlorides and sulphates from 1594 mg/L to 358 mg/L and 4196 mg/L to 8.4 mg/L, respectively (Refer page 34).

- The optimum condition obtained for chloride and sulphate precipitation was at volume ratio (VR) 1.02, pH 8, temperature 23.4 °C, and contact time 26 min (Refer page 46).
- Around 96 % - 98 % of organic solvent (IPA) was recovered which is recycled back to the system for further use.
- A comparative study of literatures with the present study shows that the use of miscible organic solvents is limited for the separation of chloride and sulphate ions from the industrial effluents (Refer Table 6).
- The method carried out in this work will be a benefaction to the steel industry in terms of handling nanofiltration rejected water containing high chlorides and sulphate ions.

Promising integrated technique for the treatment of highly saline nanofiltration rejected stream of steel industry (Refer Chapter 3):

Closed circuit reverse osmosis (CCRO) combined with solvent-based precipitation for the separation of ions especially chlorides and sulphates from highly concentrated brine of nanofiltration reject which is a major concern of blast furnace treatment unit of the steel industry was studied, and on the basis of that, the following details are found:

- Overall, water quality parameters like TDS was reduced to 1316 mg/L and that of chlorides and sulphates to 156 mg/L and 0.9 mg/L respectively by the integrated technique (Refer Table 3.1).
- At a steady-state flux of 7 L/m^2h maintaining 7 bar transmembrane pressure, the recovery was found to be as high as 82 % (Refer Figure 3.3).
- The preliminary economic assessment suggests viability because the cost of treating brine with the integration of the above-mentioned systems was estimated to be only $ 7.35 $/m^3$ (Refer Table 3.2).

- Apparently, the removal of ions presented in this study is comparably better to that presented in the literatures (Refer Table 3.3), since this work achieved a higher percentage of removal of chlorides, sulphates and TDS through integrated techniques.

Utilization of LD Slag from steel industry for the preparation of MF membrane (Refer Chapter 4):

Microfiltration ceramic membranes were fabricated using Linz-Donawitz (LD) slag which is a solid waste produced by basic oxygen furnace unit in a steel industry**.** Limitation of using direct LD slag for the fabrication was overcome by modifying the slag, following observations were found:

- All the membranes sintered at 850 ^{o}C and 950 ^{o}C showed good flexural strength in the range of 9 MPa.
- Pure water flux was found to be 341 L/(m2.h) and 319 L/(m2.h) at 950 ^{o}C for M1 and M2 membrane respectively (Refer Figure 4.7).
- The average pore diameter was estimated to be 3.6 - 8.5 µm for both the membranes which ensure that membranes are in microfiltration range.
- The membrane cost was determined to be in the range of 100 - 125 USD/m^2, which was very close to the cost of polymeric membrane (Refer Table 4.4),.
- Chromium concentration from cold roll mill wastewater of steel industry decreased from 2.26 mg/L to 0.035 mg/L and that of for iron decreased from 5.7 mg/L to 0.51 mg/L after a hybrid process of coagulation – flocculation followed by microfiltration.
- Overall, membranes sintered at 950 ^{o}C showed good results in terms of pure water flux, stability and strength when compared to membranes sintered at 650 ^{o}C and 850 ^{o}C.

Chapter 6

Removal of Chromium from Linz-Donawitz slag (Refer Chapter 5):

A process to remove chromium from LD slag as a part of solid waste management of solid waste of the iron/steel industry by roasting and leaching method using potassium hydroxide and water, respectively was studied and following observations were found.

- The best conditions for chromium (Cr) leaching by KOH roasting are a roasting temperature of 450 °C and a roasting period of 2 hours. Around 96 % Cr removal efficiency was attained under these conditions.
- The Cr leaching sharply increased from 15 % to 69 % with an increasing mass ratio from 0.041to 0.083. Therefore, the optimum mass ratio of KOH to LD slag was determined to be 0.25 (Refer Figure 5.2).
- Based on the experimental findings, the optimum mass ratio of KOH to LD slag, roasting temperature and roasting time was determined to be 0.25, 450 °C, and 3 h respectively.
- At optimum conditions, such as leaching time: 40 minutes and temperature: 30 ^{o}C, the leaching efficiency of chromium using water achieved a maximum of 95 % (Refer Figure 5.3)..
- Adsorption on residual slag followed the pseudo-second-order kinetic model depicting chemisorption, according to the kinetic study.
- The correlation coefficients also show that the Langmuir isotherm model better explains the adsorption isotherm for the current system.
- The results showed that the optimal calcium hydroxide dose and duration for recovering chromium in the form of chromium hydroxide were 900 mg/L and 30 min, respectively.

6.2. Recommendations on future work

This section highlights some of the new areas of research, that can be carried for further treatment of highly saline wastewater from coke oven unit and utilization of LD slag from steel industry. Some of the important areas of recommended research are suggested as an extension of the present study:

- Future fundamental work can include the complexity of organic-aqueous systems. Phenomenon interaction such as inorganic-inorganic interactions and inorganic-solvent interactions like ion hydration can be included in the solventing out method.
- Based on the results obtained on saline wastewater treatment, a pilot plant study is strongly recommended to treat the NF rejected stream and to investigate its feasibility in industrial scale.
- Research for the development of a possible integrated process that can generate water and salt in a desalination system with low energy, chemical, and cost consumption can be done not only in steel industry but also related brine-producing industries.
- LD slag can be used to fabricate a tubular membrane module system.
- The recovered chromium hydroxide can be further purified and used in the steel industry or for some other industrial applications.
- Besides adsorbent, the residual slag may be utilized for other applications such as road construction, pavement, and building bricks which gives monetary benefit to the industry

Appendix

Appendix

A. Error analysis

The errors in experimentally measured quantities and in parameters calculated from those measurements are important in that they determine the accuracy of calculation and predictions using those quantities. There are two types of errors viz. systematic error and random error. Systematic errors are the results of faulty assumptions or improper experimental measuring techniques. In this work, care was taken in eliminating systematic errors by appropriately designing the experiments and adopting qualified methods for analysis of the data. On the other hand, random errors result from variation in the precision of measuring parameters and the slight variations that occur in successive measurements made by the same observer under nearly identical conditions. Random errors cannot be eliminated. The focus of the error analysis presented in this section is on the random errors.

In most of the experiments performed in this work, the quantities that are measured directly are concentrations, permeate flow rates, weights and volumes which are used to determine the removal (%), rejection (%) and permeate flux.

A.1. Error in measurement of chloride and sulphate concentrations water

Chloride and sulphate concentrations in the aqueous phase was determined by measuring the absorbance value at a specific time in the ion exchange chromatography. A calibration curve was prepared by taking the absorbance values against the corresponding time as discussed in. From Figure 2.2, it is seen that the standard deviation of the predicted value from actual value of concentration is 0.9995. Thus, every measurement of chloride and sulphate concentrations is associated with an error of 0.05 % whose effect on precipitation factor can be ignored.

A.2. Error in the measurement of permeate flux

The errors in the values of permeate flux are related to the errors in the measurements used to calculate those values. In this section, statistical analysis is used for the estimation of uncertainty associated with the values of permeate flux. Determination of standard deviation is generally considered to be one of the best methods to estimate the uncertainty which is based on the following method:

If u_1, u_2, ..., u_N are the N results of the measurements of a particular quantity u, then the mean value of u (i.e. $\bar{u}$), is defined by

$$\bar{u} = \frac{u_1 + u_2 + \ldots\ldots\ldots + u_N}{N} = \frac{1}{N}\sum_{i=1}^{N} u_i \qquad \text{(A.1)}$$

The uncertainty in the result is usually expressed as "root-mean-squared-deviation", which is denoted as Δu, which is computed using the following Eq. (A.2):

$$\Delta u = \sqrt{\frac{(u_1 - \bar{u})^2 + (u_2 - \bar{u})^2 + \ldots\ldots\ldots + (u_N - \bar{u})^2}{N-1}} \qquad \text{(A.2)}$$

In the present work, the membranes used as mentioned in chapter 4, were cleaned thoroughly following each experiment. Besides, before each experiment, performance of all the membranes were checked through pure water flux (PWF) measurement; hence uncertainties involved in the PWF measurements are reported here. The uncertainties involved in different experimental measurements for (PWF) for membranes M1 and M2 are estimated and shown in Table A.1.

Table A.1. Values of uncertainties estimated in PWF measurements for membranes M1 and M2.

Membranes	Run 1	Run 2	Run 3	$\bar{u}$	Δu	Uncertainties (%)
M1	341	337.5	345	341.16	3.75	0.60
M2	319	315.6	323	319.16	3.75	0.60